

LEVEL

17

SSA-125
Contract No. AC9NX707

January 1980

ADA 084910

**CRITICALITY STUDIES OF GRAPHITE
MODERATED PRODUCTION REACTORS**

**DTIC
SELECTED
MAY 29 1980**

Prepared For

U.S. ARMS CONTROL AND DISARMAMENT AGENCY

Prepared By

S. E. Turner, Project Manager
R. M. Cole
M. K. Gurley
R. D. Keller, Jr.
K. D. Kirby
W. Mitchell, III

Southern Science Applications, Inc.
Division of Black & Veatch
P. O. Box 10
Dunedin, Florida 33528

This document has been approved
for public release and sale; its
distribution is unlimited.

DDC FILE COPY

80 5 27 153

REPORT DOCUMENTATION PAGE		1. REPORT NO. (1+) SSA-125	2. AD-A084910	3. Recipient's Accession No.
4. TITLE and Subtitle (6) Criticality Studies of Graphite Moderated Production Reactors.			5. Report Date (11) Jan 1986	
7. Author(s) (10) R.M. Cole, M.K. Gurley, R.D. Keller, Jr., K.D. Kirby, S.E. Turner			8. Performing Organization Rept. No. SSA-125	
9. Performing Organization Name and Address Southern Science Applications, Inc. PO Box 10 Dunedin, Fla. 33528		10. Project/Task/Work Unit No. (15)		11. Contract (C) or Grant (G) No. (C) No. AC9NX707 (G)
12. Sponsoring Organization Name and Address U.S. Arms Control Disarmament Agency Washington, D.C. 20451		13. Type of Report & Period Covered (9) Final rept.		14.
15. Supplementary Notes (12) 127				
16. Abstract (Limit: 200 words) The objective of the study was to examine the feasibility of using commercially available graphite in small production reactors. Three different-size reactors, each with a different coolant, were investigated, and an assessment was made of the effect of parasitic neutron-absorbing material in the graphite, either as naturally-occurring impurities or as intentionally-added spikants. In addition, a brief survey of methods of manufacturing and of purifying graphite was performed.				
17. Document Analysis a. Descriptors Nuclear Engineering				
b. Identifiers/Open-Ended Terms				
c. COSATI Field/Group				
18. Availability Statement Release unlimited		19. Security Class (This Report) Unclassified		21. No. of Pages 127
		20. Security Class (This Page) Unclassified		22. Price

TABLE OF CONTENTS

<u>Section and Title</u>	<u>Page No.</u>
1.0 INTRODUCTION	1
2.0 SUMMARY AND CONCLUSIONS	2
2.1 Analytical Bases and Procedures	2
2.2 Calculations with Pure Graphite	2
2.3 Effect of Graphite Impurities	4
2.4 Enriched Fuel	8
2.5 Poison Burnout Under Irradiation	9
2.6 Commercial Graphites	12
3.0 REFERENCE REACTOR CONCEPTS	21
3.1 Air-Cooled Reactor	22
3.2 The Gas-Cooled Reactor	25
3.3 The Water-Cooled Reactor	26
3.4 Graphite Temperatures	31
3.5 Bibliography for Section 3.0	34
4.0 NUCLEAR PERFORMANCE OF THE AIR-COOLED REACTOR	39
4.1 General	39
4.2 Lattice Optimization for the Reference Design	40
4.3 Fuel Burnup and Reactivity	42
4.4 Enriched Fuel	42
4.5 Plutonium Production	43
4.6 Graphite Impurities	45
5.0 NUCLEAR PERFORMANCE OF THE CO ₂ -COOLED REACTOR	58
5.1 General	58
5.2 Lattice Optimization for Reference Design	58

TABLE OF CONTENTS (continued)

<u>Section and Title</u>	<u>Page No.</u>
5.3 Fuel Burnup and Reactivity	59
5.4 Enriched Fuel	61
5.5 Plutonium Production	61
5.6 Graphite Impurities	63
6.0 NUCLEAR PERFORMANCE OF THE H ₂ O-COOLED CONCEPT	76
6.1 General	76
6.2 Natural-Uranium-Fueled Reference Reactor	76
6.3 Low-Enriched Uranium Fueled Reactors	78
6.4 Effects of Graphite Density	81
6.5 Effects of Graphite Impurities	81
7.0 NEUTRON BURNOUT OF IMPURITIES	98
8.0 CONSIDERATION OF COMMERCIALY AVAILABLE GRAPHITE	103
8.1 Manufacture of Graphite	103
8.1.1 Graphite Properties	106
8.1.2 After Market Graphite Purification in an Acheson Furnace	106
8.2 Suitability of Commercially Available Grades for Use in Production Reactors	112
8.3 Neutron Absorber Spikants to Deter the Use of Commercially Available Graphite in Reactors	112
8.4 Bibliography for Section 8.0	113
9.0 EFFECT OF REACTOR SIZE	117

iii

Accession For	
NTIS GTR&I	<input checked="" type="checkbox"/>
DDC TAB	<input type="checkbox"/>
Unannounced	<input type="checkbox"/>
Justification	
By _____	
Distribution/ _____	
Availability _____	
Dist	Available for special

LIST OF TABLES

<u>Table No.</u>		<u>Page No.</u>
2.1	REPRESENTATIVE REACTOR CONCEPTS	3
2.2	IMPURITY CONCENTRATIONS EQUIVALENT TO 1 PPM BORON	6
2.3	CALCULATED TOLERANCE LEVELS FOR GRAPHITE IMPURITIES	7
2.4	MINIMUM BORON (EQUIVALENT) CONCENTRATION TO INHIBIT REACTOR OPERATION WITH ENRICHED FUEL	10
2.5	FULL-POWER YEARS REQUIRED TO REDUCE BORON IMPURITY TO 10% OF THE INITIAL VALUE	11
3.1	LOW-POWER REACTOR CHARACTERISTICS	23
3.2	MEDIUM-POWER REACTOR CHARACTERISTICS	27
3.3	HIGH-POWER REACTOR CHARACTERISTICS	29
4.1	REACTIVITIES AND OPTIMUM LATTICE SPACING IN THE LOW POWER AIR-COOLED REACTOR CONCEPT	41
4.2	RATE OF PLUTONIUM PRODUCTION IN THE LOW POWER AIR-COOLED REACTOR	44
5.1	REACTIVITIES AND OPTIMUM LATTICE SPACING IN THE MEDIUM POWER CO ₂ -COOLED REACTOR CONCEPT	60
5.2	RATE OF PLUTONIUM PRODUCTION IN THE MEDIUM POWER CO ₂ -COOLED REACTOR	62
6.1	REACTIVITY EFFECTS FOR THE REFERENCE WATER-COOLED REACTOR	79
6.2	COMPARISON OF NUCLEAR CHARACTERISTICS FOR DIFFERENT FUEL ENRICHMENTS IN THE WATER- COOLED REACTOR	80
7.1	NEUTRON BURNOUT OF IMPURITIES	99
8.1	SUMMARY OF COMMERCIAL GRAPHITE PROPERTIES	107

LIST OF ILLUSTRATIONS

<u>Figure No.</u>		<u>Page No.</u>
2.1	Lattice optimization curves for the three reference design reactors with natural uranium.	13
2.2	Reactivity variation with fuel burnup, with natural uranium.	14
2.3	Burnup dependence of plutonium production rates.	15
2.4	Plutonium production rates in reference design reactors with natural uranium fuel.	16
2.5	Percentage non-fissile content in plutonium produced in the reference design reactors (natural uranium fuel).	17
2.6	Relationship between fuel burnup in Mwd/mtU and equivalent full power days of operation.	18
2.7	Uranium feed requirements as a function of fuel burnup with natural uranium fuel.	19
2.8	Fuel enrichments required for various levels of neutron-absorbing impurities (as boron).	20
3.1	Cross section of cell for low-power reactor.	36
3.2	Cross section of cell for medium-power reactor.	37
3.3	Cross section of cell for high-power reactor.	38
4.1	Lattice optimization of k_{∞} versus carbon-to-uranium atom ratio.	46
4.2	Lattice optimization of k_{eff} for several graphite densities (natural uranium fuel).	47

LIST OF ILLUSTRATIONS (Continued)

<u>Figure No.</u>		<u>Page No.</u>
4.3	Variation in reactivity with fuel burnup for natural uranium fuel (low power, air-cooled reactor).	48
4.4	Lattice optimization of k_{eff} for fuel of various enrichments (low power, air-cooled reactor).	49
4.5	Total and fissile plutonium production in the air-cooled reactor as a function of fuel burnup.	50
4.6	Dependence of the percentage of non-fissile plutonium isotopes on fuel burnup (low power, air-cooled reactor).	51
4.7	Plutonium isotopics as a function of burnup for natural uranium fuel in the air-cooled reactor.	52
4.8	Dependence of plutonium production rate on discharge fuel burnup in the 30 Mw air-cooled reactor.	53
4.9	Lattice optimization in the air-cooled reactor for various levels of graphite impurities (as boron) with natural uranium fuel.	54
4.10	Lattice optimization for various levels of graphite impurities (as boron) for 1.2% enriched fuel.	55
4.11	Variation in k_{eff} with graphite impurity levels for fuel of natural, 1.2% and 3.2% enrichment (Mg clad, air-cooled reactor).	56
4.12	Relationship between enrichment required and impurity level in graphite, for the air-cooled reactor.	57

LIST OF ILLUSTRATIONS (Continued)

<u>Figure No.</u>		<u>Page No.</u>
5.1	Lattice optimization of k_{∞} versus carbon-to-uranium atom ratio.	64
5.2	Lattice optimization of k_{eff} for several graphite densities (natural uranium fuel), CO_2 -cooled reactor.	65
5.3	Variation in reactivity with fuel burnup for burnup for natural uranium fuel (medium power, CO_2 -cooled reactor).	66
5.4	Lattice optimization of k_{eff} for fuel of various enrichments (medium power, CO_2 reactor).	67
5.5	Total and fissile plutonium production in the CO_2 -cooled reactor as a function of fuel burnup.	68
5.6	Dependence of the percentage of non-fissile plutonium isotopes on fuel burnup (medium power, CO_2 -cooled reactor).	69
5.7	Plutonium isotopics as a function of fuel burnup for natural uranium in the CO_2 -cooled reactor.	70
5.8	Dependence of plutonium production rate on discharge fuel burnup in the 250 Mw CO_2 -cooled reactor.	71
5.9	Lattice optimization in the CO_2 -cooled reactor for various levels of Graphite impurities (as boron) with natural uranium fuel.	72
5.10	Lattice optimization in the CO_2 -cooled reactor for various levels of graphite impurities (as boron) for 1.2% enriched fuel.	73
5.11	Variation in k_{eff} with graphite impurity levels for fuel of natural, 1.2% and 3.2% enrichment (CO_2 -cooled reactor).	74

LIST OF ILLUSTRATIONS (Continued)

<u>Figure No.</u>		<u>Page No.</u>
5.12	Relationship between enrichment required and impurity level in graphite for the CO ₂ -cooled reactor.	75
6.1	Lattice optimization for natural-uranium-fueled, water-cooled reactor.	83
6.2	Reactivity variation with fuel burnup for reference natural uranium-fueled, water-cooled reactor (pitch = 22.5 cm, graphite density = 1.65 g/cm ³).	84
6.3	Lattice optimization of k_{eff} for fuel of various enrichments (high-power, water-cooled reactor).	85
6.4	Variation in reactivity with burnup for low-enriched uranium-fueled, water-cooled reactor.	86
6.5	Plutonium production variation with design burnup for low-enriched uranium-fueled, water-cooled reactor.	87
6.6	Specific plutonium production for low-enriched uranium-fueled, water-cooled reactor.	88
6.7	Plutonium isotopic composition in low-enriched uranium-fueled, water-cooled reactor.	89
6.8	Reactivity variation with pitch for different graphite densities for natural natural-fueled, water-cooled reactor.	90
6.9	Reactivity variation with pitch for different graphite densities for 1.2%-enriched uranium-fueled, water-cooled reactor.	91
6.10	Reactivity variation with pitch for different graphite densities for 3.2% enriched uranium-fueled, water-cooled reactor.	92

LIST OF ILLUSTRATIONS (Continued)

<u>Figure No.</u>		<u>Page No.</u>
6.11	Variation in optimum fuel cell pitch with graphite density for water-cooled reactor.	93
6.12	Variation in optimum fuel cell pitch with fuel enrichment for water-cooled reactor.	94
6.13	Reactivity variation with pitch for various boron impurity levels; 1.2%-enriched uranium fuel, water-cooled reactor.	95
6.14	Reactivity variation with graphite impurity level for fuel of natural, 1.2% and 3.2% enrichment (water-cooled reactor).	96
6.15	Relationship between enrichment required and impurity level in graphite for the water-cooled reactor (pitch = 22.5 cm).	97
7.1	Neutron burnout of boron in the low power air-cooled reactor.	100
7.2	Neutron burnout of boron in the medium power CO ₂ -cooled reactor.	101
7.3	Neutron burnout of boron in the high power water-cooled reactor.	102
8.1	Graphite manufacturing process.	114
8.2	Packing of a normal Acheson furnace.	115
8.3	Packing of an Acheson furnace for gas purification.	116
9.1	Change in initial reactivity with reactor design power level.	118

1.0 INTRODUCTION

The work reported here was performed for the United States Arms Control and Disarmament Agency under Contract AC9NX707, Task Order 79-01. The objective of the study was to examine the feasibility of using commercially available graphite in small production reactors. Three different-size reactors, each with a different coolant, were investigated, and an assessment was made of the effect of parasitic neutron-absorbing material in the graphite, either as naturally-occurring impurities or as intentionally-added spikants. In addition, a brief survey of methods of manufacturing and of purifying graphite was performed.

2.0 SUMMARY AND CONCLUSIONS

2.1 Analytical Bases and Procedures

Three types of graphite-moderated reactors were selected as representative of possible production reactors. These concepts, which were derived from concepts that have been previously built and operated, are summarized in Table 2.1.

For each representative reactor concept, the optimum fuel channel pitch--the one giving the greatest reactivity--was determined by a series of zero-dimensional unit cell calculations using the NULIF computer code.¹ Once the optimum fuel channel pitch has been determined, fuel burnup and isotopic analyses were performed. Similar calculations were performed for several assumed graphite densities, ranging from 1.50 g/cm³ to 1.75 g/cm³, and for various assumed levels of neutron-absorbing impurities in the graphite (represented analytically by boron-10.)

2.2 Calculations with Pure Graphite

Figure 2.1 shows the optimization curves (k_{eff}) for the three reactor concepts at various values of cell pitch, with pure graphite. From these curves, the optimum fuel element spacings (square pitch) at a nominal graphite density of 1.65 g/cm³ are 21.2 cm for the air-cooled concept, 23 cm for the CO₂-cooled concept and 22.5 cm for the water-cooled concept. For higher graphite densities, the maximum reactivity (k_{eff}) is slightly higher and occurs at a smaller lattice pitch.

With irradiation, the reactivity initially decreases sharply as the fission products Xe and Sm appear, then increases as plutonium is produced, reaching a maximum value at about 1000 Mwd/mtU or slightly higher. Beyond 1000 Mwd/mtU, the

¹NULIF is a multigroup spectrum analysis and cell homogenization code, with a fuel depletion option for burnup and isotopic analysis. Details of the code are described in Babcock & Wilcox Report BAW-246, August 1976

Table 2.1 REPRESENTATIVE REACTOR CONCEPTS

Thermal power, MW	30	250	400
Coolant	Air	CO ₂	H ₂ O
Number of fuel channels	1418	1892	2155
Moderator and reflector	Graphite	Graphite	Graphite
Total graphite, mt	989	1550	2260
Fuel type	Nat. U-metal	Nat. U-metal	Nat. U-metal
Cladding	Mg or Al	Mg	Al
Base plants, previously con- structed and operated	Brookhaven, Marcoule G1	Calder Hall Marcoule G2	Hanford, Soviet Production
Approximate Pu production rate, kg/full-power yr ¹	10	80	135
Uranium require- ment, mt/full- power yr ^{1,2}	94	147	274
Fuel burnup, Mwd/mtU ¹	115	620	520
Fissile Pu content ^{1,3}	99.2	95.5	96.2

¹Assuming annual fuel cycle.

²Also equal to the total loading and to the quantity of uranium to be reprocessed in recovery of the plutonium.

reactivity will again decrease as fission products accumulate and fissile material is depleted. Figure 2.2 illustrates these variations for the three reactor concepts (nominal cases) at the optimum lattice pitches.

Normally, production reactors are operated at comparatively low fuel burnups in order to maximize the net quantity produced and to minimize the concentration of non-fissionable plutonium isotopes (Pu-240 and -242). Figure 2.3 summarizes the quantities of plutonium produced in each of the three reference reactor concepts as a function of the fuel burnup. The same data is also given in Fig. 2.4, which shows the kilograms of plutonium produced for each thermal megawatt of reactor power as a function of the discharge fuel burnup. The decrease in net quantity of plutonium produced is due to the in-situ burning of plutonium as fuel burnup increases. Due to differences in fuel specific power between the three reactor concepts, a full-power year of operation results in different fuel burnups in each of the reference reactors: the burnup is about 115 Mwd/mtU for the air-cooled concept, 620 Mwd/mtU for the CO₂-cooled concept and 520 Mwd/mtU for the water-cooled concept. Higher fuel burnups could be achieved with longer operating intervals, but only with increasing accumulation of non-fissile isotopes in the discharge fuel. Figure 2.5 illustrates the increasing percentage of non-fissile plutonium isotopes with increasing fuel burnup for the three reactor concepts.

Figure 2.6 shows the relationship between fuel burnup in Mwd/mtU and full-power days of operation. It is evident that to achieve relatively high fuel burnup in the 30 Mw air-cooled reactor, very long operating periods will be necessary (e.g., 8.6 full-power years for 1000 Mwd/mtU). Operation periods in the CO₂-and H₂O-cooled reactors are appreciably shorter because of the higher fuel specific power in these reactors. As a corollary, the quantity of natural uranium feed decreases significantly with increasing fuel burnup, as shown in Fig. 2.7.

2.3 Effect of Graphite Impurities

The presence of neutron-absorbing impurities in the graphite, whether naturally occurring or intentionally added, reduces reactivity and shifts the optimum reactivity to a smaller lattice spacing. Boron is the most significant impurity from the standpoint of both poisoning effect and difficulty of removal. For analytical purposes, the

criticality calculations were performed with various concentrations of boron assumed to simulate the presence of neutron-absorbing impurities. Table 2.2 lists the concentrations of various commonly-occurring impurities that are equivalent to 1 ppm boron, together with the incremental change in effective graphite 2000 m/s cross-section (reference $\sigma_c = 3.39$ mb) by the presence of 1 ppm of the given impurity. It may be noted that of the impurities listed only gadolinium exceeds boron in neutron poisoning effect.

The reference reactors, at the design optimum lattice spacing, can accommodate impurities of the order of 1 to 2 ppm boron or equivalent and retain sufficient reactivity to perform as designed. Table 2.3 lists the calculated tolerance levels for graphite impurities, including both the maximum permissible level for normal operation and the minimum level necessary to inhibit operation

Where the concentration of impurities in the graphite is marginal for operation with natural uranium, there are several measures that could be taken to gain a small amount of additional reactivity thereby possibly enabling the reactor to operate. These include the following:

- 1) Reduce the design lattice spacing to minimize the neutron poisoning effect of impurities.
- 2) Operate at reduced power level to minimize Xe poisoning until an appreciable reactivity increase occurs at the higher burnup values from the production of plutonium (see Figure 2.2).
- 3) Use some fuel elements of higher enrichment (spiked) to operate until plutonium grows in with its consequent reactivity addition (see Figure 2.2)
- 4) In conjunction with (2) and/or (3) above, develop a sophisticated fuel management scheme (shuffling) to realize the benefit of higher reactivity as plutonium is produced and thereby enable continued operation.

Evaluation of these factors is beyond the scope of the present study. However, it is anticipated that the maximum benefit which could be realized would be of the order of 1% in k_{eff} corresponding to approximately 0.5 ppm equivalent boron.

AC9NX707

Table 2.2 IMPURITY CONCENTRATIONS EQUIVALENT TO 1 PPM BORON

<u>Material</u>	<u>σ_a (2200 m/s)</u>	<u>Concentration (ppm) Equivalent to 1 ppm Boron</u>	<u>σ_c/ppm (millibarns)</u>
Boron	749.6	1 (Reference)	.83
Silicon		12,350	.00007
Hydrogen	.332	210	.0040
Sodium	.400	3,981	.00021
Sulfur	.51	4,627	.00019
Calcium	.43	6,453	.00013
Aluminum	.23	8,124	.00010
Iron	2.55	1,516	.00055
Titanium	6.1	544	.0015
Vanadium	5.04	700	.0012
Molybdenum	2.65	2,508	.00033
Dysprosium	930	12	.07
Europium	4600	2.3	3.6
Gadolinium	30660	.36	2.34
Samarium	5800	1.8	.46
Chlorine	33	74	.011
Lithium	71	6.8	.123
Cadmium	2390	3.3	.255

Table 2.3 CALCULATED TOLERANCE LEVELS FOR GRAPHITE IMPURITIES

Case	Maximum for Normal Operation		Minimum to Inhibit Operation	
	Boron Equiv. ppm	eff σ_a Graphite*	Boron Equiv. ppm	eff σ_a Graphite*
Air-cooled Ref. Design				
1.5 g/cm ³ graphite	1.95	5.01	2.35	5.34
1.65 g/cm ³ graphite	2.22	5.23	2.59	5.54
1.75 g/cm ³ graphite	2.35	5.34	2.76	5.68
1.65 g/cm ³ graphite (w Al clad)	1.88	4.95	2.26	5.27
CO ₂ -cooled Ref. Design				
1.5 g/cm ³ graphite	1.60	4.72	2.39	5.38
1.65 g/cm ³ graphite	1.81	4.89	2.60	5.55
1.75 g/cm ³ graphite	1.91	4.98	2.74	5.67
1.65 g/cm ³ graphite (@ 20.3 cm pitch)	2.22	5.23	3.20	6.05
H ₂ O-cooled Ref. Design				
1.5 g/cm ³ graphite	0.82	4.07	1.68	4.79
1.65 g/cm ³ graphite	0.83	4.08	1.70	4.80
1.75 g/cm ³ graphite	0.85	4.10	1.72	4.82

*effective cross-section at 2200 m/s

Assuming an uncertainty of 0.5 ppm boron equivalent (corresponding to 1% uncertainty in calculated k_{eff} values), the minimum equivalent boron concentration to inhibit operation of any of the reactors, with natural uranium, is approximately 3.7 ppm (σ a graphite @ 2200 m/s of 6.5 mb). Even allowing for intentional reactor design at a reduced lattice spacing to minimize the effect of impurity absorption, a boron equivalent of 5 ppm (σ a graphite of 7.5 mb @ 2200 m/s) would be sufficient to prevent the graphite from being useful as a moderator in natural uranium reactors, with adequate margins for all uncertainties. Many commercially available graphites (where measured) normally contain approximately 1 to 3 ppm boron equivalent, and therefore, could be used to build reactors of the type considered here, at least the air- or CO₂-cooled types

2.4 Enriched Fuel

Because the optimum lattice spacing decreases with impurity concentration, the parasitic neutron absorption of impurities can be minimized by decreasing the design lattice pitch. However, this would be of limited practical use, for it requires the use of enriched fuel to obtain sufficient reactivity, and after the impurities are burned out (by neutron absorption) the pitch would no longer be the optimum for maximum reactivity. Nevertheless, there would be an advantage in designing the reactors at slightly less than optimum pitch (by 1 or 2 cm) in order to both minimize the reactivity effect of impurities and to increase plutonium production slightly (as a result of the higher resonance capture of neutrons in U-238). Since a greatly reduced lattice pitch (optimized for a high impurity level) would also entail a commitment to continue operation with enriched fuel, this is not believed to be a logical approach, especially in view of the ease with which graphite can be purified.

The effect of enriched fuel is to increase the optimum pitch and to reduce the amount of plutonium produced. If the objective were to use low-enriched fuel initially, until the impurity level was reduced by neutron burnout, the design pitch selected would probably still be the optimum for natural uranium. Furthermore, the decrease in optimum pitch with impurity level, and the relative ease of purifying graphite, would argue against the desirability of using a lattice spacing significantly different from the optimum for natural uranium.

For the reference cases, calculations were made for several values of enrichment as a function of the assumed boron content of the graphite. Figure 2.8 and Table 2.4 shows the enrichments required to obtain an initial k_{eff} of 1.0 for various amounts of boron impurity. This initial reactivity criterion ($k_{eff} = 1.0$) would actually not permit the reactor to operate, since, if started, it would be immediately shut down by Xe and Sm fission product poisons. Thus Fig. 2.8 illustrates the approximate minimum content of boron (or equivalent) necessary to inhibit reactor operation for a given enrichment in the fuel. Higher enrichments could possibly be utilized, although above a boron concentration in the range of 50-100 ppm, B_4C particle inclusions would be expected to be formed in the graphite, affecting adversely its mechanical and physical properties.

2.5 Poison Burnout Under Irradiation

Impurities initially present in the graphite will be burned out under irradiation at a rate that depends upon the neutron flux and the effective cross-section of the isotope of significance in the impurity. In general, the fraction of an impurity remaining after an irradiation period of time t is $e^{-(\sigma^a \phi) t}$, where σ^a is the effective absorption cross-section of the significant isotope and ϕ is the effective neutron flux. With natural uranium fuel, a reduction of the boron impurity of graphite to 10% of its initial value would require 11.7 full-power years of operation in the air-cooled reactor. At higher fuel enrichments (because of the lower flux and changes in the neutron spectrum), significantly longer periods of time would be required. Table 2.5 summarizes the time required to reduce the boron impurity to 10% of its initial value in the three reference reactors.

The significant isotope of boron, B-10, has a large absorption cross-section, 3860 barns at 2200 m/s. With the exception of some of the rare earths, the impurities normally occurring in graphite (see Table 2.2) have cross-sections sufficiently low that burnout over the lifetime of the reactor is essentially negligible. Some of the rare earths have isotopes whose cross-sections are comparable to or greater than that of boron-10. For example, the significant isotope of europium (Eu-151) has a cross-section comparable to boron-10, while gadolinium has two significant isotopes (Gd-155 and Gd-157), both of whose cross-sections (58,000 and 240,000 b at 2200 m/s) are significantly higher than that of boron-10. As a result, any gadolinium impurity would

AC9NX707

Table 2.4 MINIMUM BORON (EQUIVALENT) CONCENTRATION TO INHIBIT
REACTOR OPERATION WITH ENRICHED FUEL

	Air-Cooled		CO ₂ -Cooled		H ₂ O-Cooled	
	ppm B(2)	Reference Design graphite(3)	ppm B(2)	Reference Design graphite(3)	ppm B(2)	Reference Design graphite(3)
Natural U Fuel	2.59	5.54	2.60 (3.2)(4)	5.55 (6.05)(4)	1.70	4.80
1.2% Enriched Fuel	15.8	16.5	16.0 (19.6)	16.7 (19.7)	15.0	15.9
3.2% Enriched Fuel	49.8	44.8	49.7 (68.7)	44.7 (60.48)	46.5	42.0

1) Reference design at 1.65 g/cm³ graphite density and optimum lattice spacing for pure graphite with natural uranium.

2) or equivalent.

3) cross-section in millibarns.

4) Parentetical values for CO₂-cooled reactor at 20.3 cm lattice spacing.

AC9NX707

Table 2.5 FULL-POWER YEARS REQUIRED TO REDUCE BORON
IMPURITY TO 10% OF THE INITIAL VALUE

	<u>Air-Cooled time, years</u>	<u>CO₂-Cooled time, years</u>	<u>H₂O-Cooled time, years</u>
Natural U	11.7	2.0	2.3
1.2% Enrichment	16.9	3.0	3.4
3.2% Enrichment	26.9	5.4	4.8

burn out faster than boron; i.e., months rather than years. Therefore, except for a few very high cross-section impurities, burnout by irradiation does not appear to be an attractive method of purifying graphite, requiring time periods of the order of years to reduce boron impurity levels by a factor of 10. The relative ease of purifying graphite by conventional means is good argument against depending upon neutron burnout to purify the graphite, unless the impurity is a very high cross-section material such as gadolinium

2.6 Commercial Graphites

A review of the reported characteristics of commercial grades of graphite reveals that the impurity levels in some grades are sufficiently low to permit their use in reactors. In some cases, the nominal content of boron and other neutron absorbers is not of commercial interest and therefore has not been reported. However, the graphite vendors contacted indicated that they would anticipate the boron content to normally be less than 5 ppm and probably of the order of 1 to 3 ppm. "Nuclear grade" graphites are unique, primarily because the boron content is measured and limits on boron as well as other poisoning impurities are imposed in the specifications, but other grades may also be of low equivalent boron content.

Production of graphite appears to be a relatively simple and inexpensive procedure, although details of the processes remain proprietary to the various vendors. Furthermore, additional purification of commercial graphite, in furnaces of the Acheson type, does not appear to present any formidable difficulties. The graphite vendors contacted were not aware of any impurity, naturally-occurring or intentionally added, that would be virtually impossible to remove. In their opinion, boron is probably the most difficult impurity to remove, although it is readily removed in a halogen gas atmosphere (modified Acheson type furnace). Therefore, intentional spiking of commercial graphite with a neutron-absorbing impurity does not appear to be an effective way of preventing its use as a reactor moderator. If spiking is used, however, boron (or the enriched boron-10 isotope) would be the most attractive spikant because of the difficulty of removal and the nuclear characteristics. Gadolinium might be another possible spikant, but the very high cross-section would make it easier to purify the graphite by neutron burnout.

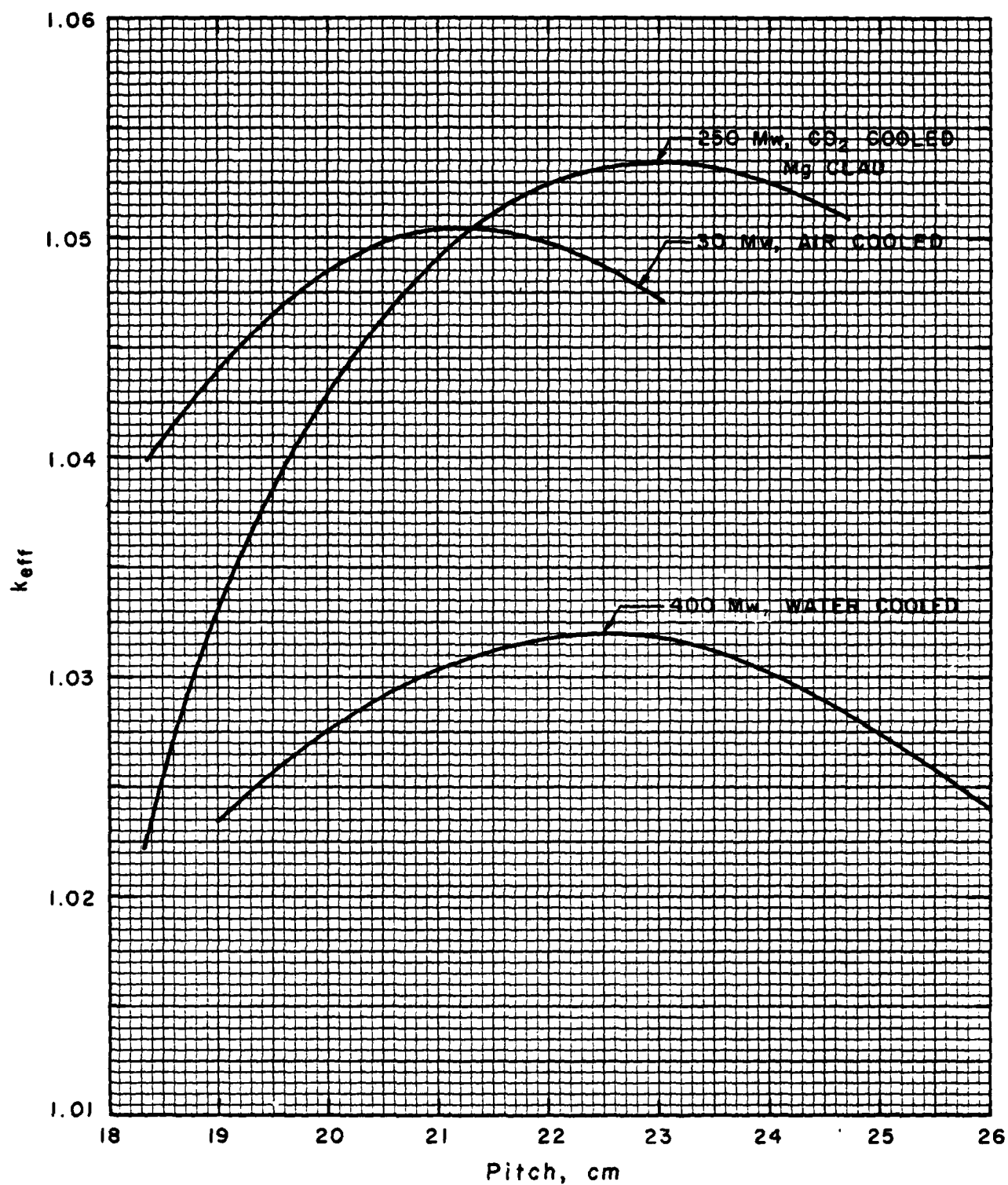


Fig. 2.1 Lattice optimization curves for the three reference design reactors with natural uranium.

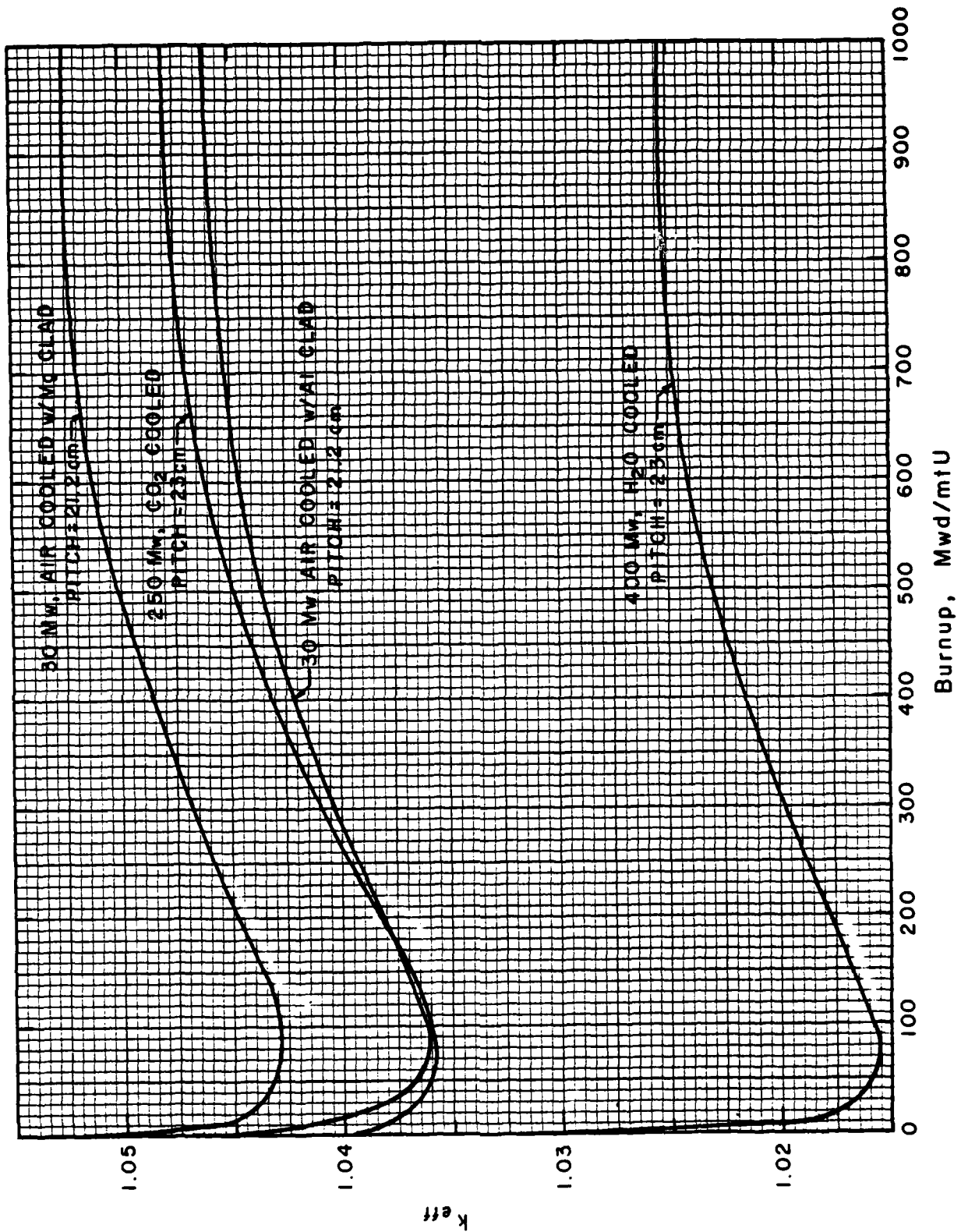


Fig. 2.2 Reactivity variation with fuel burnup, with natural uranium.

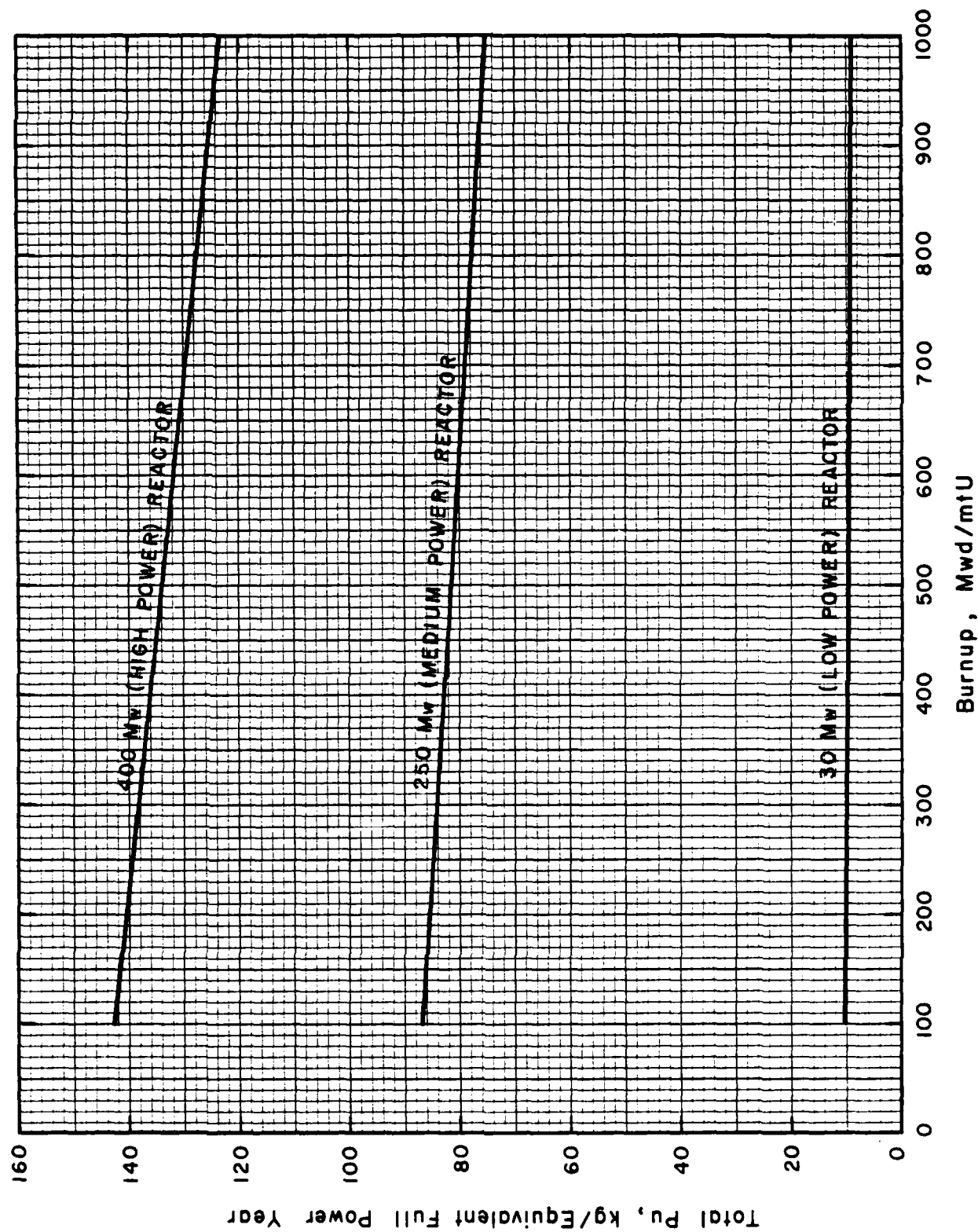


Fig. 2.3 Burnup dependence of plutonium production rates.

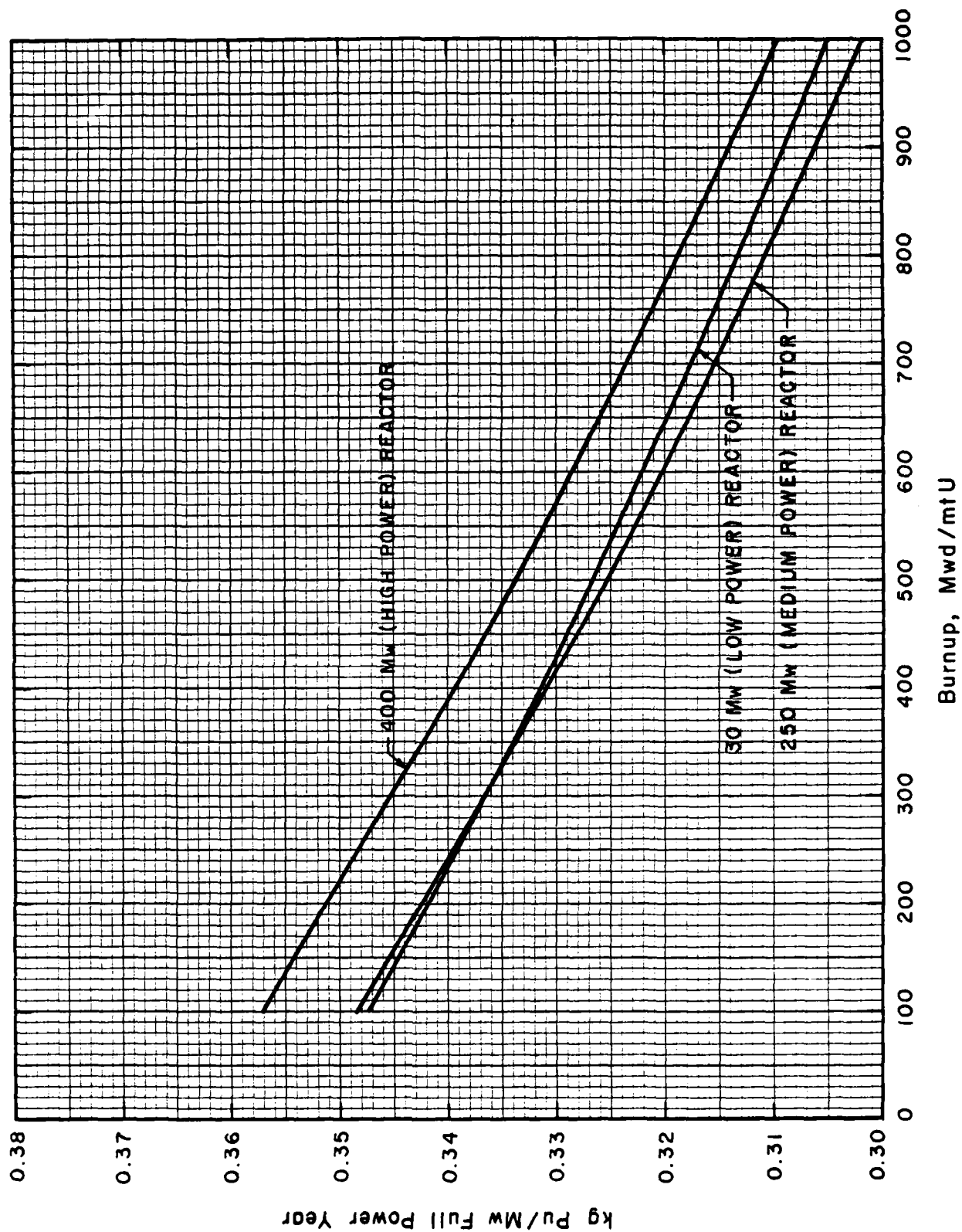


Fig. 2.4 Plutonium production rates in reference design reactors with natural uranium fuel.

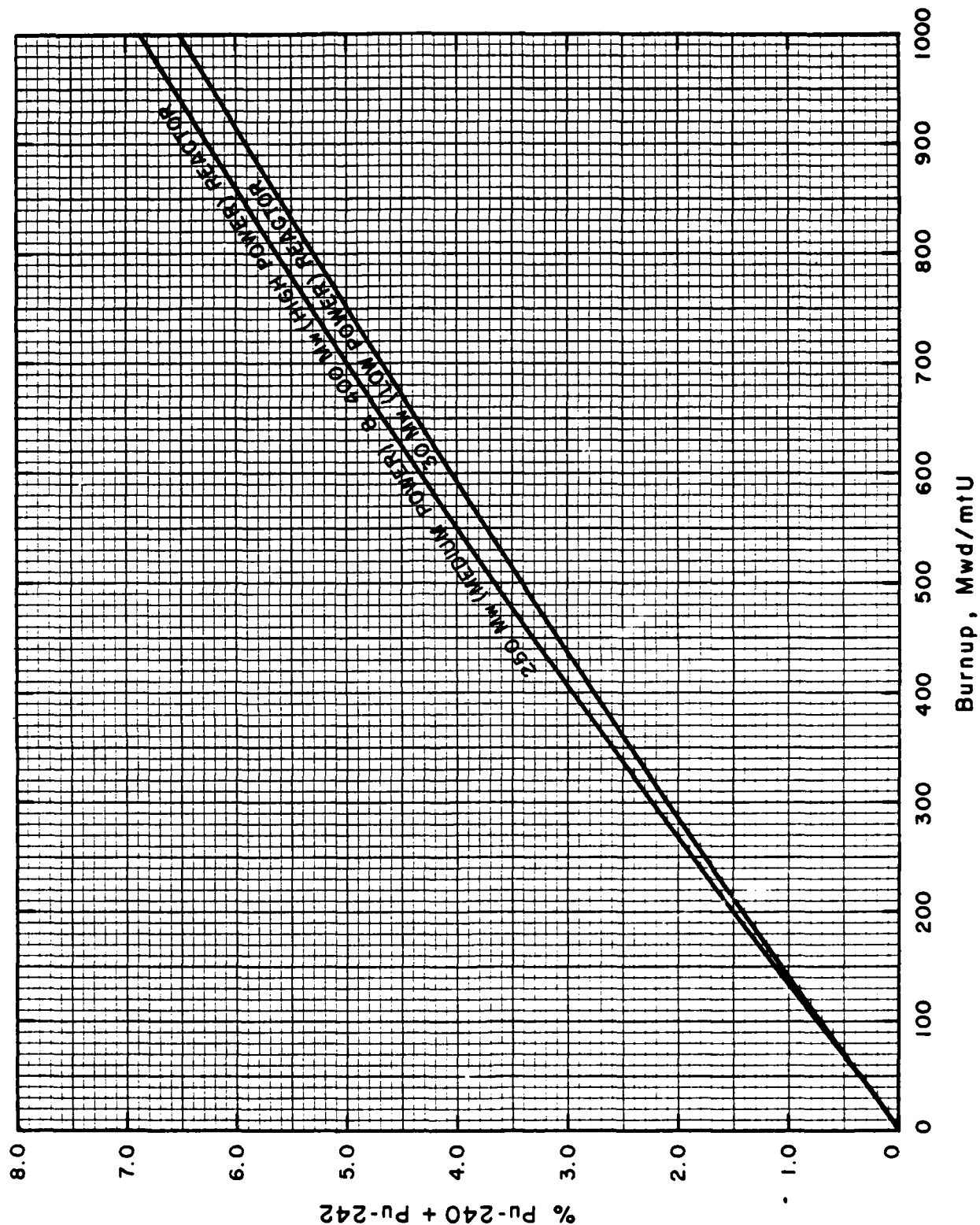


Fig. 2.5 Percentage non-fissile content in plutonium produced in the reference design reactors (natural uranium fuel).

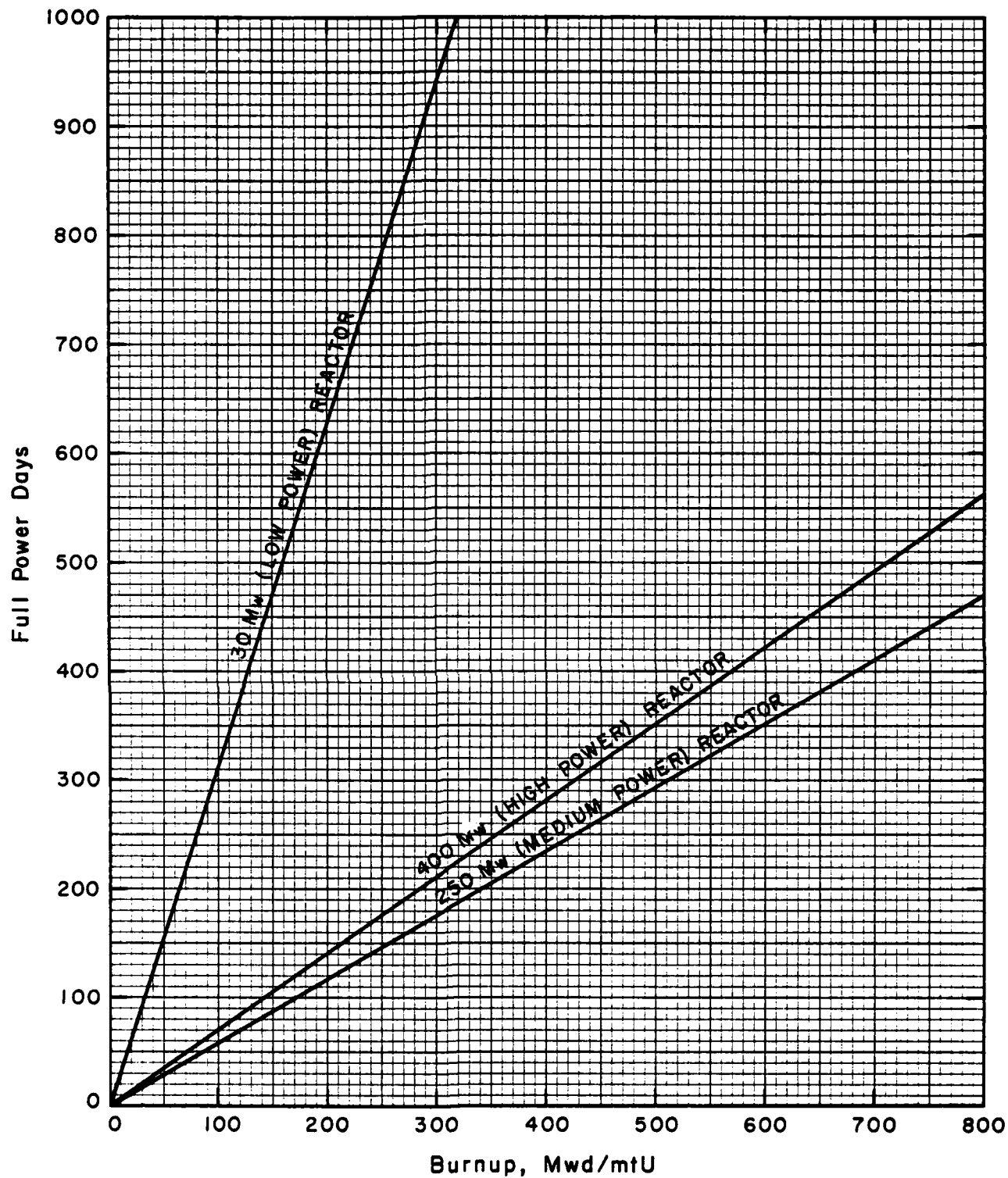


Fig. 2.6 Relationship between fuel burnup in Mwd/mtU and equivalent full power days of operation.

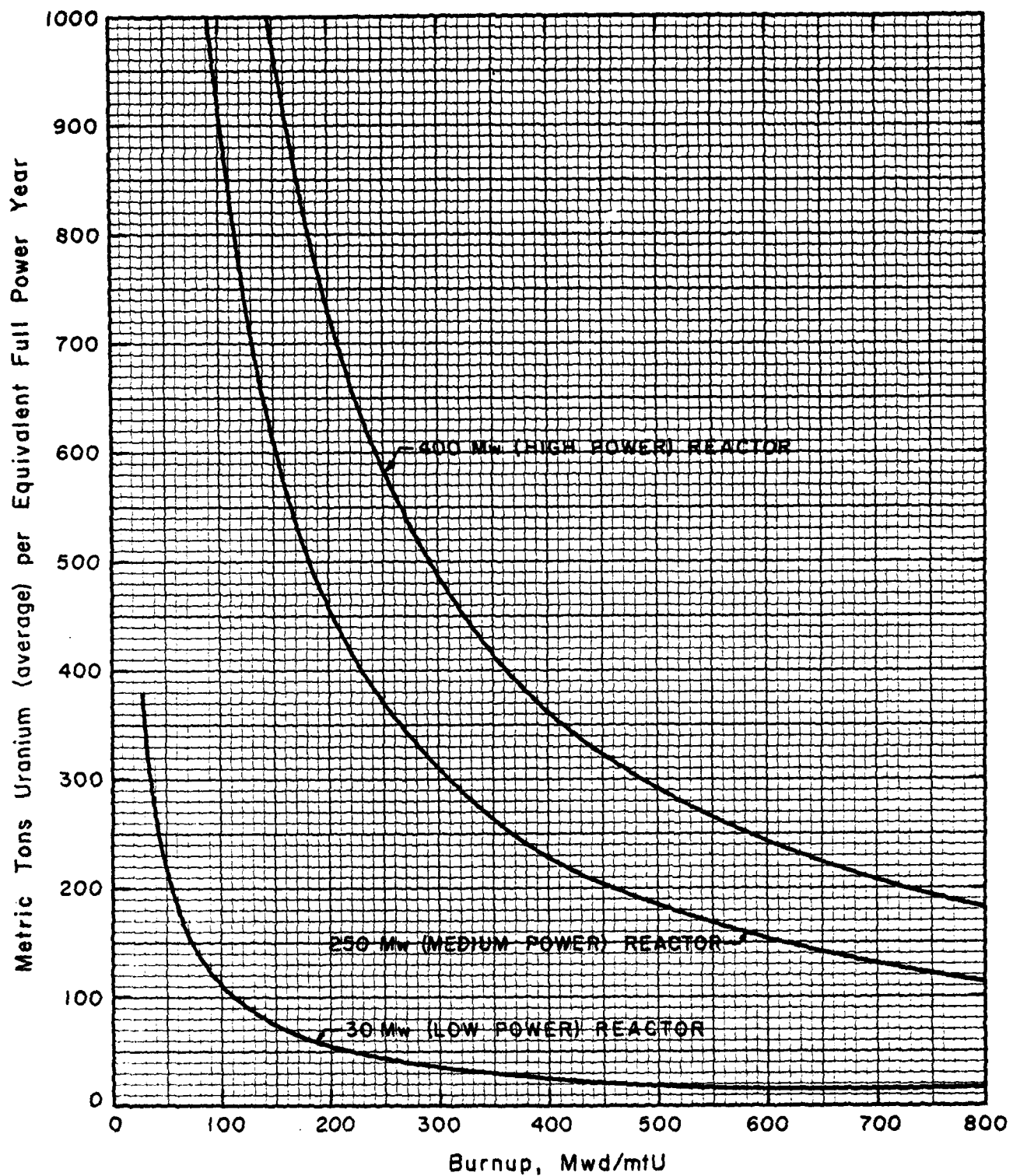


Fig. 2.7 Uranium feed requirements as a function of fuel burnup with natural uranium fuel.

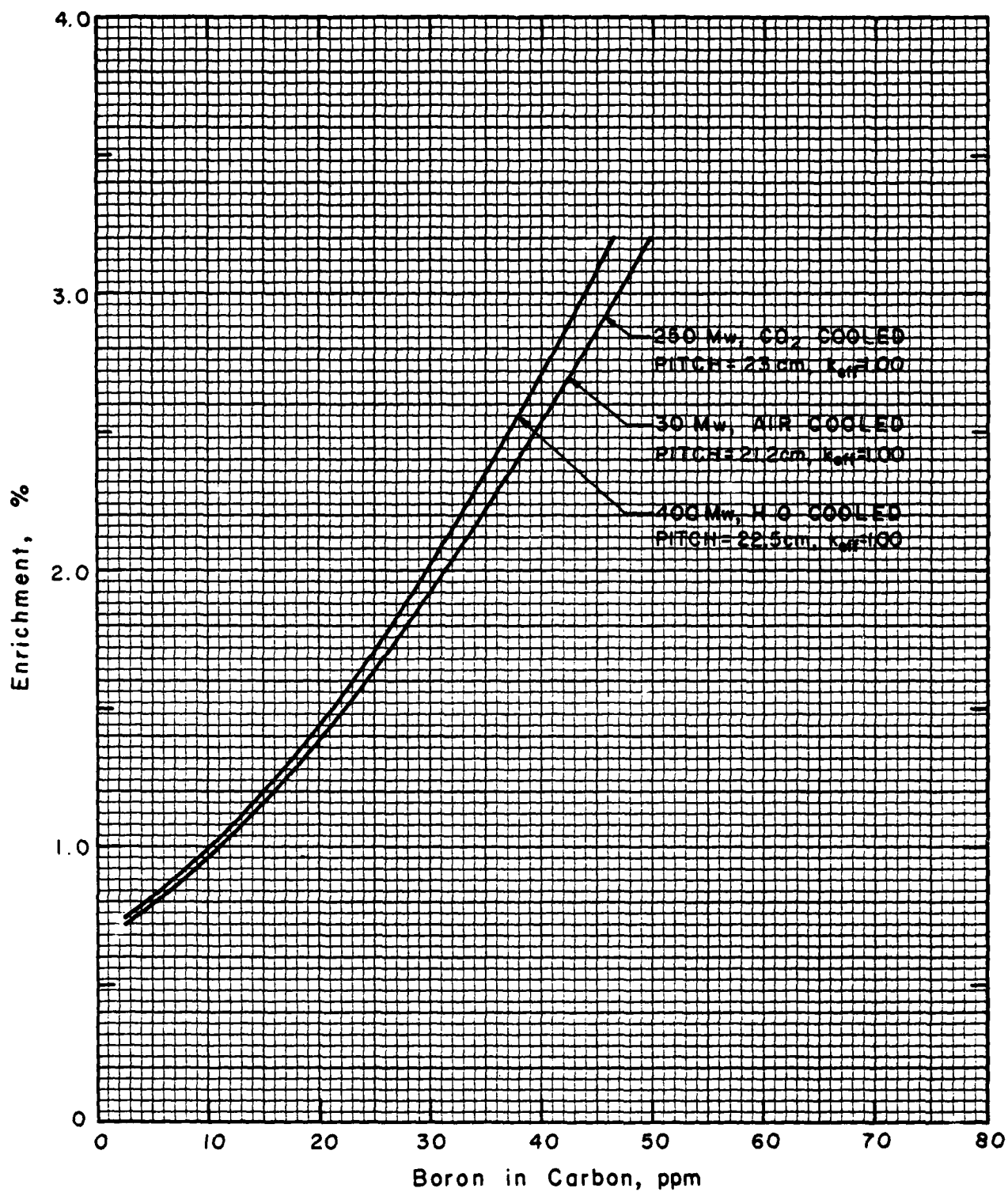


Fig. 2.8 Fuel enrichments required for various levels of neutron-absorbing impurities (as boron).

3.0 REFERENCE REACTOR CONCEPTS

The reactor designs chosen as models for the low-, medium-, and high-power (10, 250, and 400 Mw(t) reactor concepts are cooled by air, carbon dioxide, and water, respectively. The moderator in each reactor is graphite, and the fuel is natural uranium metal.

For the low-power, air-cooled reactor, the Brookhaven Graphite Research Reactor (BGRR) and the French G1 reactor were selected as models. Construction of the BGRR, located at Brookhaven National Laboratories, Upton, New York, began in the fall of 1947, and the reactor attained first criticality in August, 1950. Full power operation at 28 Mw(t) on natural uranium fuel occurred in April 1951. The reactor was designed primarily for research purposes, with isotope production a secondary objective. In 1957-1958, it was converted to use enriched fuel. The French G1 reactor at the Marcoule Plutonium Production Center was modeled after the Brookhaven reactor, but incorporated several advanced features in its design. Notable among these was the specification of magnesium fuel cladding in place of the aluminum cladding adopted early in the design of the Brookhaven reactor.² Construction of G1 commenced in May, 1954, initial criticality was in January, 1956, and the full design power of 38 Mw(t) was reached in September, 1956. The principal uses of the reactor are for research and plutonium production. After the design of the reactor had been completed, heat-exchange equipment and an electric-power generating system were added: the overall design was not optimized, and the facility consumes more electric power (10.2 Mw) than it produces (1.7 Mw).

The medium-power CO₂-cooled reactor design used in the study is based on the Calder Hall reactors in England. In September, 1950, a conference was held at the Atomic Energy Research Establishment, Harwell, to discuss the possibility of using natural uranium fuel for the simultaneous production of power and plutonium. The participants in the conference recommended a design study, which started at Harwell in January, 1951. By January, 1953, the general design for a 150 Mw(t) reactor and steam plant to generate 35 Mw net of electric power had been completed. At that point, the Production Establishment at Risley undertook the detailed

²The low neutron capture cross-section of magnesium became known in 1948.

design and construction, giving greater emphasis to plutonium production. Construction of the four-reactor Calder Hall station began in August, 1953, and the first unit reached initial criticality in May, 1956. Full design power of 180 Mw(t) was attained in October, 1956, and the power of each unit was subsequently raised to 225 Mw(t). At that thermal power level,³ each unit produce 51 Mw of electric power, 10 Mw of which is consumed by the unit itself.

The high-power, water-cooled reactor analyzed in this study derives its general design from the production reactors at Hanford, Washington, and incorporates features selected on the basis of experience gained in the analysis of other graphite/water systems. Development of the Hanford reactors began in 1942, and construction of the cooling water facilities for the first reactor started in August, 1943. The initial power run of the first Hanford reactor commenced in September, 1944.

The following subsections present descriptions of the reference designs selected for the three reactors analyzed in this study. Also a discussion is given of significant temperature effects in graphite.

3.1 The Air-Cooled Reactor

The low-power, air-cooled reactor, like the other systems considered here, is a large graphite structure pierced by process channels that contain the uranium fuel. Cooling fluid passes through the process channels, flowing over the fuel elements to remove their heat and providing the principal heat-removal mechanism for the energy deposited in the moderator graphite. Basic characteristics of the reactor are listed in Table 3.1.

The 30-Mw(t) core is cooled by approximately 275,000 standard cubic feet per minute (SCFM) of filtered air that enters the reactor at a nominal temperature of 18°C. Outlet coolant temperature is 135°C, and the hot air is discharged, through a stack, to the atmosphere in the simplest system. Recovery of energy from the heated air would require an air-to-water heat exchanger, flash boilers, a turbine-generator set, a condenser, etc. The low temperature and pressure of the reactor coolant air could make the equipment for electric power generation very costly, and the process would be inefficient, as it is in the G1 facility.

³Many years later, the reactors were de-rated slightly because of materials-compatibility problems.

AC9NX707

Table 3.1 LOW-POWER REACTOR CHARACTERISTICS

Type	Graphite moderated, open-cycle air cooled
Thermal power, Mw	30
Core	
Active length, m	5.7
Active diameter, m	8.8
Power density, w/cm ³	0.087
Control	B ₄ C rods
Refueling	Off-line
Moderator	
Material	Graphite
Density, g/cm ³	1.65 (nominal)
Average temperature, °C	200
Process channel holes	
Number	1418
Diameter, mm	67.8
Square pitch, mm	212
Approx. total weight, mt	551
Reflector	
Material	Graphite
Thickness, cm	80
Approx. total weight, mt	451
Coolant	
Material	Air
Nominal pressure	Atmospheric
Inlet/Outlet temperature, °C	18/135
Fuel	
Material	Natural uranium metal
Geometry	Cylindrical slugs
Slug diameter, mm	27.94
Average temperature, °C	220
Fuel loading, mtU	94
Specific power, Mw/mtU	0.319

AC9NX707

Table 3.1 LOW-POWER REACTOR CHARACTERISTICS
(Continued)

Fuel cladding	
Material	Magnesium
Geometry	Finned tubes
Diameter, mm	29.57 OD, 28.04 ID
Average temperature, °C	212
Nuclear characteristics*	
Initial k_{∞} (operating)	1.0892
Initial k_{eff} (operating)	1.0502
k_{eff} (equilibrium Xe and Sm)	1.0430
Neutron flux levels	
Fast (>1.86 ev)	1.6×10^{12}
Thermal (<1.86 ev)	2.5×10^{12}
Maximum plutonium production, kg per full power year	10.6

*Nominal design, no boron or other impurities in the graphite.

Active length of the core is about 5.7 meters, and the active diameter is 8.8 meters. A graphite reflector of 80-cm thickness surrounds the active core, and the total weight of graphite in the moderator and reflector is approximately 1000 metric tons. The 1418 process channels are longitudinal holes in the graphite, and the 67.8 mm diameter holes are located on a square pitch of 212 mm. A cross-section through the lattice cell of the low-power reactor is given in Fig. 3.1.

The core power density is 0.087 w/cm^3 , and the average moderator temperature is 200°C . The cylindrical fuel slugs are 27.94 mm in diameter, and they are enclosed in finned, magnesium cladding tubes having an inside diameter of 28.04 mm. Average temperature of the cladding is 212°C , and the low specific power of the metallic fuel combines with its high thermal conductivity to give an average fuel temperature of only 220°C , despite the high temperature rise from the coolant to the cladding. In the reference reactor, the uranium loading of 94 metric tons gives a maximum plutonium production of 10.6 kilograms per full power year.

3.2 The Gas-Cooled Reactor

The medium-power reactor is cooled by carbon dioxide at a nominal pressure of 8 kg/cm^2 , or slightly more than 100 psi. The 6.4 m long by 11.3 m diameter core contains 1892 process channels 97 mm in diameter. The CO_2 coolant flows at a rate of 1300 kg/sec, and, in removing the reactor heat, its temperature is raised from an inlet value of 145°C to 340°C at the reactor outlet. Reflector thickness is nominally 80 cm, and total weight of graphite in the reactor is about 1552 metric tons. A cross-section drawing of the lattice cell for the reactor is given in Fig. 3.2.

The primary system is closed cycle, and the relatively high temperature of the reactor coolant permits the use of a moderately-efficient power generation system. A steam cycle typical of that used at Calder Hall would enable the plant to produce a gross electric power of about 50 or 60 Mw.

At full core power of 250 Mw(t), and with the optimum process-channel square spacing of 230 mm, the average moderator temperature is 250°C . Average temperature in the 147 metric tons of metallic uranium fuel is 425°C , and the finned magnesium cladding tubes operate at an average temperature of 260°C .

As shown in Table 3.2, the reference design is capable of producing up to 89 kilograms of plutonium per full power year.

3.3 The Water-Cooled Reactor

Basic characteristics of the water-cooled, high-power reactor are given in Table 3.3, page 29. The thermal power produced by the reactor (400 Mw) is removed by an open-cycle water system in which the fluid flows through the reactor in aluminum process tubes. Dimensions of these tubes, which are used to prevent contact between the cooling water and the graphite moderator, are given in Table 3.3. Note that average temperatures of the process tubes and the fuel cladding are not given in Table 3.3: the physics model utilized in the nuclear analysis of the reactor combines the process tubes, coolant, and cladding materials in a single region and uses the average temperature. Actual temperatures in the aluminum are acceptable from the standpoints of corrosion and material strength.

The graphite moderator, which operates at an average temperature of 250°C, weighs approximately 1289 metric tons. The axial and radial reflectors have a nominal thickness of 100 cm, bringing the total graphite weight in the plant to approximately 2260 metric tons.

With 2155 process channels, the average channel power is 186 kilowatts; the maximum channel power is 325 kilowatts, assuming a radial max-to-average peaking factor of 1.75. The coolant flow required to maintain an acceptable coolant-discharge temperature from the hot channel is approximately 18 gpm, which gives a coolant velocity of 4.64 m/sec in the channel. Orificing permits the matching of channel flow to channel power, but a 10% safety margin is provided for mismatch. Under these conditions, the total water required for reactor cooling is 23,800 gpm. Provision of this quantity of treated water, with a storage reserve, requires substantial facilities in the form of a chemical addition building, settling basins, filters, clearwells, and storage tanks. Such facilities are not necessary for the low-and medium-power reactors, and the coolant filtration or supply systems

AC9NX707

Table 3.2 MEDIUM-POWER REACTOR CHARACTERISTICS

Type	Graphite moderated, closed-cycle, CO ₂ cooled
Thermal power, Mw	250
Core	
Active length, m	6.4
Active diameter, m	11.3
Power density, w/cm ³	0.390
Control	Boron steel rods
Refueling	Off-line
Moderator	
Material	Graphite
Density, g/cm ³	1.65 (nominal)
Average temperature, °C	250
Process channel holes	
Number	1892
Diameter, mm	97
Square pitch, mm	230
Approx. total weight, mt	910
Reflector	
Material	Graphite
Thickness (nominal), cm	80
Approx. total weight, mt	642
Coolant	
Material	CO ₂
Nominal pressure, kg/cm ²	8
Inlet/outlet temperature, °C	145/340
Fuel	
Material	Natural uranium metal
Geometry	Cylindrical rods
Rod diameter, mm	29.2
Average temperature, °C	425
Fuel loading mtU	147
Specific power, Mw/mtU	1.71

AC9NX707

Table 3.2 MEDIUM-POWER REACTOR CHARACTERISTICS
(Continued)

Fuel cladding	
Material	Magnesium
Geometry	Finned tubes
Diameter, mm	32.2 OD, 29.2 ID
Average temperature, °C	260
Nuclear characteristics*	
Initial k_{∞} (operating)	1.0863
Initial k_{eff} (operating)	1.0520
k_{eff} (equilibrium Xe and Sm)	1.0360
Neutron flux levels	
Fast (<1.86 ev)	7.7×10^{12}
Thermal (<1.86 ev)	1.3×10^{13}
Maximum plutonium production, kg per full power year	89

*Nominal design, no boron or other impurities in the graphite.

AC9NX707

Table 3.3 HIGH-POWER REACTOR CHARACTERISTICS

Type	Graphite moderated, open-cycle water cooled
Thermal power, mw	400
Active length, m	7.4
Active diameter, m	11.8
Power density, w/cm ³	0.50
Control	Boron carbide rods
Refueling	Off-line
Moderator	
Material	Graphite
Density, g/cm ³	1.65 (nominal)
Average Temperature, °C	2.50
Process channel holes	
Number	2155
Diameter, mm	47
Square pitch, mm	225
Approx. total weight, mt	1289
Reflector	
Material	Graphite
Thickness (nominal), cm	100
Approx. total weight mt	971
Process tubes	
Material	Aluminum
Dimensions, mm	43.6 OD, 40 ID
Average temperature	See text
Coolant	
Material	H ₂ O
Nominal pressure	Atmospheric
Average temperature, °C	80

Table 3.3 HIGH-POWER CHARACTERISTICS
(continued)

Fuel	Natural uranium metal
Material	Cylindrical rods
Geometry	34
Slug diameter, mm	120
Average temperature, °C	274
Fuel loading, mtU	1.46
Specific power, Mw/mtU	
Fuel cladding	Aluminum
Material	Tubes
Geometry	36 OD, 34 ID
Diameter, mm	See text
Average temperature	
Nuclear characteristics*	1.050
Initial k (operating)	1.032
Initial k _{eff} (operating)	1.016
k _{eff} (equilibrium Xe and Sm)	
Neutron flux levels	8.2 x 10 ¹²
Fast (>1.86 ev)	1.4 x 10 ¹³
Thermal (<1.86 ev)	
Maximum plutonium production,	145
kg per full power year	

*Nominal design, no boron or other impurities in the graphite.

in those reactors are far less conspicuous than the components of the water-treatment system in the high-power reactor.

3.4 Graphite Temperatures

Graphite temperatures affect the physics performance of the various reactors studied here, and are accommodated in the cell calculations by temperature-dependent, multi-group cross-sections. Temperature also affects the rate of oxidation of carbon in certain media, and the 1950s and early 1960s, in particular, saw a substantial amount of work on this subject. These studies involved principally the high temperatures that result from the use of the power densities and coolant temperatures considered for advanced gas-cooled reactors.

Irradiation affects many of the properties of graphite, and some of these influence the operating temperatures of moderator structures. In 1943, Wigner suggested that fast particles from nuclear fission could displace carbon atoms from their normal lattice positions, thereby increasing the stored energy of the graphite. If released suddenly, this stored energy could cause a spontaneous rise in temperature. Experiments show that Wigner's hypothesis was correct, but that the stored energy was annealed out continuously if the operating temperature of the moderator was relatively high (typical, say, of the temperatures that exist in modern power reactors). For early, low-temperature reactors, a technique of releasing the stored energy by operating at low power without cooling was developed in the 1950s (at Brookhaven). Irradiation effects on thermal conductivity are marked, particularly at the relatively-low temperatures that exist in the systems of interest in this study.

The effects of temperature on graphite oxidation are not important for this study, nor are the effects of irradiation, except on the thermal conductivity. In essence, the factors that affect the results of the study are those that are seen in the average moderator (graphite) temperature. The bases for selection or specification of the values for the air-, or gas-, and water-cooled reactors are given below.

The existing reactors that served as models for the systems studied here are described in the literature. For the air-cooled and the gas-cooled models, information is sufficient; data on the specific water-cooled reactor is rather limited,

so specification of the average moderator temperature at operating conditions required analyses of some of the thermal aspects of that system.

Average moderator temperature in the air-cooled reactor is 200°C, while that in the gas-cooled reactor is 250°C. The air-cooled value is taken from a 1948 report on the original "Brookhaven Nuclear Reactor" prepared for the Reactor Safeguards Committee, while the gas-cooled value is listed for Calder Hall in the 1962 IAEA publication Directory of Nuclear Reactors, Vol. IV. In these reactors, it is important to note that the coolant gas serves as the moderator blanket gas, since the designs do not incorporate metallic process tubes for the fuel channels. Without the barrier provided by the process tube, the coolant and blanket gas are inherently the same.

The water-cooled reactor, by virtue of its use of process tubes to prevent contact between the reactor coolant and the graphite moderator, can operate with a blanket gas of the designer's choice. The blanket gas provides an environment in the reactor to remove moisture and foreign gases, and it serves as the heat-transfer medium between the graphite and the process tubes in removing heat from the moderator. It can also be used to detect water leaks into the moderator region. In practice, the designer's choice of gas has been limited to helium, nitrogen, or a mixture of the two, although a mixture of helium and carbon dioxide has been used at Hanford. In the range of temperatures of interest (and up to about 600°C), the thermal conductivity of CO₂ is even lower than that of nitrogen, so obtaining a reasonable overall conductivity from a He-CO₂ mixture would require a correspondingly higher fraction of (relatively-high-conductivity) helium than would be needed in a He-N mixture. For this reason, CO₂ was not considered further in this study.

Although helium is not as common as nitrogen, it is used as a blanket gas, or a component of a helium-nitrogen mixture, in foreign countries (the Soviet Union, for example), and its heat-transfer properties and its inertness generally make it the preferred gas. Thermal conductivity and its effect on graphite temperature will be discussed later, but it should be observed here that a helium blanket gas gives a lower graphite temperature than a nitrogen one, and the lower temperature of the moderator yields a higher reactivity in the water-cooled reactor, an important consideration in a system that can be marginally critical when natural uranium fuel is used. Consequently, helium was chosen as the "reference" blanket gas in the calculation of average moderator temperature in the water-cooled reactor.

AC9NX707

Temperature in the graphite is a function of the following parameters:

- Volumetric energy deposition (heat generation) rate in graphite;
- thermal conductivity of graphite, of blanket gas, and of process tube material;
- heat transfer coefficient to reactor coolant
- temperature of reactor coolant;
- lattice pitch;
- diameter and thickness of process tube; and
- diameter of hole in graphite for process tube.

Whereas the conductivities of the blanket gas and the process tube are functions of material temperature, the thermal conductivity of the graphite varies with both temperature and irradiation. The trend in unirradiated graphite is for rapid increases in conductivity from very low temperatures up to room/reactor temperatures, followed by a decrease or a slowing in rate of increase over the temperature range that typically exists in reactors. Following irradiation, the curve of graphite conductivity versus temperature generally follows the unirradiated-material curve, but is displaced downward to substantially lower values. For the present study, a graphite thermal conductivity value of 11.1 Btu/hr-ft-°F was used: This value is at the low end of the range of conductivity values for irradiated graphite at elevated temperatures, and its use results in a relatively high graphite temperature and a relatively low reactivity. The variation of conductivity is a complex function of irradiation history and time-dependent operating temperature, as well as the type of graphite. A detailed evaluation of thermal conductivity and its effect on core reactivity is beyond the scope of this study.

The use of the irradiated-graphite thermal conductivity given above, a helium blanket gas, and a nominal process-tube to graphite gap (1.7 mm), when combined with other physical parameters of the reactor, gives a reference average moderator temperature in the water-cooled reactor of 250°C.

AC9NX707

In the nominal-temperature region of the reactor, the graphite temperature at the surface of the process-tube holes is 229°C, and the maximum temperature at the lattice-cell boundary is slightly greater than 253°C.

Changes in blanket gas change the conductivity across the process-tube to graphite gap, resulting in changes in the graphite temperature. For example, with the gas gap specified in the reference water-cooled reactor design, the use of a helium blanket gas gives a gap temperature rise of 149°C. The corresponding average graphite temperature is 250°C, as stated above. If the blanket gas were changed to a mixture of half helium, half nitrogen, the average graphite temperature would rise to 350°C. A pure-nitrogen blanket gas would result in an unacceptably-high average graphite temperature (probably approaching 850°C) if the reference gas gap were maintained and radiant heat transfer ignored.

The high temperatures reached with a pure-nitrogen blanket gas in the reference design make the use of that gas alone unfeasible. If the gas gap between the process tube and the graphite could be reduced in thickness, the gap temperature rise and, hence, average graphite temperature could probably be reduced to acceptable values. There is, however, a fabrication-tolerance and assembly-clearance limit on the size of the gap (hole in graphite), and we have specified a clearance that should make fabrication of the moderator stack and insertion and removal of process tubes relatively easy. Some reduction is no doubt possible, but, since the use of nitrogen in place of helium reduces reactivity for any given gap size, we did not attempt to determine how small the gap would have to be if nitrogen were used.

3.5 Bibliography for Section 3.0

Information on existing reactor designs was taken from the following publications; in each case, more than one publication was used in determining the parameters for the model reactors from which the reference reactor designs described above were established.

Nuclear Reactor Project, Progress Report, Brookhaven National Laboratory, Report BNL-14, January 1, 1948.

Report on the Brookhaven Nuclear Reactor, prepared for the Reactor Safeguard Committee of the Atomic Energy Commission, Brookhaven National Laboratory, Report BNL-18, June 22, 1948.

AC9NX707

Glasstone, S., Principles of Nuclear Reactor Engineering,
D. Van Nostrand Company, Inc. New York, 1955.

The Journal of the British Nuclear Energy Conference,
Symposium: Calder Works Nuclear Power Plant, Vol. 2, No. 2,
April 1957.

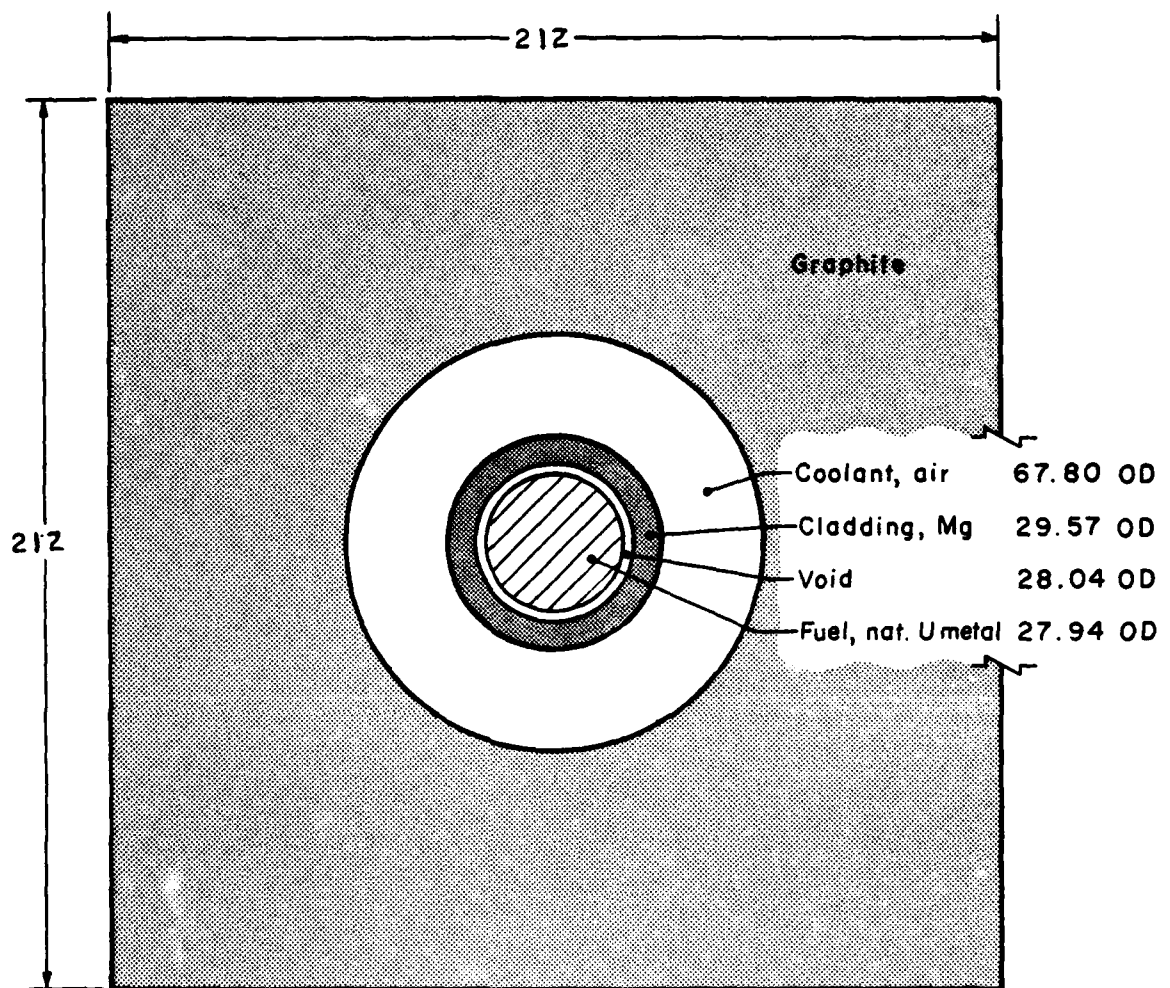
Directory of Nuclear Reactors, Vol. II, Research, Test and
Experimental Reactors, International Atomic Energy Agency,
Vienna, 1959.

Directory of Nuclear Reactors, Vol. IV, Power Reactors,
International Atomic Energy Agency, Vienna, 1962.

Hazards Summary Report, Vol. 3 - Description of the 100-B
100-C, 100-D, 100-DR, 100-F, and 100-H Production Reactor
Plants, Report HW-74094 Vol. 3, Hanford Atomic Products
Operation, Richland, Washington, April 1, 1963
(Declassified).

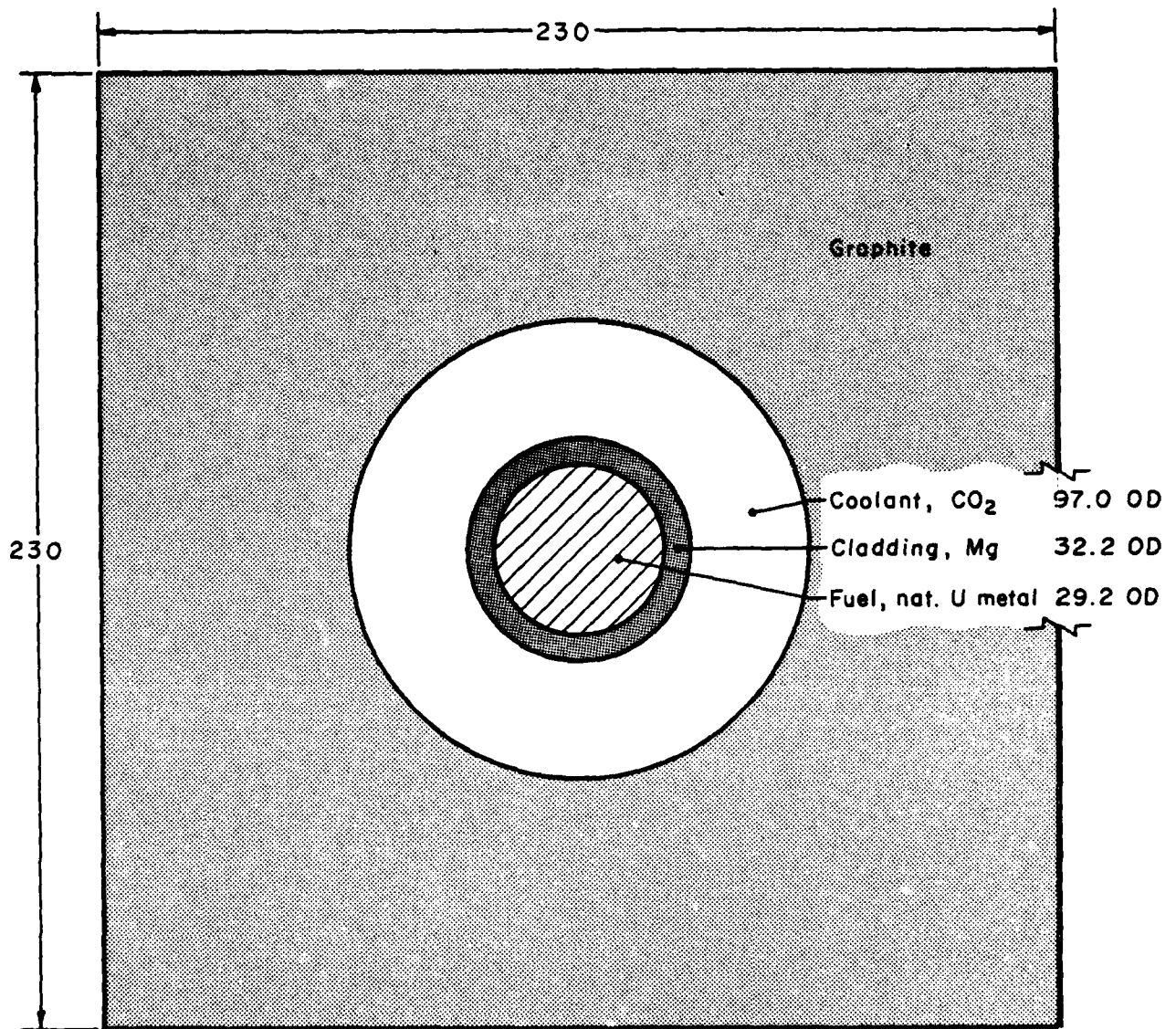
Bilan et Perspectives, Commissariat a l'Energie Atomique,
Paris, Juin 1967.

Hewlett, R. G., and Anderson, O. E., Jr. The New World, a
History of the United States Atomic Energy Commission, Vol.
1, 1939/1946, Report WASH 1214, USAEC, 1962, reprinted 1972.



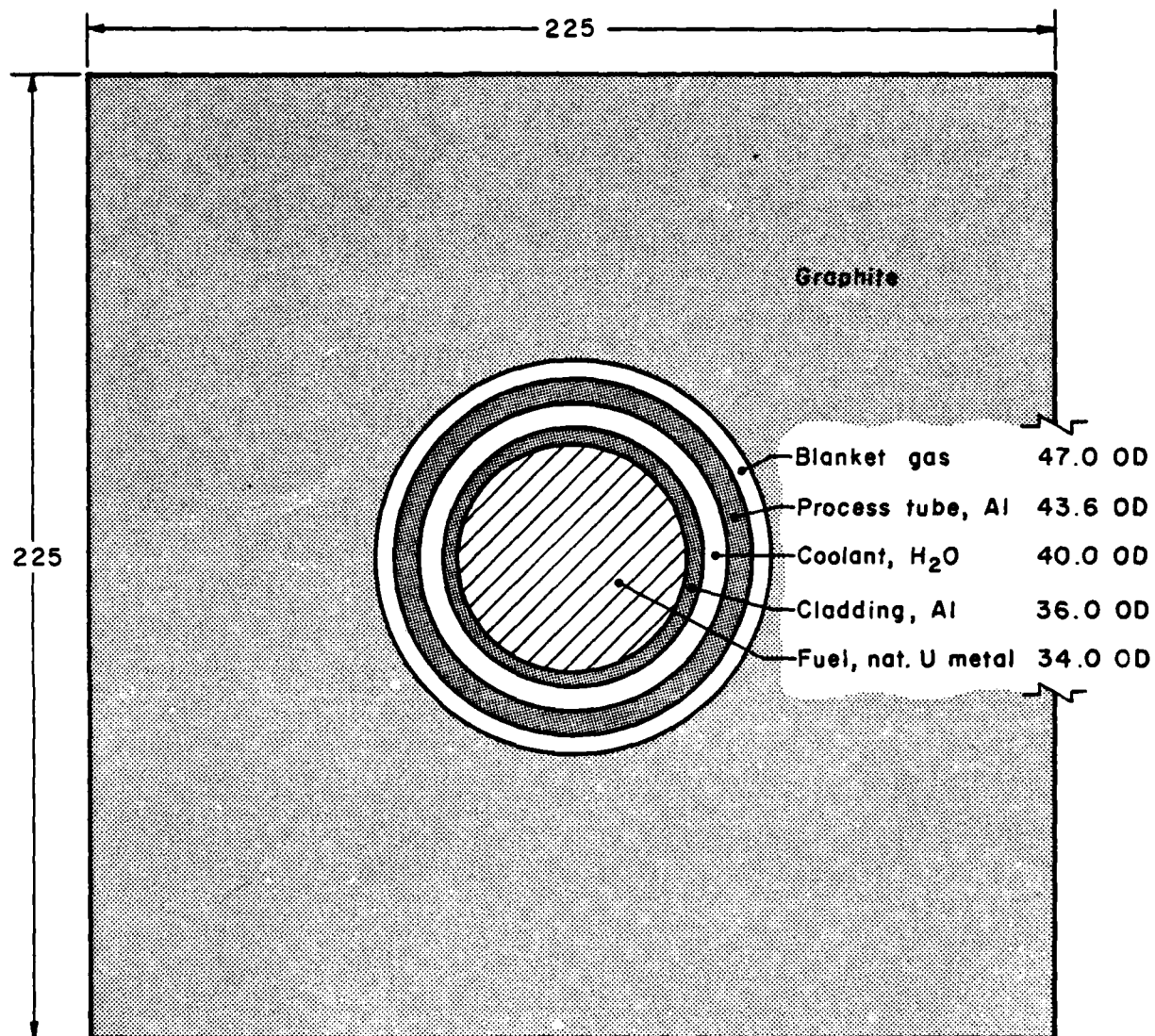
Not to scale,
All dimensions in mm.

Fig. 3.1 Cross section of cell for low-power reactor.



Not to scale,
All dimensions in mm.

Fig. 3.2 Cross section of cell for medium-power reactor.



Not to scale,

All dimensions in mm.

Fig. 3.3 Cross section of cell for high-power reactor.

4.0 NUCLEAR PERFORMANCE OF THE AIR-COOLED REACTOR

4.1 General

The nuclear performance of the low power (30 Mw(t)) air-cooled reactor concept was evaluated using the NULIF unit cell spectrum analysis and homogenization code. Average (typical) thermal performance characteristics are described in Table 3.1. The reference design used in this study closely resembles the original Brookhaven reactor and the French G1 plutonium production reactor at Marcoule. For the reference design, the calculated k_{∞} is 1.088 (with no impurities in the graphite) compared to a reported k_{∞} of 1.074⁴ (Brookhaven) and 1.077⁵ (Marcoule G1) with an unknown graphite impurity level. This is considered to be good agreement in view of the uncertainty in graphite purity actually used at Brookhaven and Marcoule.

Brookhaven used AGOT graphite, but the impurity level of the 1948 vintage graphite is unknown. Marcoule probably used an early version of the "Lockport" graphite, also of unknown impurity level.

K_{eff} values were estimated from the core dimensions (geometric buckling), using a reflector savings of 46 cm estimated from measurements in the Calder Hall graphite-reflected reactor and the M^2 calculated by the NULIF code. Using the reference design, calculations were made of the effect of lattice spacing, graphite density, fuel enrichment, graphite impurity levels (in terms of the equivalent boron concentration) and plutonium production rates. Results of these calculations are described in the following paragraphs.

⁴Report on the Brookhaven Nuclear Reactor, prepared for the Reactor Safeguard Committee of the Atomic Energy Commission, Brookhaven National Laboratory, Report BNL-18, June 22, 1948.

⁵Directory of Nuclear Reactors, Vol. IV, Power Reactors,
International Atomic Energy Agency, Vienna, 1962.

4.2 Lattice Optimization for the Reference Design

Calculations of the k_{∞} values for various lattice spacings and graphite densities are shown in Fig. 4.1 as a function of the carbon-to-uranium (N_c/N_u) atom ratio. The band shown on the figure encompasses calculated values for graphite densities ranging from 1.5 g/cm^3 to 1.75 g/cm^3 . In terms of the N_c/N_u ratio, graphite density over the given range has an almost negligible effect on calculated values of k_{∞} . Single point calculations to investigate the effect of variations in fuel element diameter and in coolant channel size also show only a small effect ($\sim 0.3\% \Delta k$ maximum). Since the fuel element diameter and coolant channel size are determined primarily by thermal performance requirements, no further evaluation of the effect of variations in these parameters was made.

Despite the consistency in k_{∞} values, the k_{eff} values differ for graphite of various densities, primarily because of differences in migration area and, hence, differences in neutron leakage effects. Figure 4.2 shows the calculated k_{eff} values as a function of lattice spacing (pitch). These data show that, as the graphite density increases, the core reactivity (k_{eff}) increases and the optimum pitch (maximum k_{eff}) decreases. For a nominal graphite density of 1.65 g/cm^3 (reference), the optimum k_{eff} of 1.050 occurs at a square lattice spacing of 21.2 cm. Table 4.1 summarizes the reactivities and optimum lattice spacing for the three graphite densities investigated.

For subsequent calculations, the nominal graphite density of 1.65 g/cm^3 was adopted as a reference, recognizing that different densities could increase or decrease reactivities by $\sim \pm 0.5\% \Delta k$ and lattice spacing by $\sim 1 \text{ cm}$ or less. With natural uranium, the relationships, $\Delta k_{\text{eff}} = 0.033 (\rho_c - 1.65)$ and $\text{pitch} = 20.7 + 6.8 (1.75 - \rho_c)$ may be used to extrapolate to other graphite densities (ρ_c). For example, at a graphite density of 1.72 g/cm^3 , the optimum pitch would be 20.9 cm and would result in a k_{eff} $\sim 0.23\%$ higher than the reference case of 1.65 graphite density.

With aluminum cladding rather than the reference magnesium, the k_{eff} (at 1.65 g/cm^3 graphite density) is reduced from 1.050 to 1.043, a loss of $\sim 0.7\% \Delta k$.

Table 4.1 REACTIVITIES AND OPTIMUM LATTICE SPACING
IN THE LOW POWER AIR-COOLED REACTOR CONCEPT (1)

	Graphite Density		
	<u>1.5 g/cm³</u>	<u>1.65 g/cm³</u>	<u>1.75 g/cm³</u>
Optimum square pitch, cm	22.4	21.2	20.7
k_{eff} at optimum	1.045	1.050	1.053
k_{eff} from reference (2)	-.005	reference	+.003
(k_{eff} with Al clad)		(1.043)	

(1) Natural uranium metal fuel, magnesium cladding.

(2) $k_{eff} = 0.033 (\rho_g - 1.65)$

Optimum pitch = $20.7 + 6.8(1.75 - \rho_g)$, where ρ_g is the graphite density.

4.3 Fuel Burnup and Reactivity

With fuel burnup, the initial reactivity typically decreases rapidly as xenon and samarium fission products are produced. Later, as plutonium accumulates, the reactivity increases to a burnup of about 1000 Mwd/mtU, then again decreases as other fission product poisons accumulate. Figure 4.3 illustrates the reactivity variation at the optimum lattice spacing with natural uranium for graphite densities of 1.50, 1.65 and 1.75 g/cm³. Also shown in Fig. 4.3 is the effect of using aluminum cladding rather than the reference magnesium cladding.

In all cases, the minimum reactivity determines the capability of the reactor to operate as intended without shutting down as xenon and samarium accumulate. The four cases illustrated in Fig. 4.3 all have excess reactivity at the minimum of the reactivity curve and can accommodate impurities ranging from 1.9 to 2.4 ppm boron equivalent. After the initial cycle, fuel management programs (fuel shuffling) could utilize the greater reactivity of the higher burnup fuel to achieve a higher core reactivity. Such programs, however, are beyond the scope of the present study.

4.4 Enriched Fuel

With graphite impurity levels greater than about 2 ppm boron, enriched fuel is necessary for the reactor to operate satisfactorily. Calculations were made at fuel enrichments of 1.2 and 3.2% U-235,⁶ to illustrate the effect of higher enrichments. As shown in Fig. 4.4, the optimum lattice spacing increases with increasing enrichment. However, as will be seen in a later section, the presence of higher impurity levels in the graphite tends to reduce the optimum pitch, thus counteracting (and exceeding) the effect of higher enrichment. Since the objective of using enriched

⁶Attempts to calculate for 20% enriched fuel quickly revealed that unreasonably high boron contents (~200 ppm boron equivalent or more) would be necessary to reduce the reactivity to levels normally associated with this reactor concept and amenable to reasonable reactivity control schemes. Consequently, the effort was terminated.

fuel is to overcome reactivity losses due to graphite impurities, there does not appear to be any incentive to design for a pitch greater than the reference design. Furthermore, after the graphite impurity level is reduced by neutron burnout, the required enrichment would be less and the lattice spacing would therefore no longer be optimum. The use of enriched fuel also reduces the production of plutonium, as shown in Section 4.5 below.

4.5 Plutonium Production

As fuel burnup progresses, the quantity of plutonium in the fuel increases. The increase in plutonium content is not linear, since some of the plutonium is consumed in-situ. Figure 4.5 shows the accumulation of both total and fissile plutonium in the fuel, for natural, 1.2% and 3.2% enrichments at optimum pitch. Graphite density, over the range from 1.5 to 1.75 g/cm³, has a negligible effect on plutonium production. At burnups employed in production reactors, (typically 200-600 Mwd/mtU) the plutonium is primarily the Pu-239 isotope, although the Pu-240 (and Pu-242) content increases with burnup as indicated in Figs. 4.6 and 4.7.

The data in Figs. 4.5 to 4.8 extends to a burnup of 1000 Mwd/mtU, although, in practice, burnups would not likely exceed 100 to 200 Mwd/mtU because of the long time periods (~8.6 full power years) needed to reach 1000 Mwd/mtU.

The rate of plutonium production, shown in Fig. 4.8, decreases slightly with increased burnup as more of the plutonium is burned in the reactor. Enriched fuel, however, produces a more pronounced effect on plutonium production, decreasing the rate of production significantly with increased enrichment. Assuming an annual fuel cycle, for illustration purposes, the discharge fuel burnup would correspond to 115 Mwd/mtU and the corresponding rates of plutonium production are listed in Table 4.2.

Thus, increased parasitic absorption in the graphite would necessitate the use of enriched fuel, with a corresponding reduction in the rate of plutonium production.

AC9NX707

Table 4.2 RATE OF PLUTONIUM PRODUCTION IN THE LOW POWER
AIR-COOLED REACTOR

Plutonium Production Rate*		
<u>Enrichment</u>	<u>Pu, kg/EFP yr</u>	<u>Fissile Pu, kg/EFP yr</u>
Natural, Mg clad	10.4	10.3
Natural, Al clad	10.4	10.3
1.2%	6.9	6.9
3.2%	3.5	3.5

*Assuming 115 Mwd/mtU burnup; production in kilograms per
equivalent full power.

4.6 Graphite Impurities

Calculations with various assumed impurity levels in the graphite (represented analytically as equivalent boron concentrations) indicate that the optimum lattice space is reduced with increased parasitic absorption in the graphite. This effect is shown in Figs. 4.9 and 4.10 for natural and 1.2% enriched fuel, respectively. However, since it is likely that a reactor would be built at the optimum pitch for natural uranium, calculations were made at the reference lattice spacing of 21.2 cm, with various amounts of boron poisoning in the graphite, for natural, 1.2% and 3.2% enriched fuel. Results of these calculations, shown in Fig. 4.11, indicate that there is a minimum concentration of boron (or equivalent) in the graphite that is just adequate to prevent the reactor from operating. These values of equivalent boron poisoning (for $k_{eff} = 1.0$) are 2.6 ppm for natural uranium fuel, 16 ppm for 1.2% enriched fuel and 50 ppm for 3.2% enrichment (graphite density of 1.65 g/cm³). Corresponding values of the effective 2200 m/s cross-section of graphite are 5.5, 16.5 and 44.8 millibarns. Figure 4.12 shows the boron concentration as a function of enrichment for an initial k_{eff} of 1.0 and for a k_{eff} of 1.050 (the initial reactivity with natural uranium in the absence of graphite impurities). These curves may be used to estimate the enrichment required to overcome a given boron (equivalent) poisoning level in the graphite. It should also be remembered that, if necessary, the reactor could be built on a closer lattice spacing to reduce the effect of poisoning.

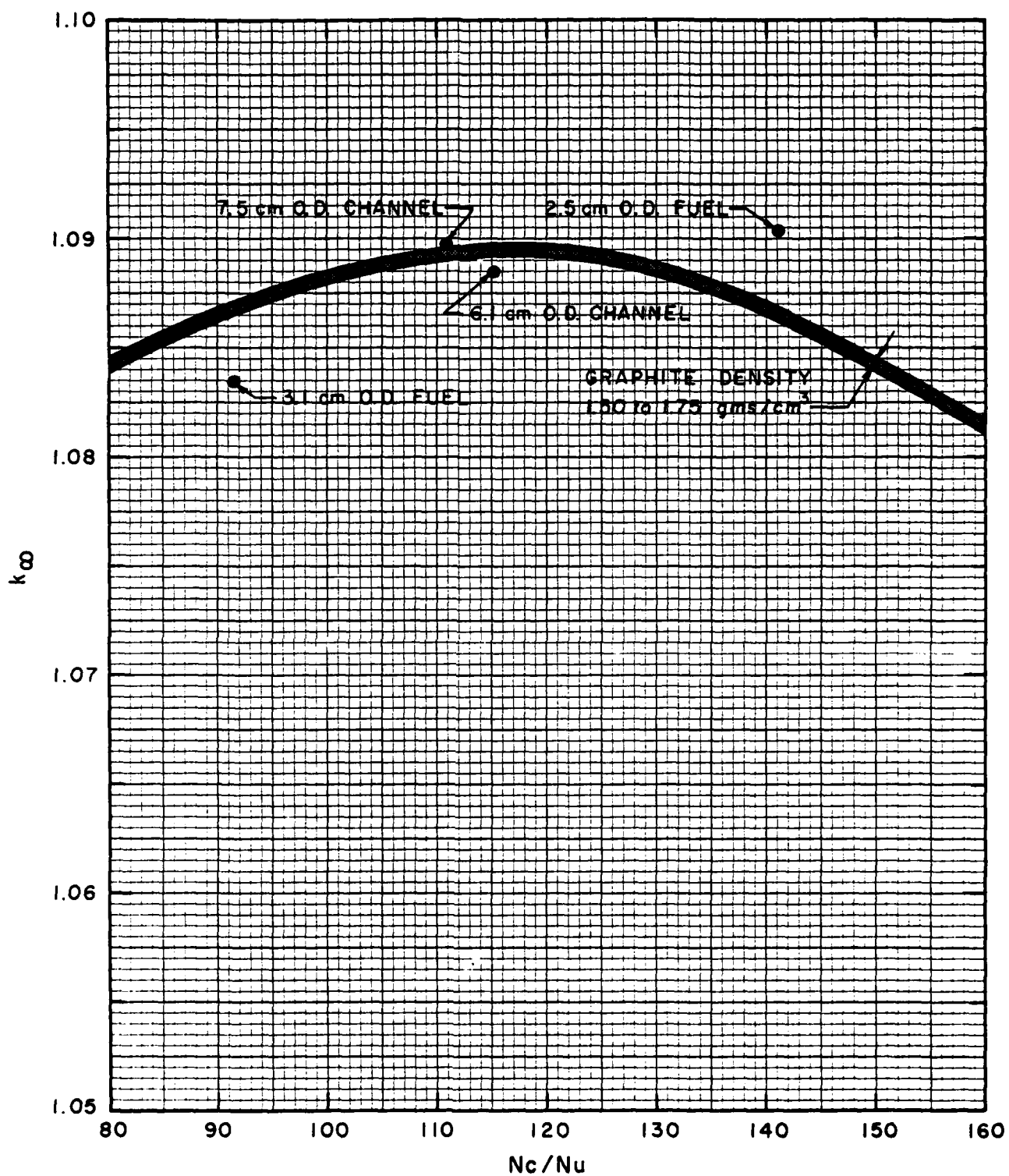


Fig. 4.1 Lattice optimization of k_{∞} versus carbon-to-uranium atom ratio.

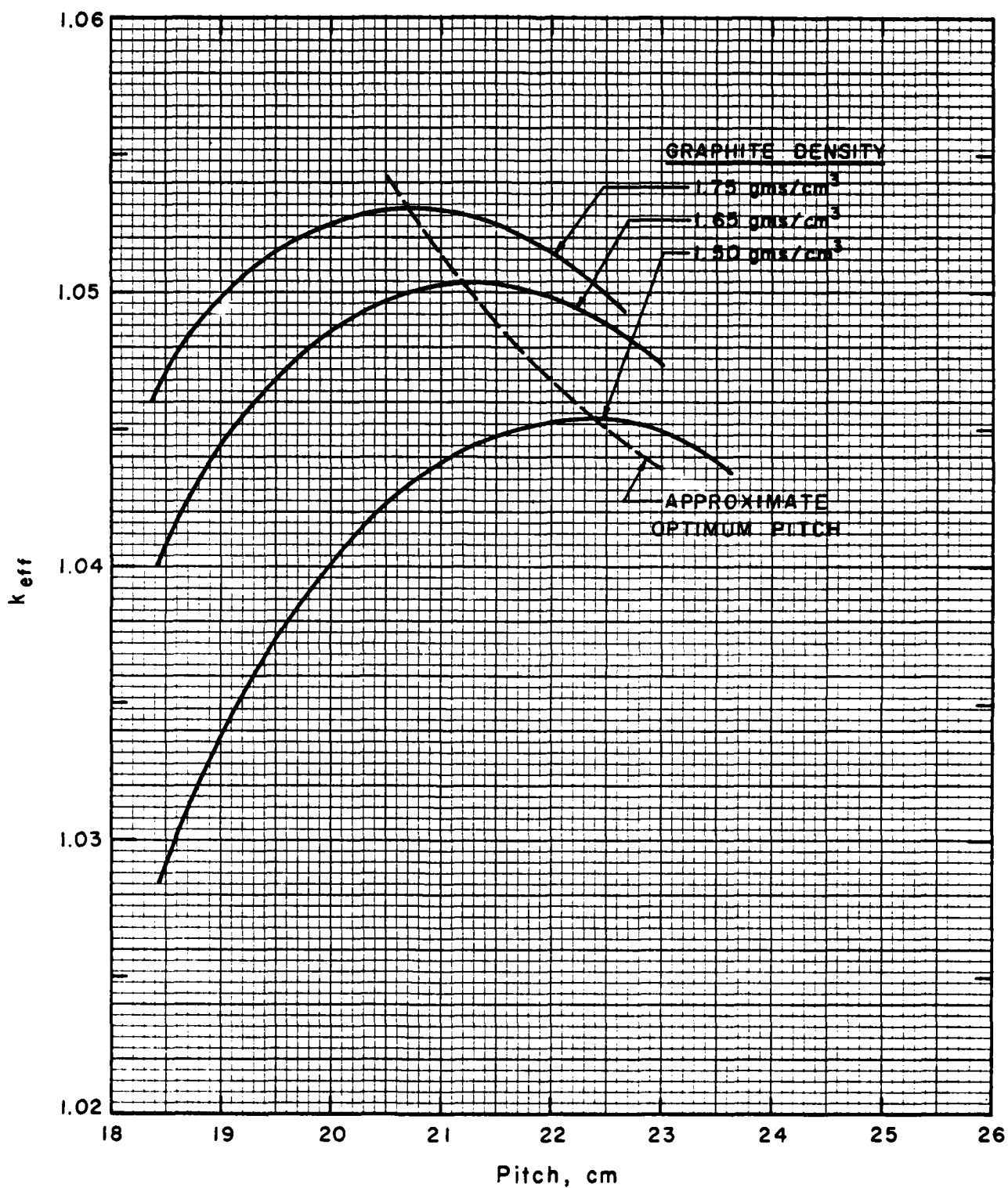


Fig. 4.2 Lattice optimization of k_{eff} for several graphite densities (natural uranium fuel).

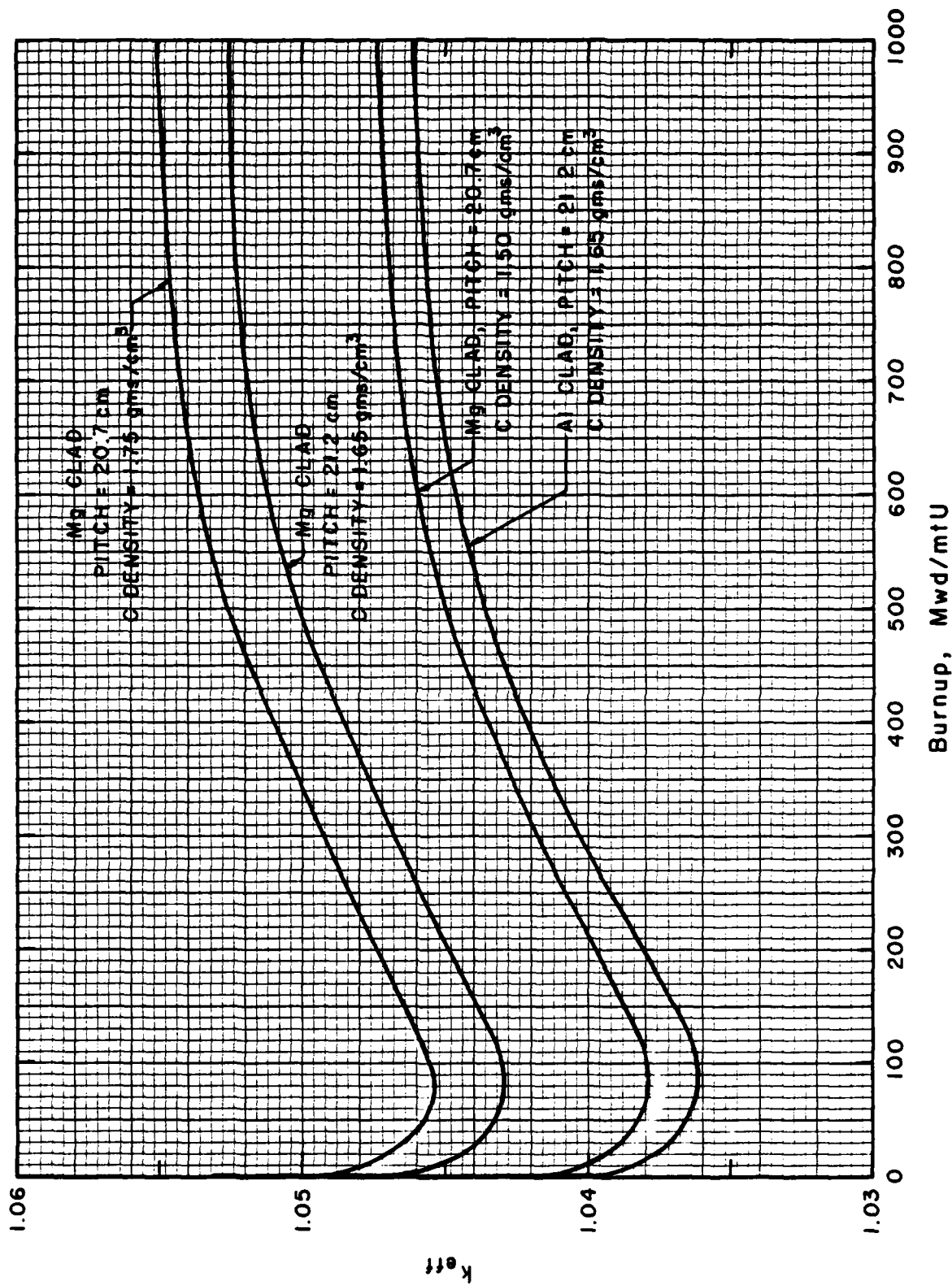


Fig. 4.3 Variation in reactivity with fuel burnup for natural uranium fuel (low power, air-cooled reactor).

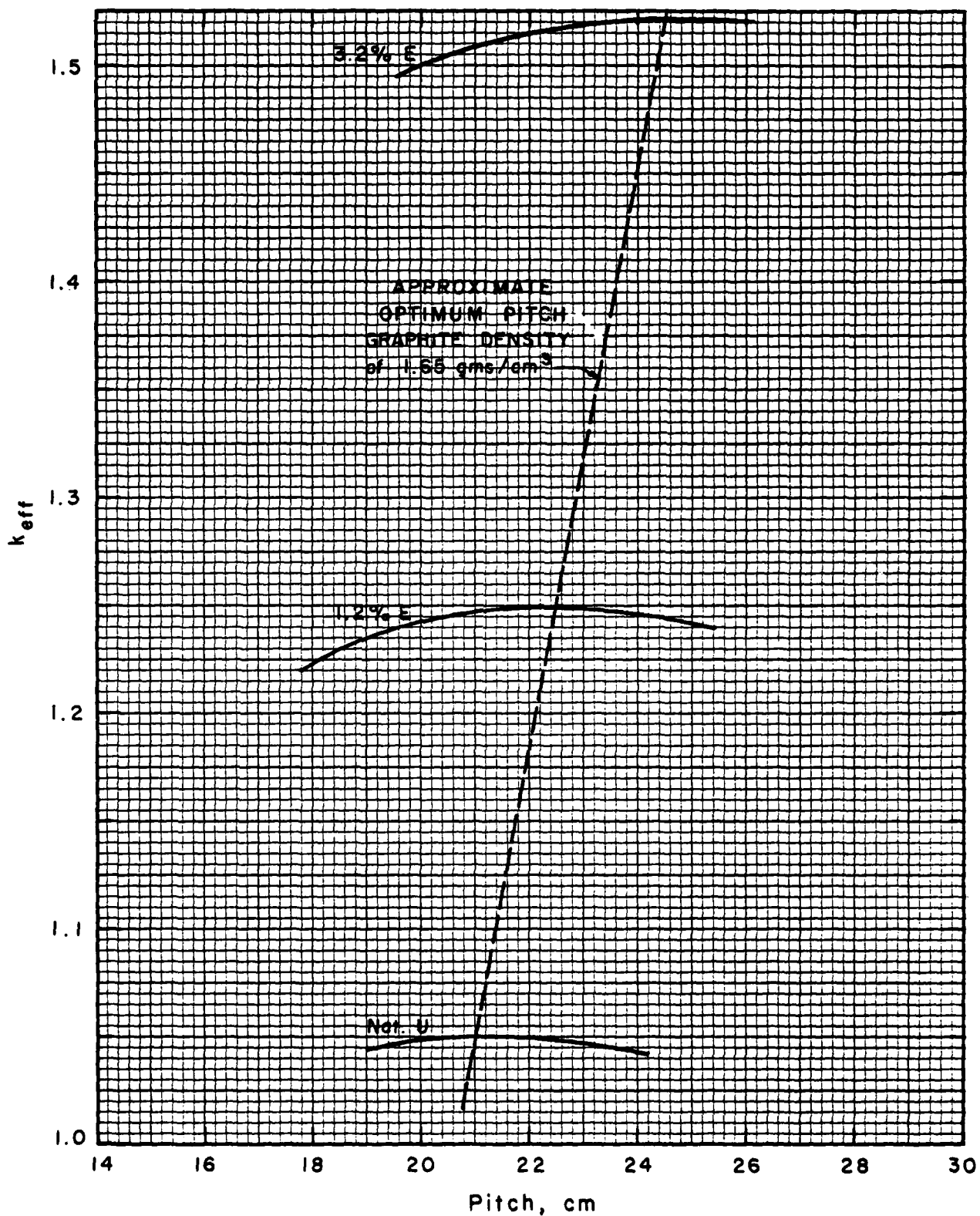


Fig. 4.4 Lattice optimization of k_{eff} for fuel of various enrichments (low power, air-cooled reactor).

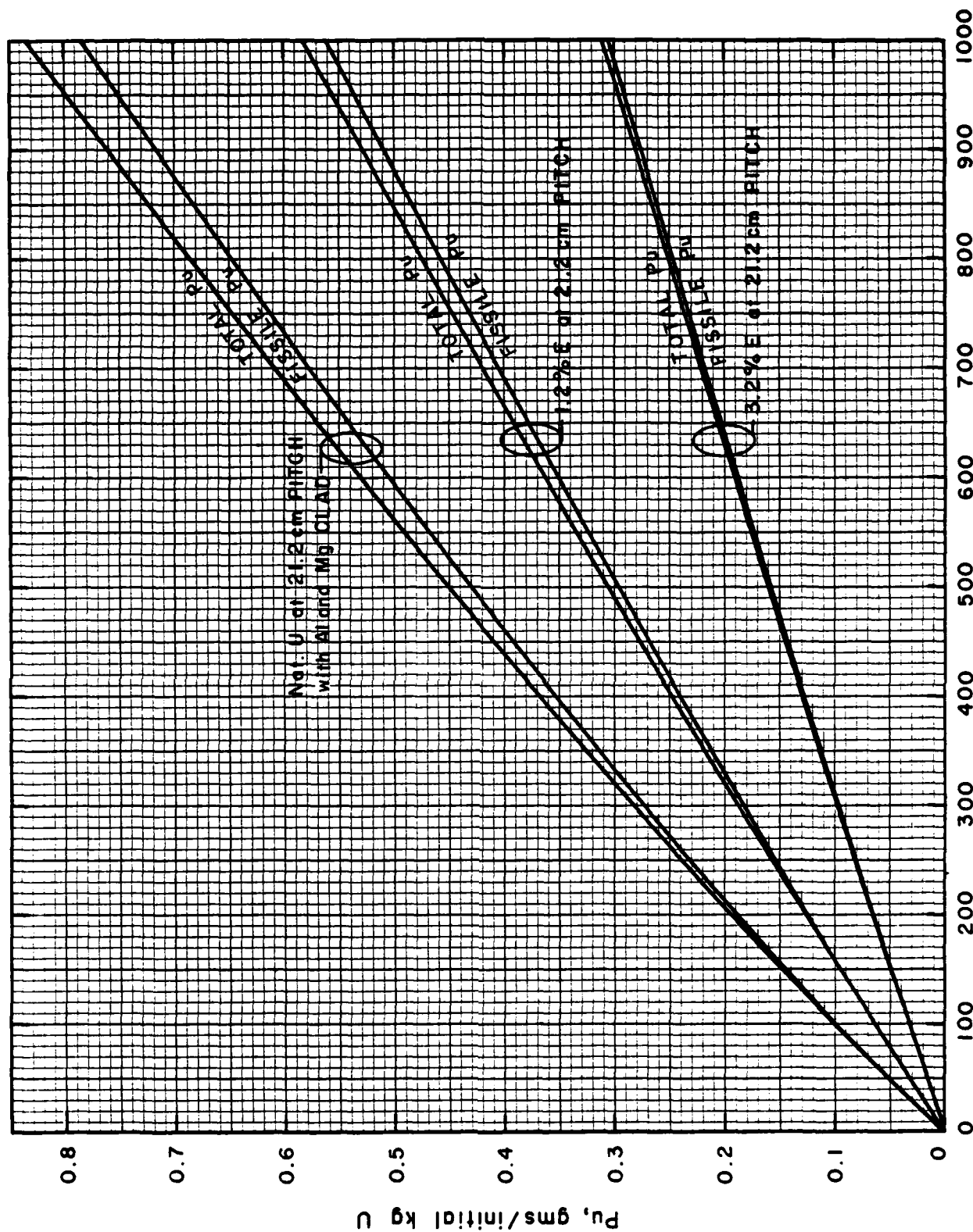


Fig. 4.5 Total and fissile plutonium production in the air-cooled reactor as a function of fuel burnup.

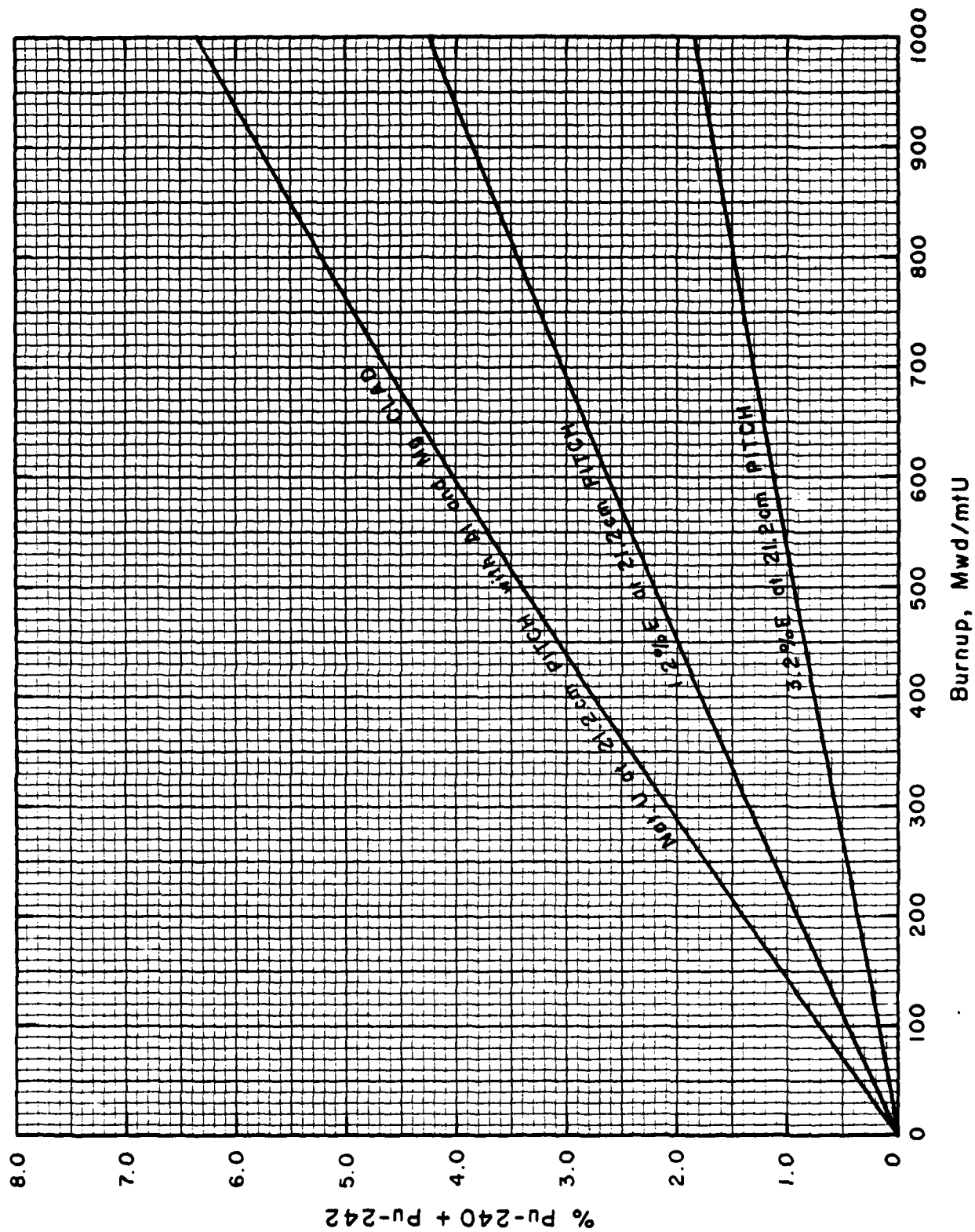


Fig. 4.6 Dependence of the percentage of non-fissile plutonium isotopes on fuel burnup (low power, air-cooled reactor).

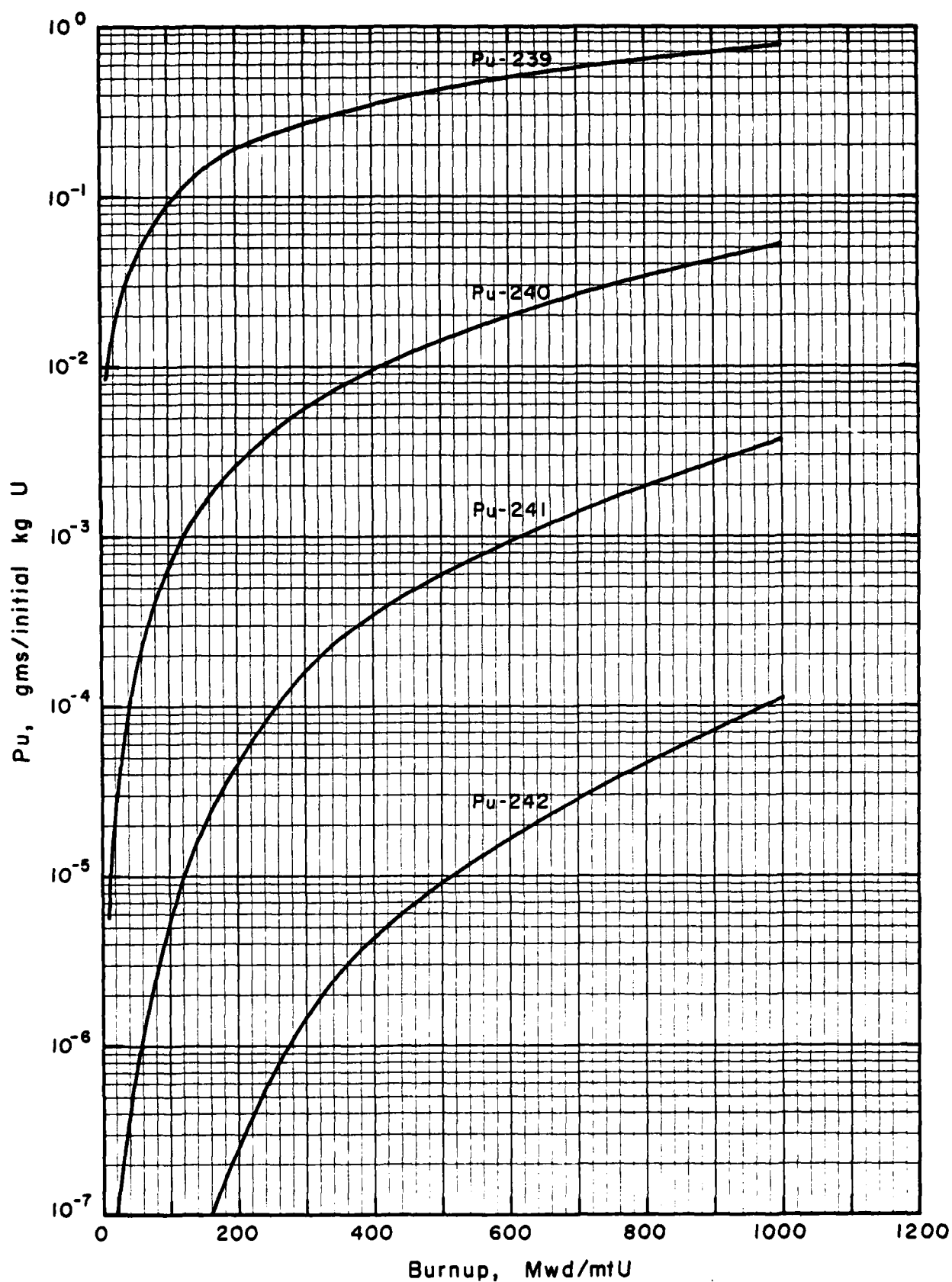


Fig. 4.7 Plutonium isotopics as a function of burnup for natural uranium fuel in the air-cooled reactor.

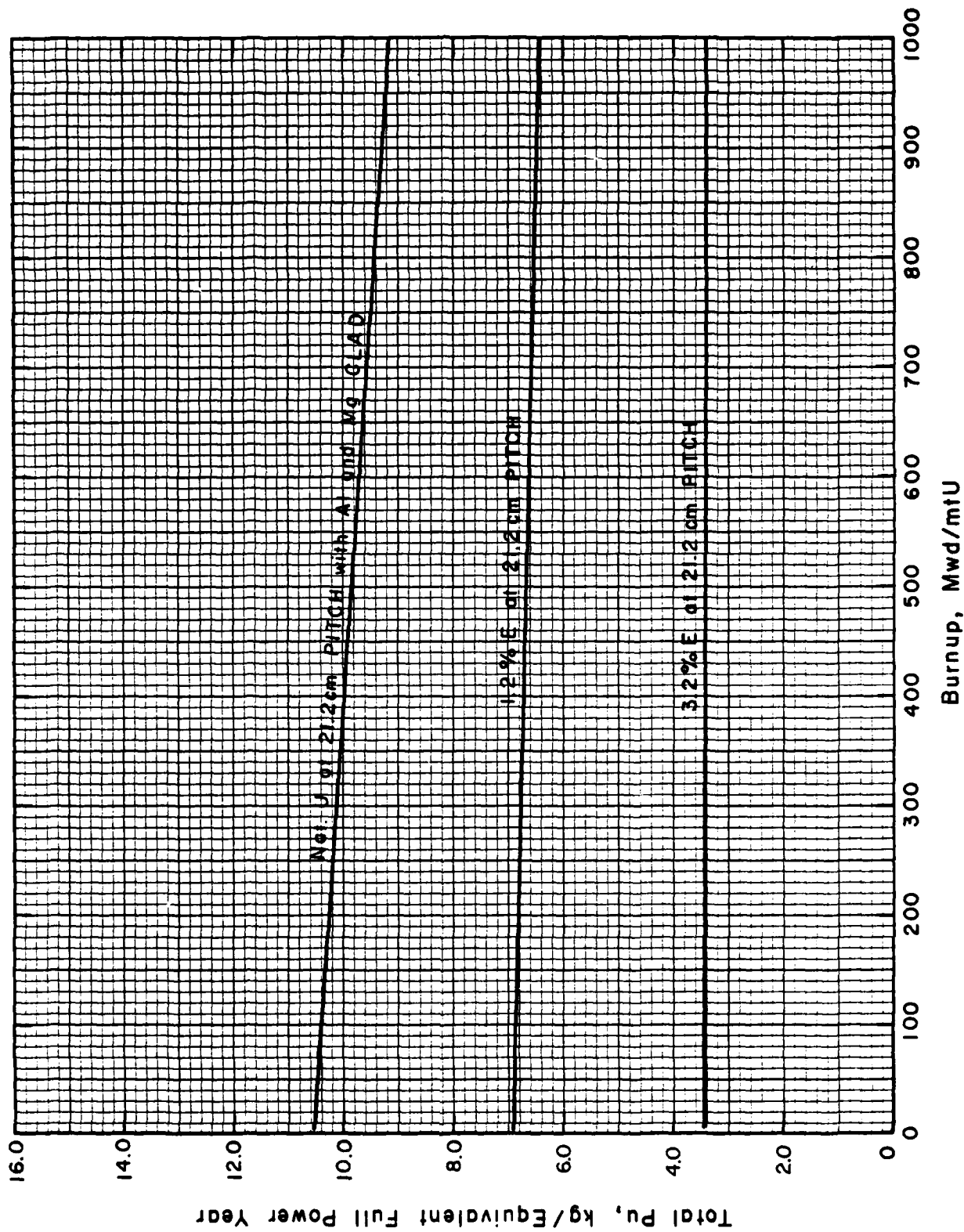


Fig. 4.8 Dependence of plutonium production rate on discharge fuel burnup in the 30 Mw air-cooled reactor.

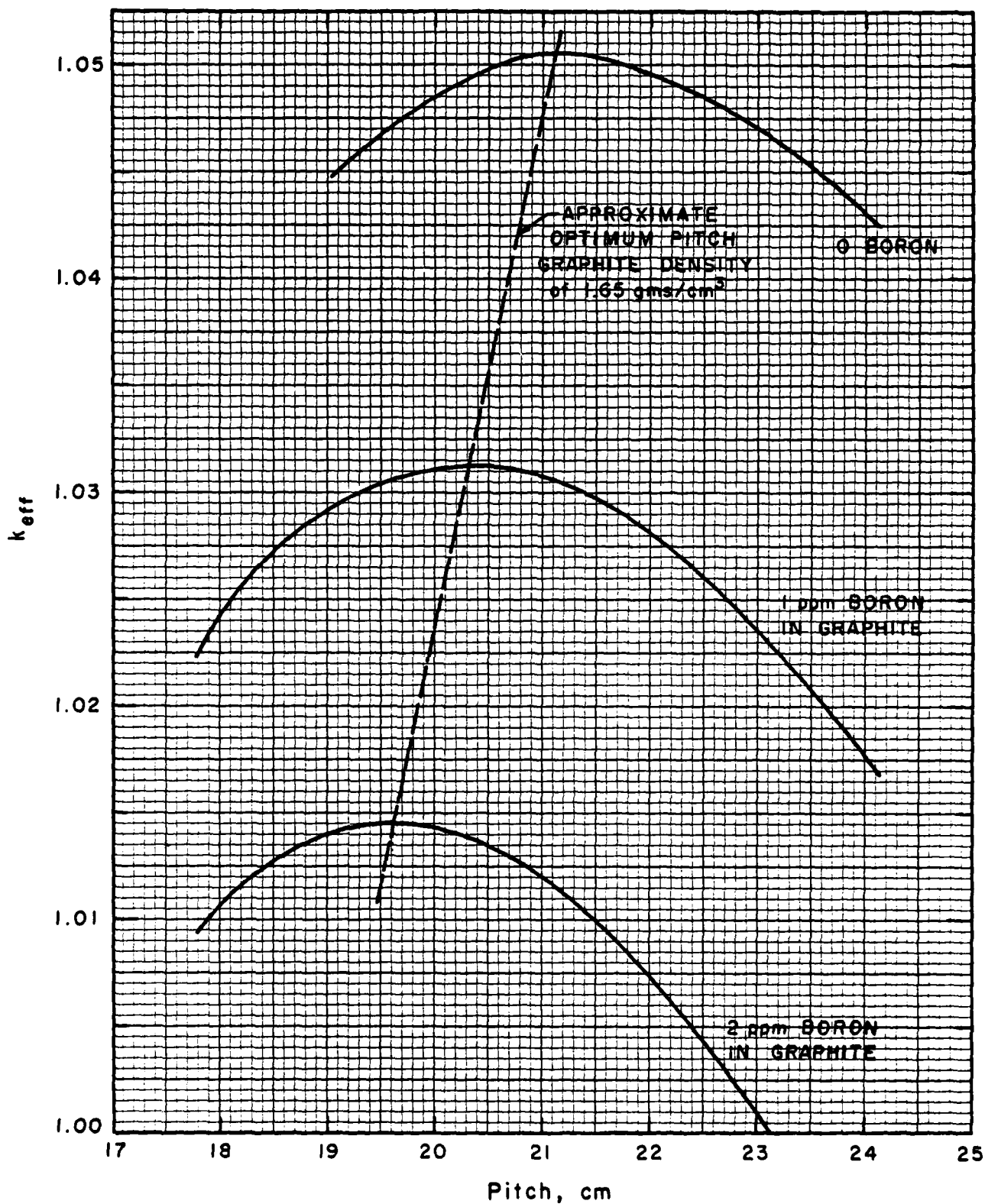


Fig. 4.9 Lattice optimization in the air-cooled reactor for various levels of graphite impurities (as boron) with natural uranium fuel.

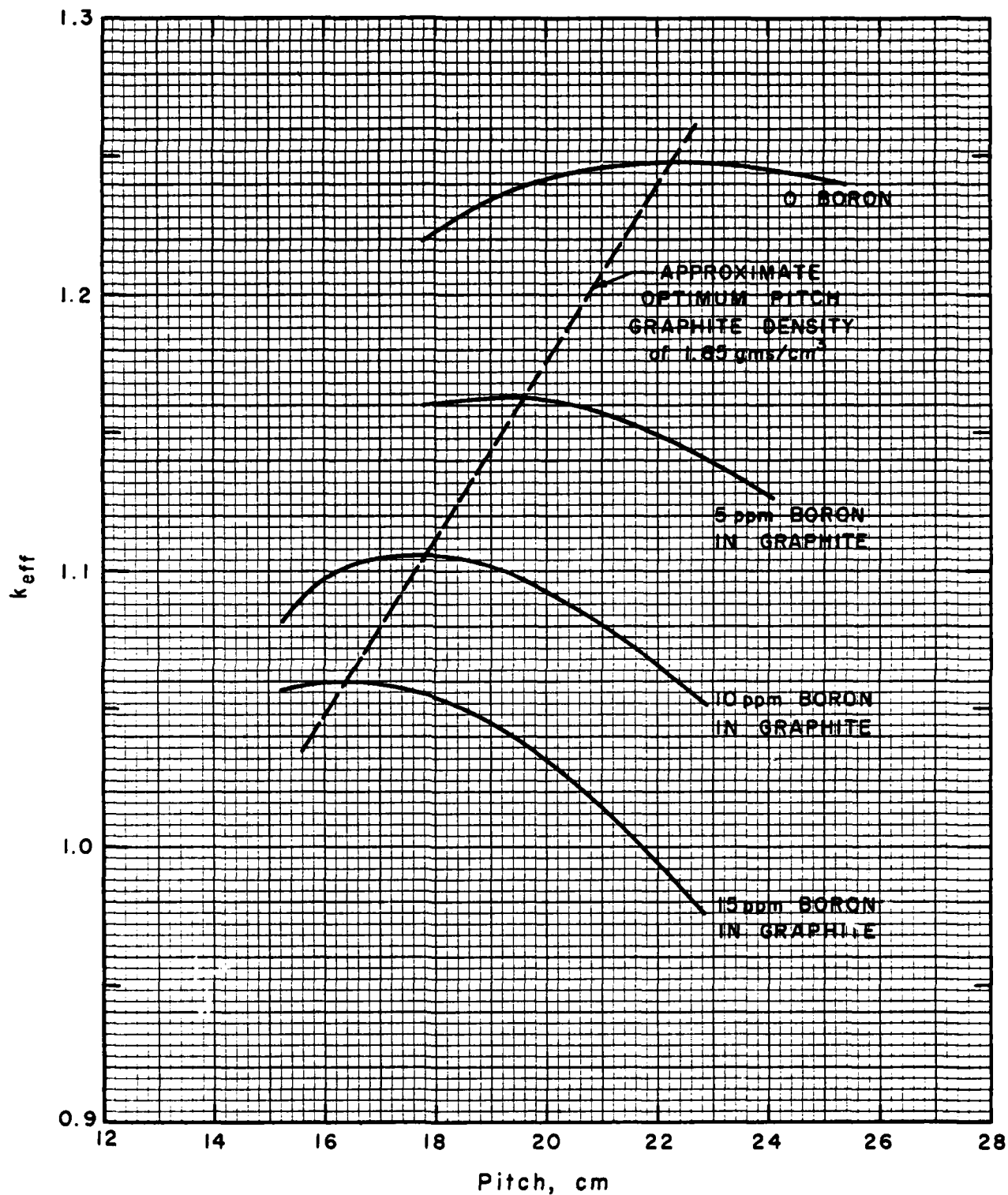


Fig. 4.10 Lattice optimization for various levels of graphite impurities (as boron) for 1.2% enriched fuel.

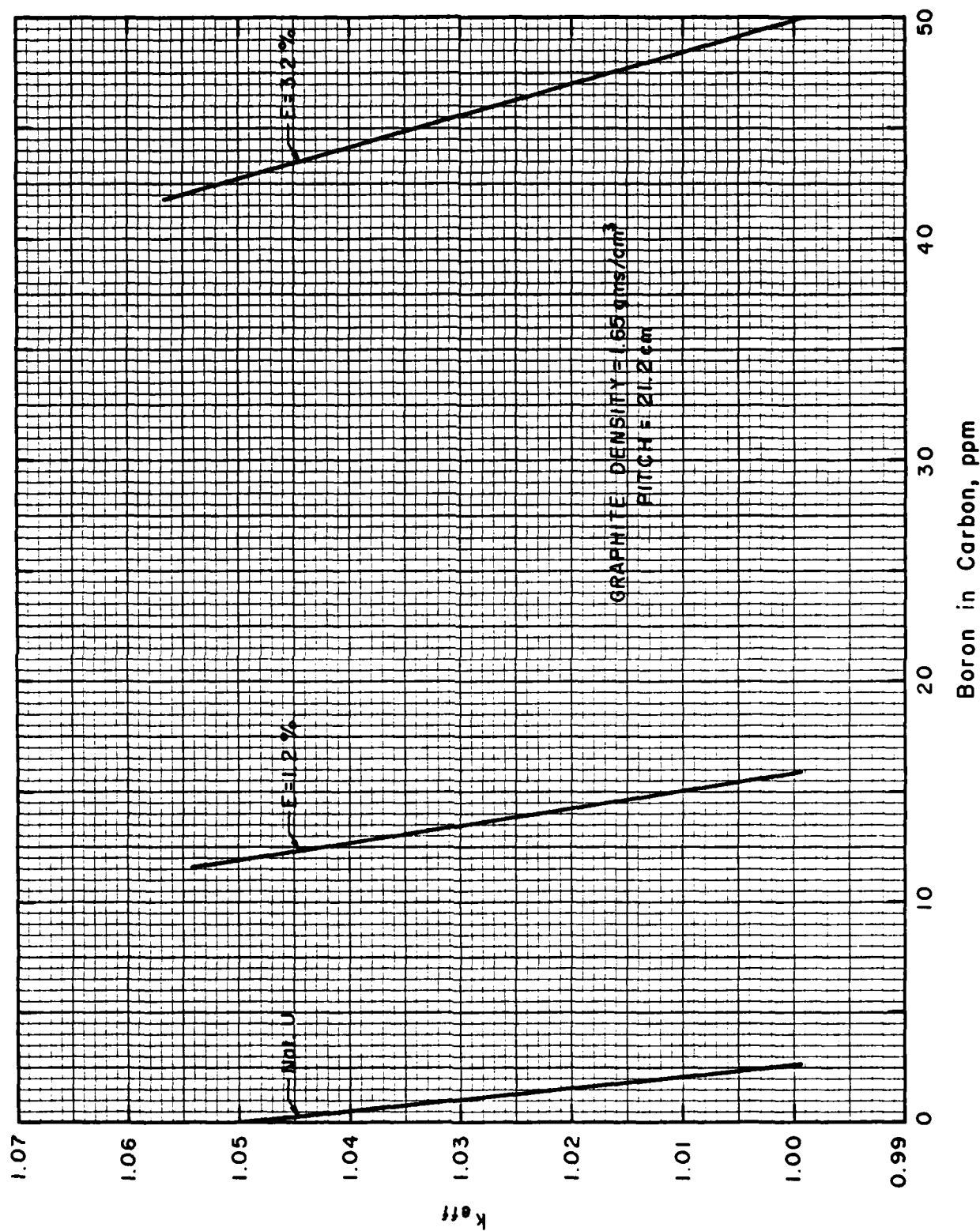


Fig. 4.11 Variation in k_{eff} with graphite impurity levels for fuel of natural, 1.2% and 3.2% enrichment (Mg clad, air-cooled reactor).

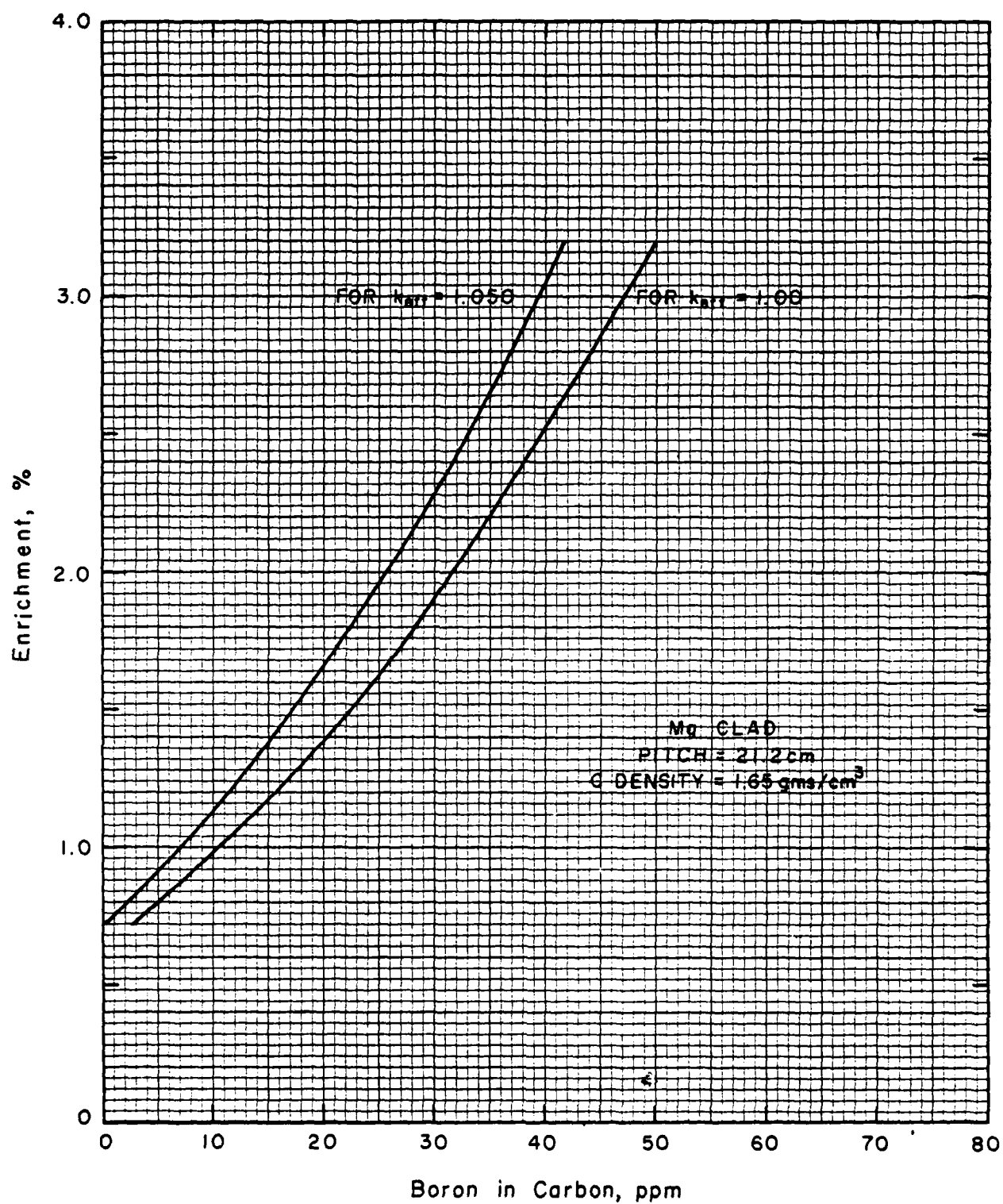


Fig. 4.12 Relationship between enrichment required and impurity level in graphite, for the air-cooled reactor.

5.0 NUCLEAR PERFORMANCE OF THE CO₂-COOLED REACTOR

5.1 General

The 250 Mw(t) CO₂-cooled reactor in this study is based upon the British Calder Hall and the French Marcoule G-2 and G-3 reactor designs. Calculations of the nuclear performance were made with the NULIF multigroup cell homogenization code. Table 3.2 gives the fuel element design and the average thermal performance characteristics of the reference design. For the reference design at a lattice spacing of 8 inches,⁷ the calculated k_{∞} is 1.081 compared to an experimental value of 1.079 reported for the Calder Hall reactor.⁸ The reported values of k_{∞} and k_{eff} measured in the Calder Hall reactor were used to derive a reflector savings of 46 cm, which was then used in subsequent estimates of k_{eff} from the k_{∞} calculated by NULIF. Calculations were made of the effect of lattice spacing, graphite density, fuel enrichment, graphite impurity levels and plutonium production rates. Results of these calculations are described below.

5.2 Lattice Optimization for Reference Design

The effect of lattice spacing and graphite density is shown in Fig. 5.1, in terms of the carbon-to-uranium atom ratio. In addition, variations of fuel element diameter and coolant channel diameter are also indicated in Fig. 5.1. None of the variables investigated, including graphite density, appears to have significant effect on the optimum lattice spacing (pitch). Subsequent calculations were made at the mid-range graphite density (1.65 g/cm³), recognizing that lattice spacings calculated for a graphite density of 1.65 g/cm³ could be corrected for other graphite densities (ρ_c) on the basis of equivalent carbon-to-uranium atom ratio, $k_{eff} = .028 (\rho_c - 1.65)$. The optimum lattice spacing may also be estimated from the relationship, $pitch = 22.37 + 6.32 (1.75 - \rho_c)$.

⁷Directory of Nuclear Reactors Vol. IV, Power Reactors, International Atomic Energy Agency, Vienna, 1962.

⁸1.73 g/cm³ graphite density.

Despite the lack of sensitivity of k_{∞} values to graphite density, there are differences in k_{eff} values, as shown in Fig. 5.2. The optimum lattice spacing decreases with increasing graphite density and the k_{eff} values are slightly higher. Table 5.1 summarizes the optimum lattice spacings and reactivities for the three graphite densities investigated.

The optimum square pitch of 23.0 cm derived here is slightly larger than that employed in the British or French gas-cooled reactors (20.3 cm). At a pitch of 20.3 cm, the calculated k_{eff} for the reference reactor at a graphite density of 1.75 is approximately 1.050 (clean graphite without impurities) compared to 1.053 reported for Calder Hall with unspecified graphite impurities. This is considered to be good confirmation of the analytical model used in the present study. Since a pitch of 20.3 cm was used in Calder Hall and the French G-2 and G-3 reactors, calculations of plutonium production and the effect of neutron-absorbing impurities were made at this pitch, as well as at the calculated optimum lattice spacing of 23 cm.

5.3 Fuel Burnup and Reactivity

Fuel burnup results initially in a rapid decrease in reactivity as xenon and samarium poisons are generated. As plutonium accumulates, the reactivity increases, reaching a maximum value at about 1000 Mwd/mtU (or somewhat greater), and thereafter decreasing as fission product poisons accumulate. The variation in k_{eff} with fuel burnup at the optimum lattice spacings is shown in Fig. 5.3, for graphite densities of 1.50, 1.65 and 1.75 g/cm³. These curves are essentially parallel, showing that the difference in k_{eff} is the same as the initial difference, with little or no change with burnup.

Also shown in Fig. 5.3, is the variation in k_{eff} with burnup for a lattice spacing of 20.3 cm (8 inches) as used in the British and French reactors.

The minimum reactivity determines the capability of the reactor to tolerate graphite impurities and to operate as designed without shutting down when xenon and samarium accumulate. Later in the reactor life, fuel shuffling could be employed in a fuel management scheme utilizing the greater reactivity of the higher burnup fuel to achieve a higher overall core reactivity.

AC9NX707

Table 5.1 REACTIVITIES AND OPTIMUM LATTICE SPACING
IN THE MEDIUM POWER CO₂-COOLED REACTOR CONCEPT*

	<u>Graphite Density</u>		
	<u>1.50 g/cm³</u>	<u>1.65 g/cm³</u>	<u>1.75 g/cm³</u>
Optimum square pitch, cm	24.0	23.0	22.4
k _{eff} at optimum	1.049	1.053	1.056
k _{eff} from reference (2)	-.004	reference	+.003
(k _{eff} at 20.3 cm pitch)		(1.045)	

(1) Natural uranium metal fuel, magnesium cladding.

(2) $k_{eff} = .028 (\rho_c - 1.65)$
Optimum pitch = $22.37 + 6.32 (1.75 - \rho_c)$, where ρ_c is the
graphite density.

5.4 Enriched Fuel

With enriched fuel (and without graphite impurities), the optimum lattice spacing increases with increasing enrichment, as shown in Fig. 5.4, for natural, 1.2% and 3.2 enrichments. Enriched fuel, however, would not normally be used in plutonium production reactors, except as necessary to overcome high levels of neutron absorbing impurities in the graphite moderator. Neutron absorbing impurities tend to cause the optimum lattice to decrease. Consequently, burnup calculations were not made at the higher lattice spacings; rather, the burnup calculations were made at the reference pitch and at the 20.3 cm pitch used in Calder Hall.

5.5 Plutonium Production

The accumulation of plutonium in the reactor fuel with increasing fuel burnup is shown in Fig. 5.5, for natural, 1.2%, and 3.2% enrichments. Over the range of graphite densities studies, the density has a negligible effect on the quantity produced. Increased enrichment, however, markedly reduces the yield of plutonium for a given fuel burnup, as revealed in Fig. 5.5. The amount of plutonium produced at 20.3 cm pitch is slightly higher than at 23 cm pitch because of the greater resonance capture of neutrons in U-238 at the smaller lattice spacing.

The quality of the plutonium produced, as measured by the amount of non-fissile plutonium present (Pu-240 and Pu-242), decreases with increasing fuel burnup. Figure 5.6 shows the increase in percentage of Pu-240 and Pu-242 with increasing fuel burnup, and Fig. 5.7 shows the isotopic composition of the plutonium produced.

The rate of plutonium production, Shown in Fig. 5.8, decreases slightly with increasing fuel burnup as more of the plutonium is burned in the reactor. For illustrative purposes, annual fuel cycle (full power year) would correspond to a fuel burnup of 620 Mwdm/tU. At this burnup, the quantities of plutonium produced, and of feed uranium required, in a full power year are shown in Table 5.2. Increased fuel burnup would result in a lower net average rate of plutonium production, but would require less uranium feed.

AC9NX707

Table 5.2 RATE OF PLUTONIUM PRODUCTION IN THE MEDIUM
POWER CO₂-COOLED REACTOR

<u>Enrichment</u>	<u>Plutonium Production Rate *</u>	
	<u>Pu, kg/EFP yr</u>	<u>Fissile Pu, kg/EFP yr</u>
Natural (@ 23 cm pitch)	80	77
Natural (@ 20.3 cm pitch)	82	79
1.2% (@ 23 cm pitch)	59	57
3.2% (@ 23 cm pitch)	28	28

* For 620 Mwd/mtU burnup; production in kilograms per
equivalent full power year.

5.6 Graphite Impurities

Calculations were made with various assumed impurity levels in the graphite, representing the impurity analytically as boron. Results of these calculations indicate that the optimum pitch decreases with increasing impurity poison level, as shown in Figs. 5.9 and 5.10 for natural and 1.2% enriched fuel. Although the parasitic neutron poisoning effect could be reduced by reducing the design lattice spacing, it is not likely that a reactor would be designed for appreciably reduced pitch. Consequently, calculations were made of the effect of the poison level for both the nominal design optimum lattice spacing and for a pitch of 23 cm used in the Calder Hall type reactors. Results of these calculations are shown in Fig. 5.11 for the two lattice spacings. These data may be cross-plotted, as given in Fig. 5.12, to show the enrichment required to overcome the effect of neutron poisons (as boron) in the graphite. Two curves are shown in Fig. 5.12; one relates poison concentration and enrichment for a k_{eff} equal to that of the unpoisoned lattice with natural enrichment. The second curve is for a k_{eff} of 1.0, and indicates the minimum boron (equivalent) concentration required for a given enrichment to prevent the reactor from operating (i.e., if started, it would quickly be shut down by xenon poisoning). The effect of reduced lattice spacing in minimizing the effect of graphite impurities is clearly evident.

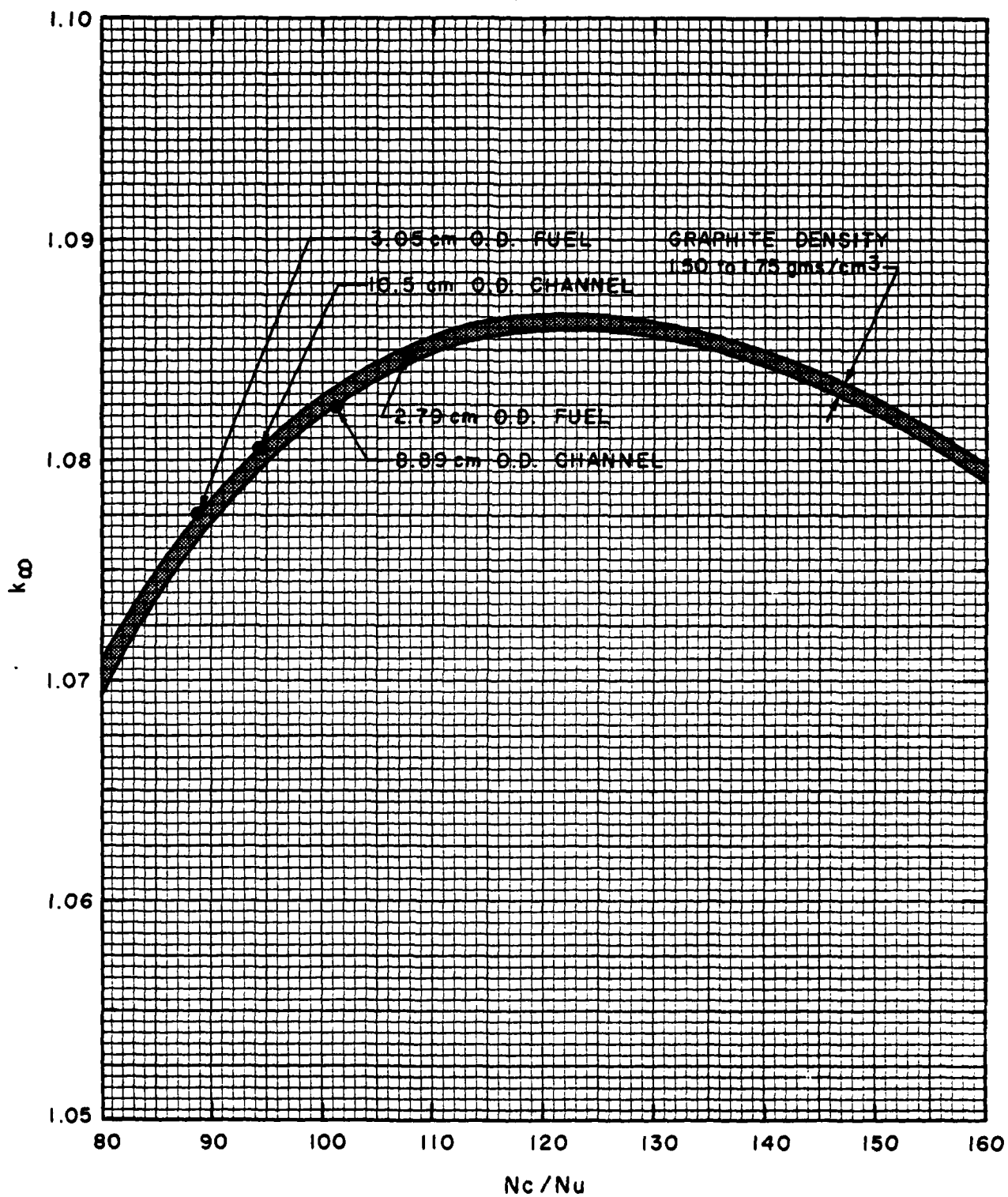


Fig. 5.1 Lattice optimization of k_{∞} versus carbon-to-uranium atom ratio.

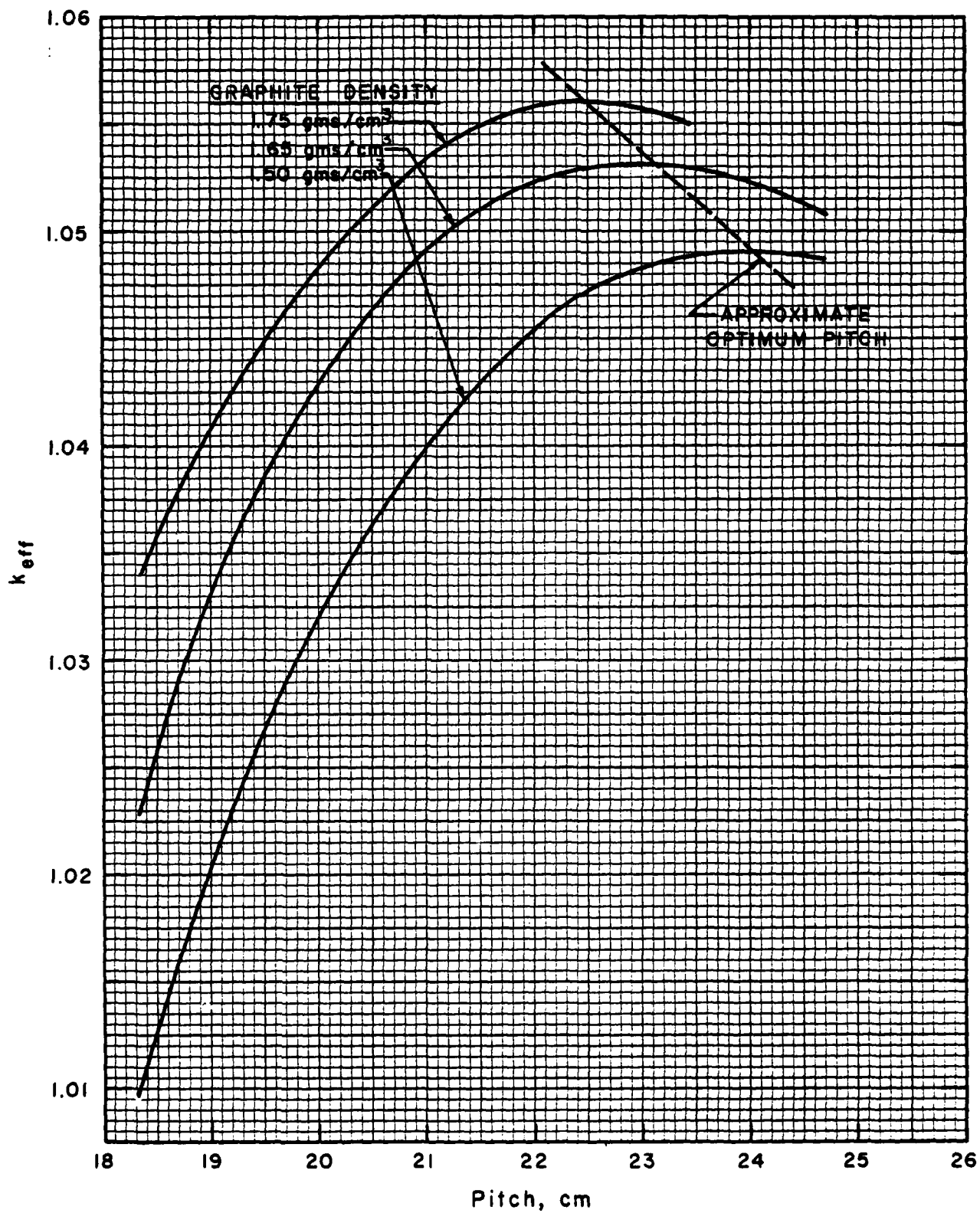


Fig. 5.2 Lattice optimization of k_{eff} for several graphite densities (natural uranium fuel), CO_2 -cooled reactor.

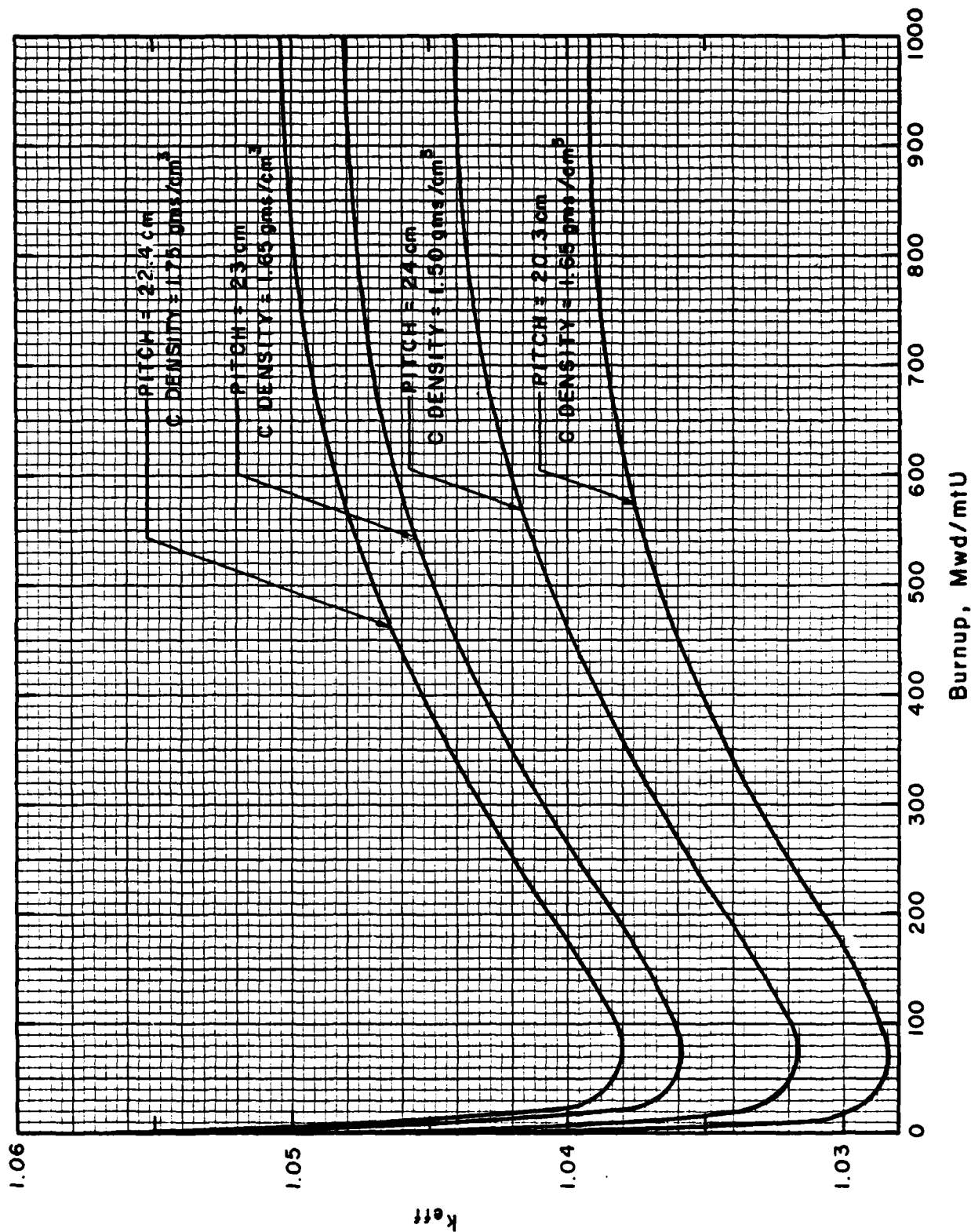


Fig. 5.3 Variation in reactivity with fuel burnup for natural uranium fuel (medium power, CO₂-cooled reactor).

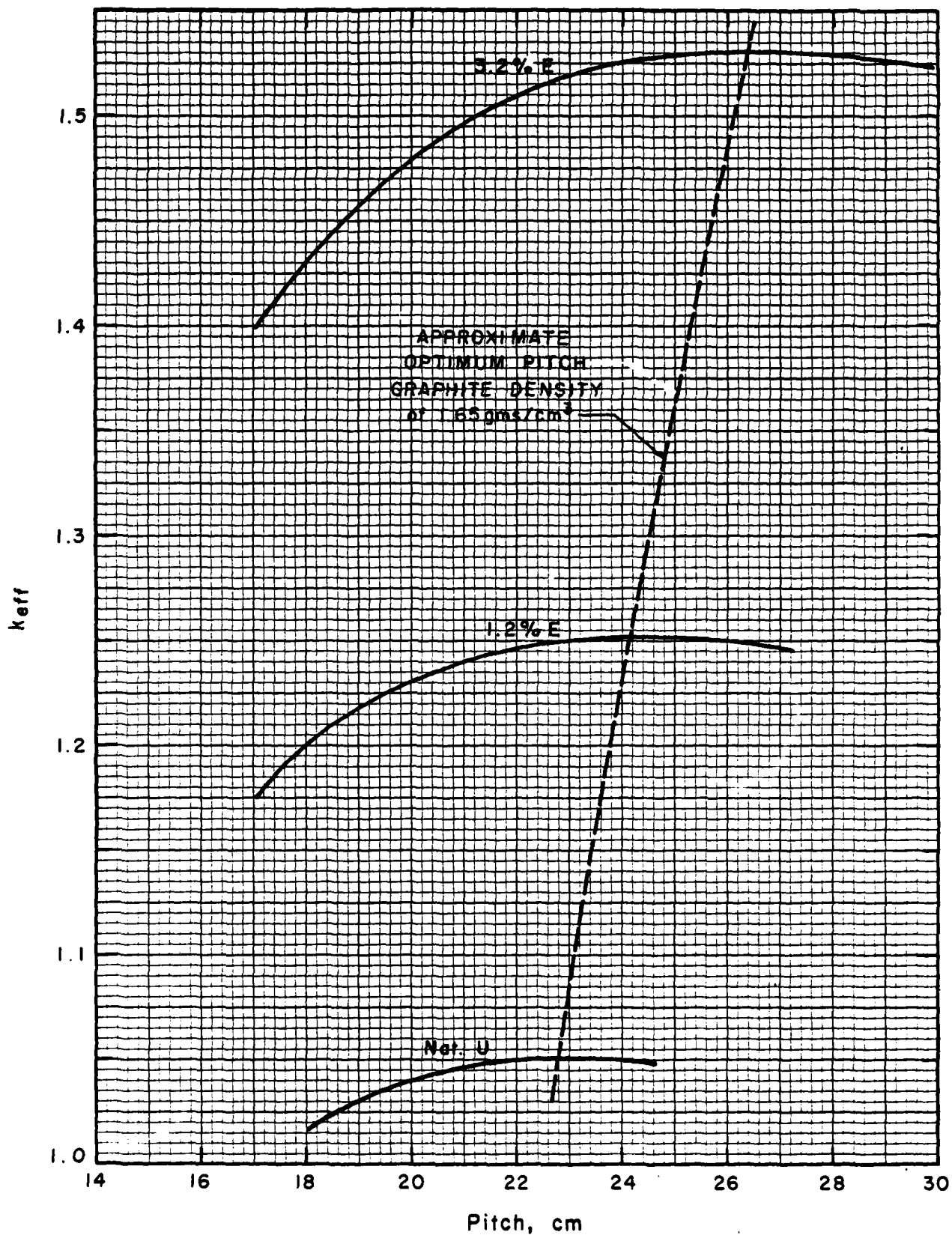


Fig. 5.4 Lattice optimization of k_{eff} for fuel of various enrichments (medium power, CO_2 reactor).

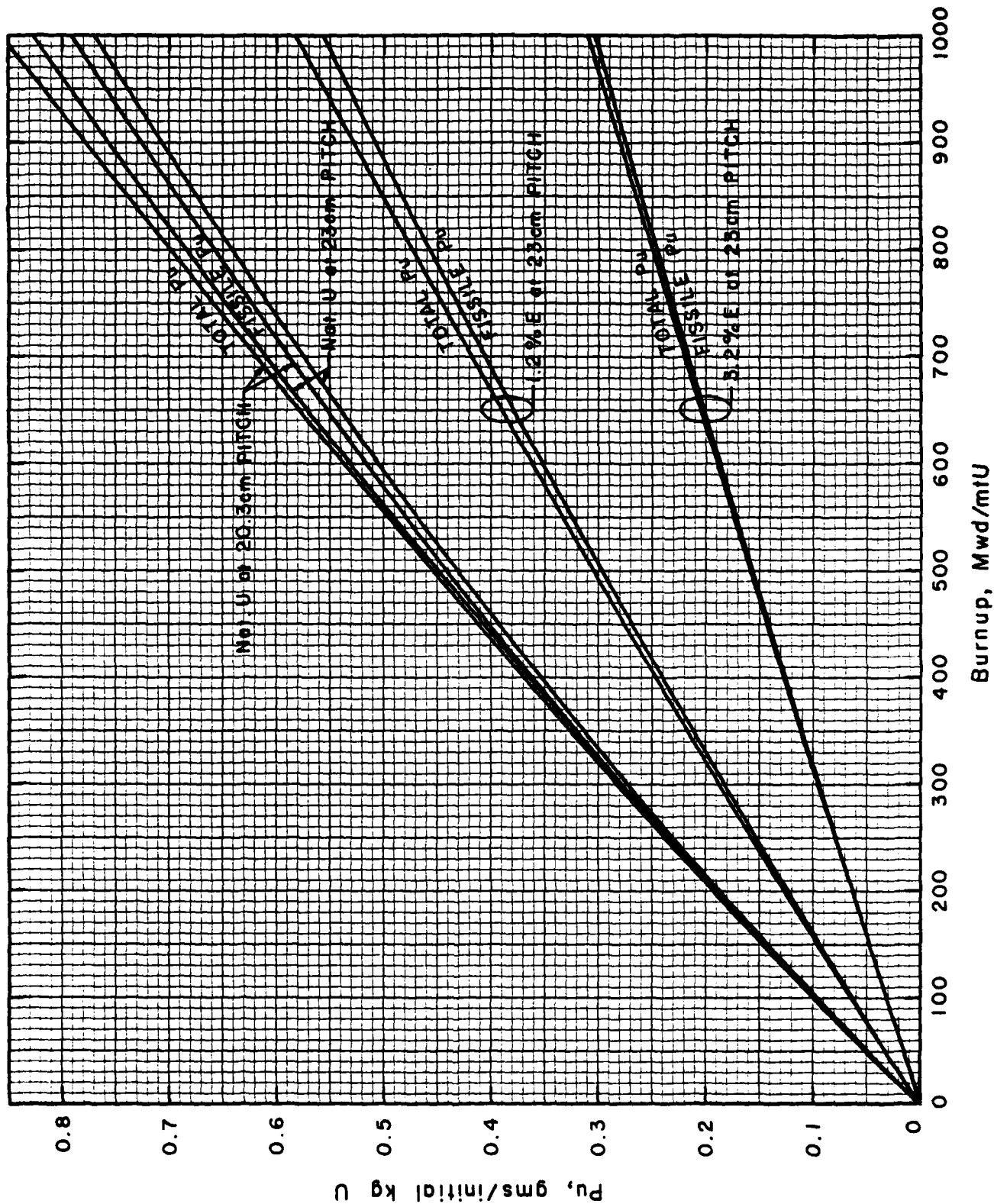


Fig. 5.5 Total and fissile plutonium production in the CO₂-cooled reactor as a function of fuel burnup.

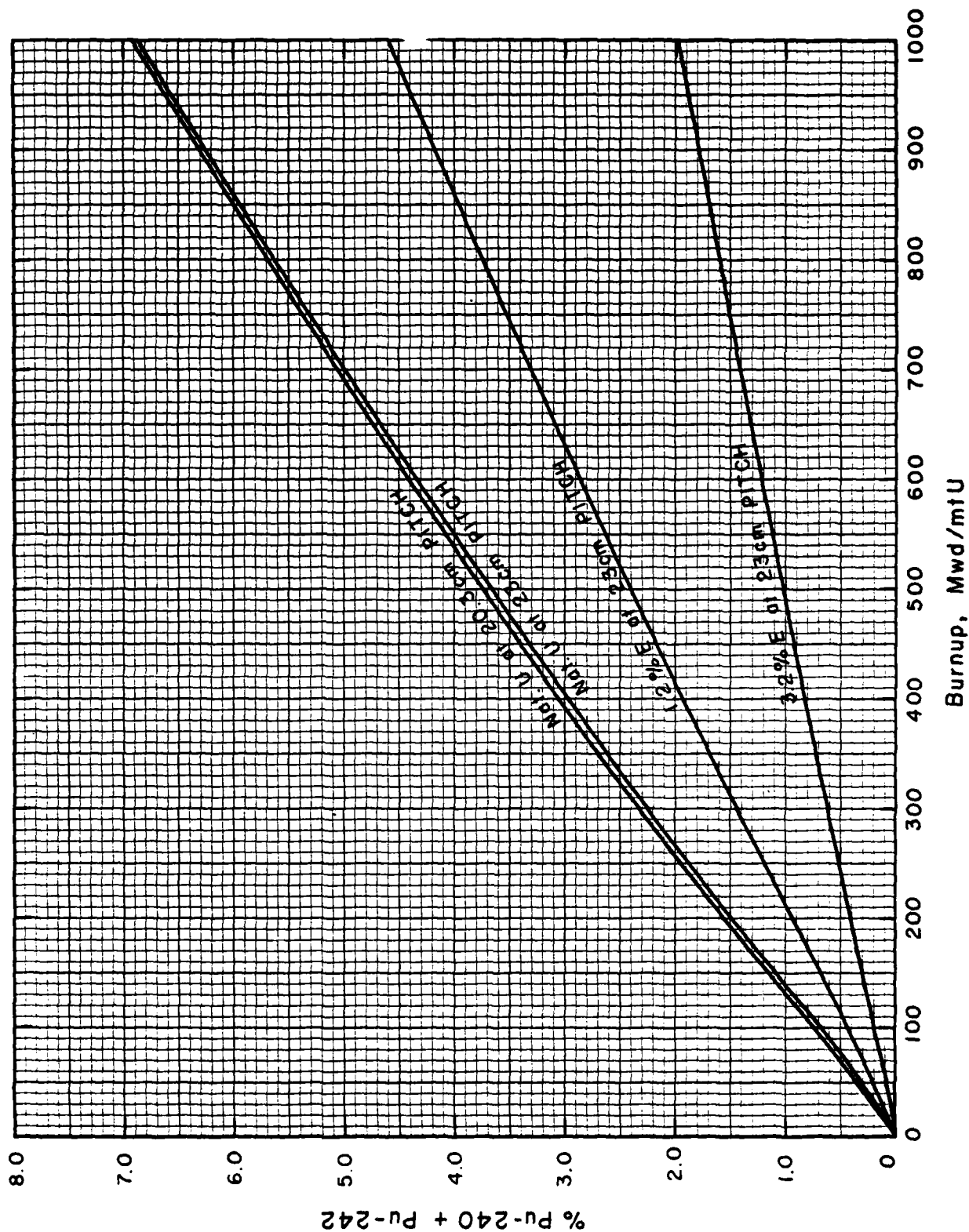


Fig. 5.6 Dependence of the percentage of non-fissile plutonium isotopes on fuel burnup (medium power, CO₂-cooled reactor).

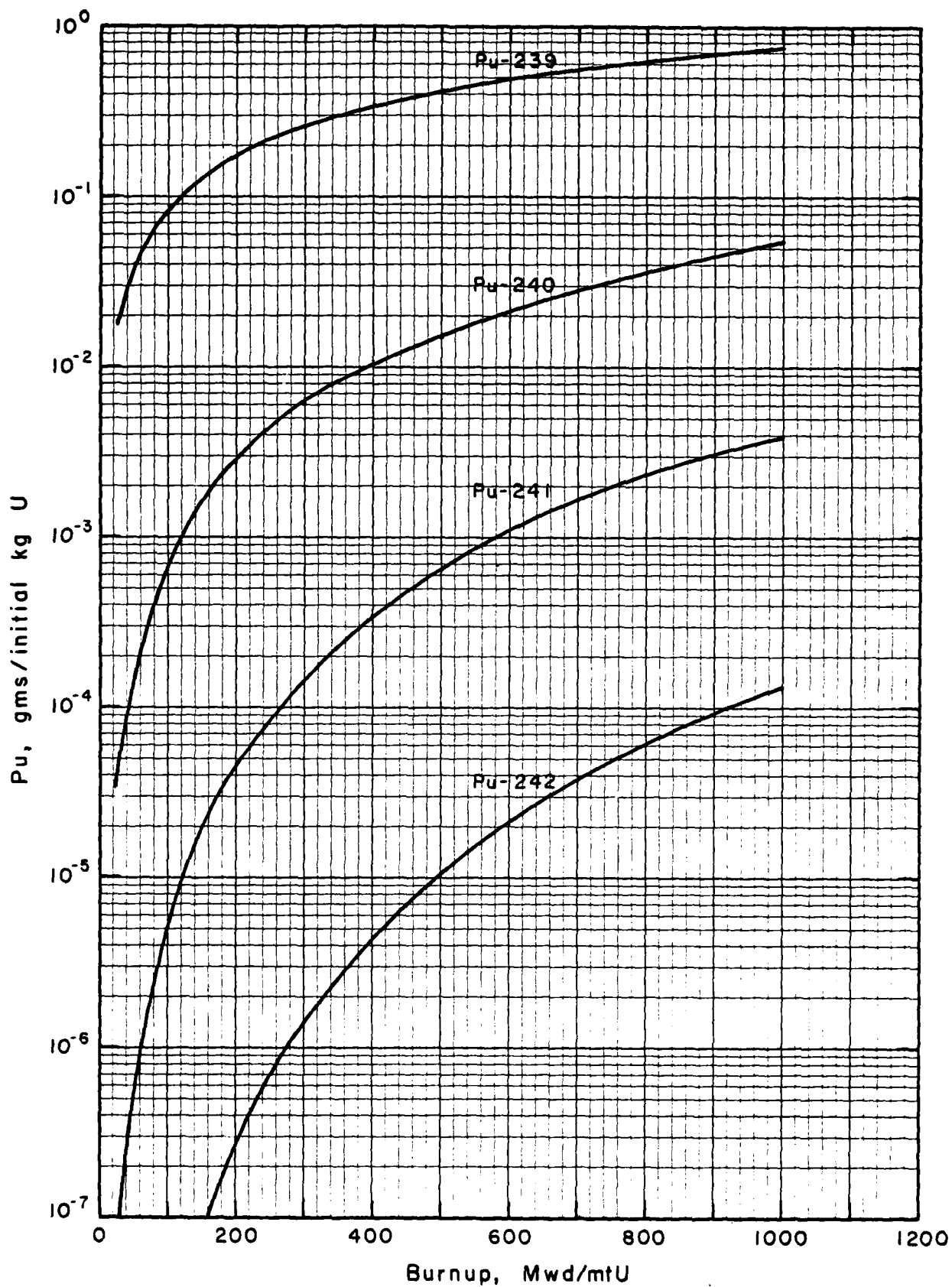


Fig. 5.7 Plutonium isotopics as a function of fuel burnup for natural uranium in the CO₂-cooled reactor.

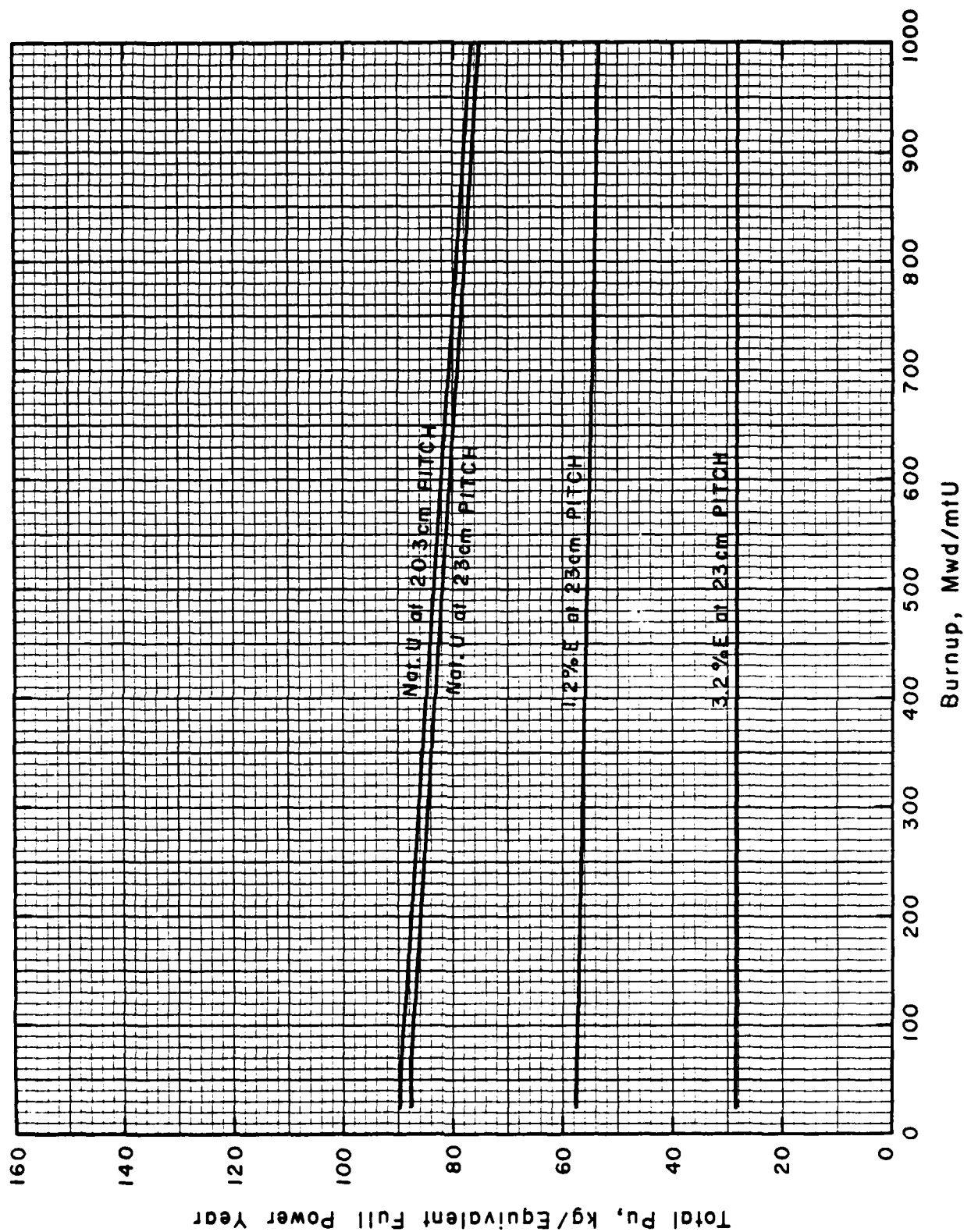


Fig. 5.8 Dependence of plutonium production rate on discharge fuel burnup in the 250 Mw CO₂-cooled reactor.

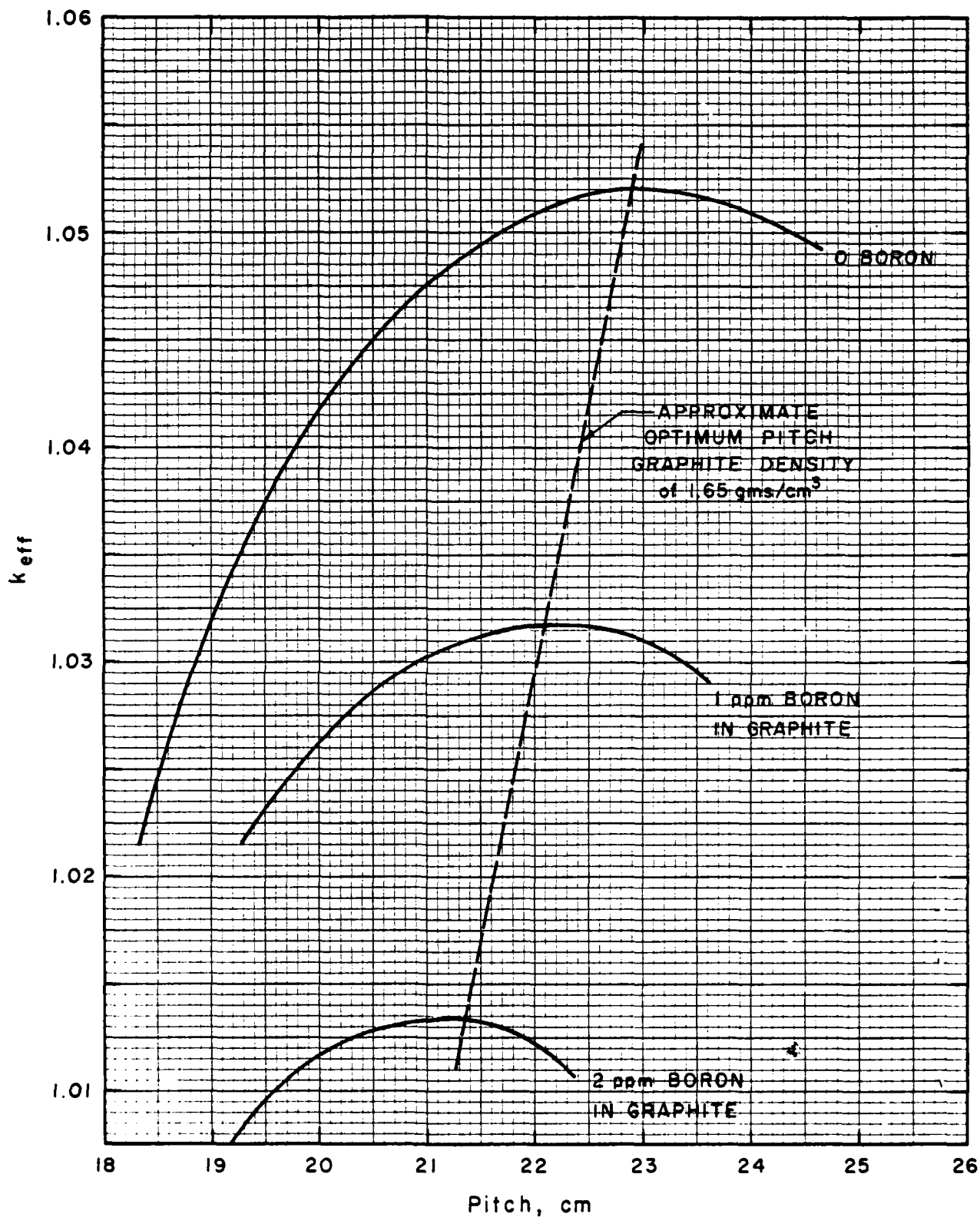


Fig. 5.9 Lattice optimization in the CO₂-cooled reactor for various levels of graphite impurities (as boron) with natural uranium fuel.

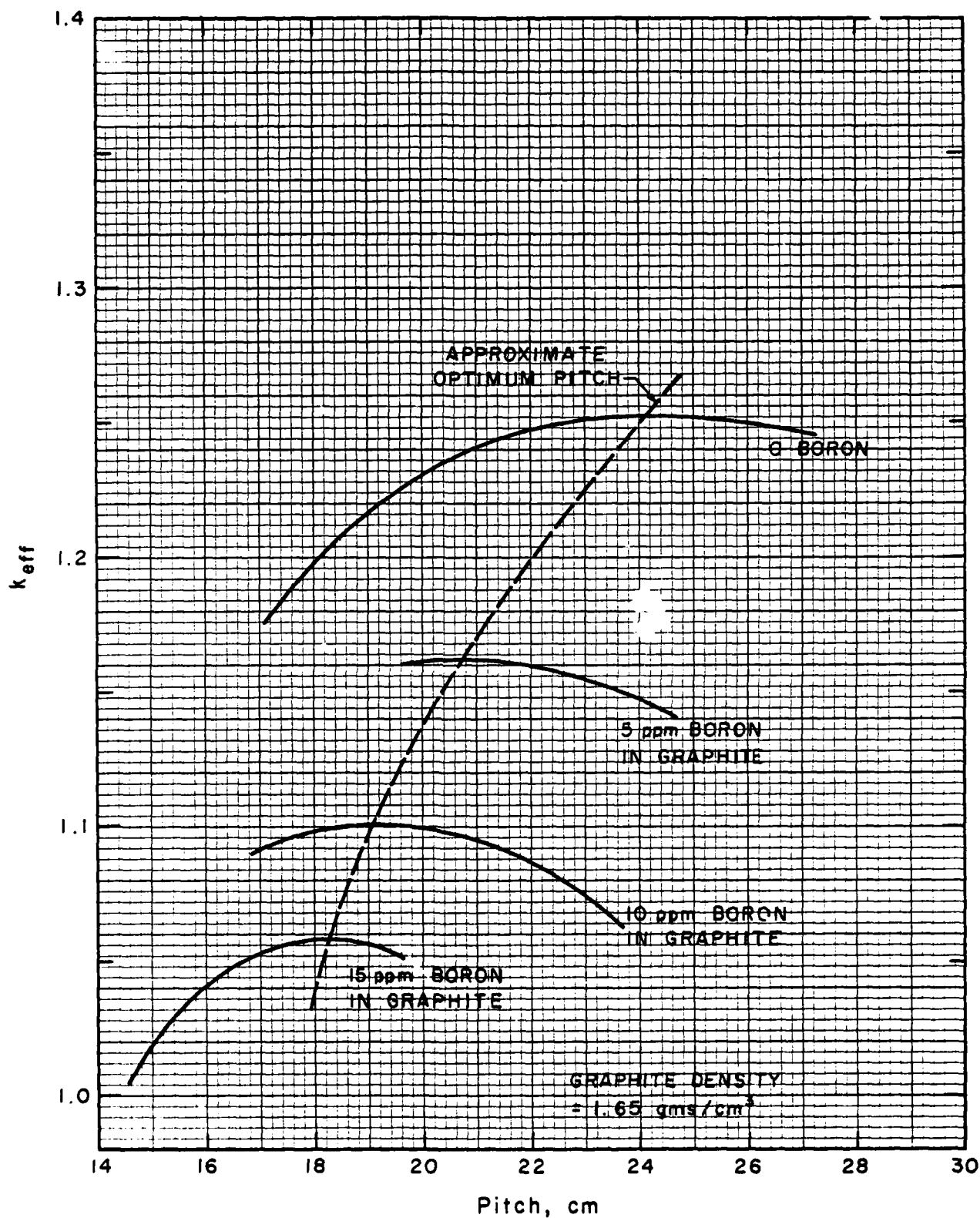


Fig. 5.10 Lattice optimization in the CO₂-cooled reactor for various levels of graphite impurities (as boron) for 1.2% enriched fuel.

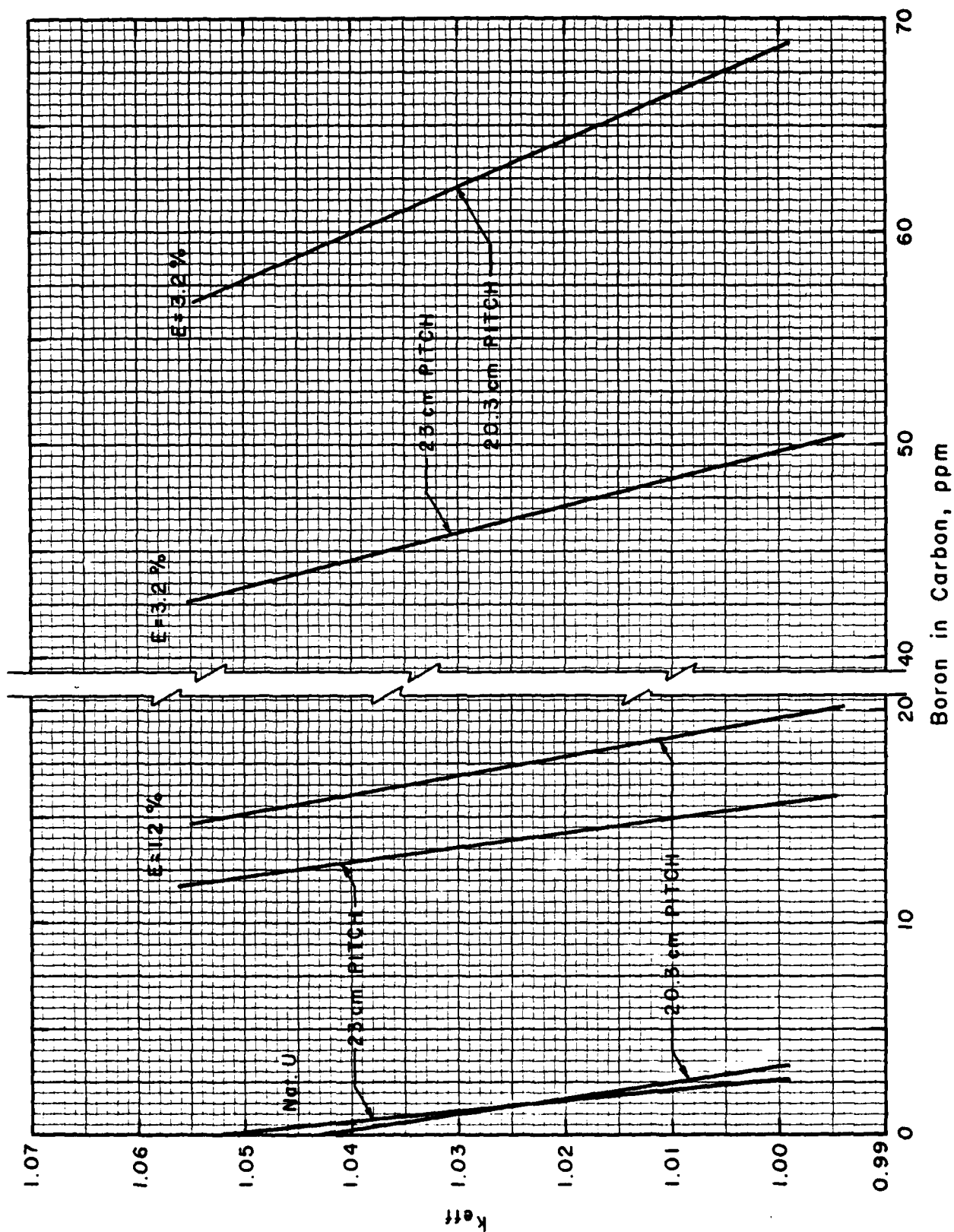


Fig. 5.11 Variation in k_{eff} with graphite impurity levels for fuel of natural, 1.2% and 3.2% enrichment (CO_2 -cooled reactor).

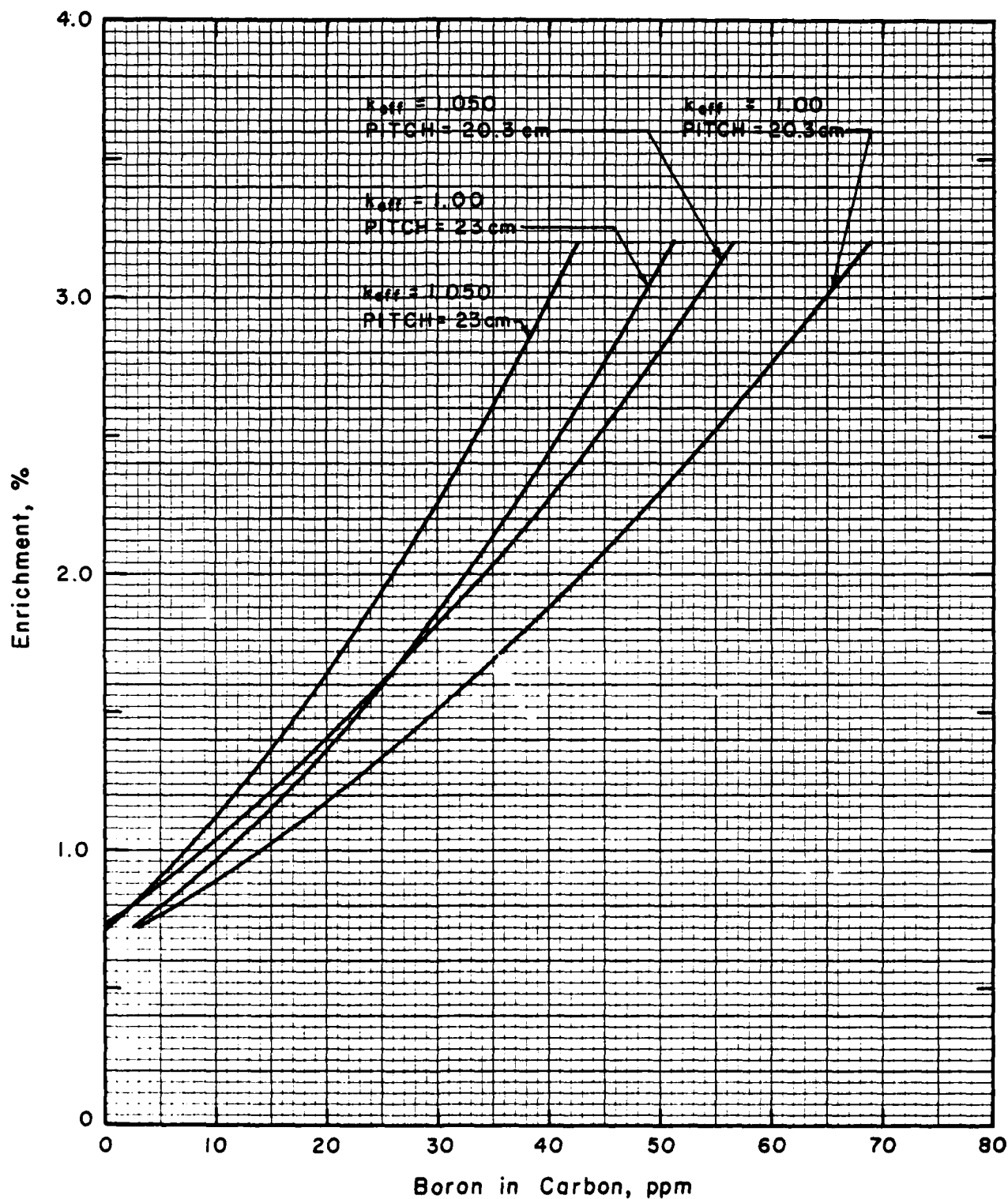


Fig. 5.12 Relationship between enrichment required and impurity level in graphite for the CO₂-cooled reactor.

6.0 NUCLEAR PERFORMANCE OF THE H₂O-COOLED CONCEPT

6.1 General

The nuclear characteristics and performance of a 400 Mw(t), water-cooled, graphite moderated reactor concept have been investigated to determine the effects of graphite density, fuel enrichment and impurity content of the graphite. This section summarizes the results of these investigations. A reference concept as described in Section 3.3 has been utilized as the basis for comparative assessments. The physical dimensions of the fuel slug, cladding, water gap and process tube remain constant at the reference values while examining the effects of alternate graphite and fuel parameters. The number of fuel channels is also held constant throughout the comparisons in order to assure reasonably equal thermal-hydraulic performance for the various alternatives.

Nuclear performance was investigated by point-criticality and burnup calculations utilizing the NULIF code. The fuel cell of the water-cooled reactor concept was modeled as three regions consisting of the fuel slug, a homogenized annulus containing the aluminum cladding, process tube and water, and an outer region for the graphite moderator. Heterogeneous self-shielding and other spatial effects are handled by analytical models within NULIF based on that description. Independent calculations utilizing the THERMOS⁹ code with five separate regions were made to verify the modeling approach, and the thermal spectrum and average cross-sections were found to be in good agreement.

6.2 Natural-Uranium-Fueled Reference Reactor

Initial nuclear analyses were undertaken to establish a design for a natural-uranium-fueled, water-cooled, graphite-moderated reactor. Calculations were performed to establish reasonably simple design using natural uranium fuel and to establish a reference design from which to also investigate the effects of low-enriched uranium fuel, graphite density, and impurity content of the graphite.

⁹Honeck, H. B. "THERMOS: A Thermalization Transport Theory Code for Reactor Lattice Calculations, "BNL-5826 (September 1961).

The fuel and reactor design parameters chosen and described in Section 3.3 are reasonably typical of the range of parameters associated with the Hanford production reactor plants.¹⁰ For the purpose of this study, the reactor design would be assumed to be developed from a conservative, low technology approach for both nuclear and thermal-hydraulic performance. Hence many features of the early Hanford plants might be expected. The fuel slug and process tube design was initially fixed, then scoping calculations for nuclear performance and thermal-hydraulic acceptability were utilized to establish the reference design.

Criticality calculations were performed for various fuel cell spacings (square pitch) to determine the optimum pitch using natural uranium fuel. A graphite density of 1.65 g/cm³ was assumed for the reference design. As shown in Fig. 6.1, the maximum value of the infinite multiplication factor (k_{∞}) occurs at a pitch of approximately 22.5 cm (8.86 in.). The (k_{∞}) value at this pitch was calculated to be 1.050.

Further calculations were performed to obtain a design size with adequate excess reactivity margin to accommodate equilibrium fission product effects, leakage, structure, and calculational uncertainty appropriate to the level of design technology expected to be applied. A reflected, cylindrical reactor with a core size of 11.8 m (38.7 ft) diameter by 7.4 m (24.3 ft) height containing 2155 fuel channels provides about 1.5 percent margin at equilibrium xenon and samarium and yields acceptable and conservative thermal-hydraulic performance. It would be expected that less conservatism and refined designer efforts could yield a smaller reactor size for the design power level of 400 Mw(t), but a low technology approach might be more apt to construct the conservative, larger size initially and then refine operation or increase power level as experience is gained. The description above was thus selected as the reference design for the water-cooled, graphite-moderated reactor concept.

Nuclear characteristics of the reference design of the water-cooled reactor were calculated to assess various reactivity effects. In addition to the effect of pitch on k_{∞} ,

¹⁰Hazards Summary Report, Vol. 3 - Description of the 100-B, 100-C, 100-D, 100-DR, 100-F, and 100-H Production Reactor Plants, Report HW-74094 Vol. 3, Hanford Atomic Products Operation, Richland, Washington, April 1, 1963 (Declassified).

Fig. 6.1 also depicts the effective multiplication factor (k_{eff}) for various cell pitches for the reference number of fuel channels. Figure 6.2 illustrates reactivity variation with burnup revealing the effect of fission product poisoning and fissile plutonium buildup. Table 6.1 presents a summary of the reactivity effects due to fission product poisoning, fuel and graphite temperatures, amount of water and cover gas. Temperature coefficients for the fuel and moderator are negative, and loss of water yields a positive reactivity insertion. Reducing the coolant gap to one-half the reference gap area and increasing the fuel slug diameter to compensate yields a positive reactivity insertion of about 0.25 percent. Moderator temperature could be strongly affected by choice of cover gas, as discussed in Section 3.4; reactivity effects due to increased temperature and neutron absorption for a nitrogen cover gas are given in the table.

6.3 Low-Enriched Uranium Fueled Reactors

The nuclear performance of the water cooled concept utilizing low-enriched uranium fuel was also investigated. The optimum pitch for low-enriched fuel was first examined utilizing the reference fuel slug, clad, water gap and process tube size. Figure 6.3 compares the variation in k_{eff} with pitch for enrichments of 1.2% and 3.2% U^{235} with that for natural uranium fuel. The number of fuel channels for each of these cases is held constant at the reference number of 2155 channels. The intersections with the vertical line indicates the k_{eff} value for the enriched fuel at the design pitch that is optimum for natural uranium fuel. The slanted line indicates the trend in optimum pitch with enrichment. The optimum values increase from 22.5 cm to approximately 24 cm and 26 cm as enrichment is increased from natural to 1.2% and 3.2%, respectively. Separate calculations for 20% enriched fuel yield an optimum pitch of about 29 cm.

Burnup characteristics and plutonium production for the low-enriched fuel were also examined. Figure 6.4 compares k_{eff} as a function of burnup for the natural uranium case and the 1.2% and 3.2% enriched cases. Burnup characteristics vary between the different cases due to differences in spectrum, absolute flux, size and associated power density. Table 6.2 describes these differences and the resultant effects on plutonium production. Figures 6.5, 6.6, and 6.7 illustrate the plutonium production and isotopic composition as a function of burnup for the same cases.

AC9NX707

Table 6.1 : REACTIVITY EFFECTS FOR THE REFERENCE
WATER-COOLED REACTOR

<u>Condition</u>	k_{eff}	Δk <u>(Percent from Reference)</u>
Reference - Hot, BOL	1.032	0.0
Fuel - 120°C (248°F)		
Water - 80°C (185°F)		
Graphite - 250°C (482°F)		
Equilibrium Xe and Sm	1.016	-1.6
Elevated Fuel Temperature		
177°C (350°F)	1.031	-0.08
260°C (500°F)	1.030	-0.19
Elevated Graphite Temperature		
371°C (700°F)	1.030	-0.24
482°C (900°F)	1.028	-0.39
848°C (1558°F)	1.023	-0.87
Dry, Cold (20°C, 68°F)	1.050	+1.7
Dry, Reference Temperatures	1.040	+0.78
One-half Coolant Gap (Fuel Slug-3.065 cm O.D.)	1.035	+0.25
Nitrogen Cover Gas (for 20% void)	1.029	-0.28

AC9NX707

Table 6.2 COMPARISON OF NUCLEAR CHARACTERISTICS FOR
DIFFERENT FUEL ENRICHMENTS IN THE WATER-COOLED REACTOR

<u>Characteristics</u>	<u>Enrichment</u>		
	<u>Natural</u>	<u>1.2%</u>	<u>3.2%</u>
Optimum pitch (cm)	22.5	24	16
k_{eff} , BOL	1.032	1.229	1.499
Core size, Dia x Ht (m)	11.8x7.4	12.6x7.9	13.6x8.6
Fuel loading, mtU	274	293	319
Moderator graphite, Mt	1289	1574	2015
Reflector graphite, Mt	971	1095	1271
Specific power, Mw/mtU	1.46	1.36	1.26
Power density, w/cm ³	0.50	0.41	0.32
Neutron flux levels			
Fast (>1.86 eV)	8.2×10^{12}	5.7×10^{12}	3.6×10^{12}
Thermal (<1.86 eV)	1.4×10^{13}	9.1×10^{12}	5.2×10^{12}
Maximum plutonium production, kg per full power year	145	91	42

6.4 Effects of Graphite Density

The effects of graphite density on nuclear characteristics and performance of the water-cooled reactor concept are reasonably similar to those exhibited by the air-cooled and gas-cooled reactors. One similarity is the negligible effect of graphite density on k_{∞} when examined in terms of the carbon-to-uranium ratio. The optimum fuel cell pitch for varying graphite density is thus essentially set by the optimum carbon-to-uranium ratio. For natural uranium fuel, the optimum atom ratio is approximately 94; for 1.2% and 3.2% enriched fuel the optimum ratios are about 102 and 125, respectively.

The reactivity effects and optimum fuel cell pitches for graphite densities of 1.50, 1.65 and 1.75 g/cm³ were investigated for the water-cooled reactor with natural uranium fuel and with 1.2% and 3.2% enriched fuel. Figures 6.8, 6.9, and 6.10 depict k_{eff} for the different fuels as a function of pitch for the three graphite densities. The optimum pitches show shifts inversely related to changes in graphite density as required to reach the optimum carbon-to-uranium ratio. Maximum reactivity (k_{eff}) maintains essentially the same value within calculational accuracy for a given fuel as graphite density varies, indicating that leakage is not significantly affected for the water-cooled concept. This is due to the large overall reactor sizes and possibly to the constant amount of water associated with each fuel cell regardless of graphite density.

Figures 6.11 and 6.12 summarize the effects of graphite density and fuel enrichment, respectively, on optimum fuel cell pitch.

6.5 Effects of Graphite Impurities

The effects of possible impurities in the graphite on the nuclear characteristics of the water-cooled reactor have been examined with boron as a representative impurity. The boron equivalence of other substances are given in Table 2.2. As with the other reactor concepts, boron impurity causes the core reactivity to decrease, but part of the decrease can be regained by a shift to smaller fuel cell

AC9NX707

pitch. Figure 6.13 illustrates this effect for 1.2% enriched uranium fuel. An impurity level equivalent to 11 ppm boron can yield a decrease in reactivity of about 0.2 Δk from the optimum value for no impurity. About 0.06 Δk can be regained, however, by reducing the pitch from 24 cm to 17 cm. Reactor operation at the 24 cm pitch design may be precluded with an impurity level of about 15 ppm boron, but to preclude operation at a smaller pitch, an impurity level in excess of about 25 ppm would be required. As discussed in Section 7.4, an impurity such as boron will deplete (burn-out) with reactor operation: consequently, reactor performance optimization considering impurity effects at beginning-of-life may be offset later in operation.

For the water-cooled reactor design optimized for natural uranium fuel (pitch = 22.5 cm) without graphite impurity, the combined effects of substituting enriched fuel and adding boron to the graphite were examined. Figure 6.14 illustrates the effect on k_{eff} for these substitutions. A boron concentration of greater than 1.7 ppm is seen to preclude operation with natural uranium fuel. Concentrations of 14.9 and 46.6 ppm are seen to preclude operation with 1.2% and 3.2% enriched uranium fuel, respectively. Figure 6.15 illustrates the minimum required enrichment for criticality for varying levels of boron content in the graphite moderator of the water-cooled reactor concept.

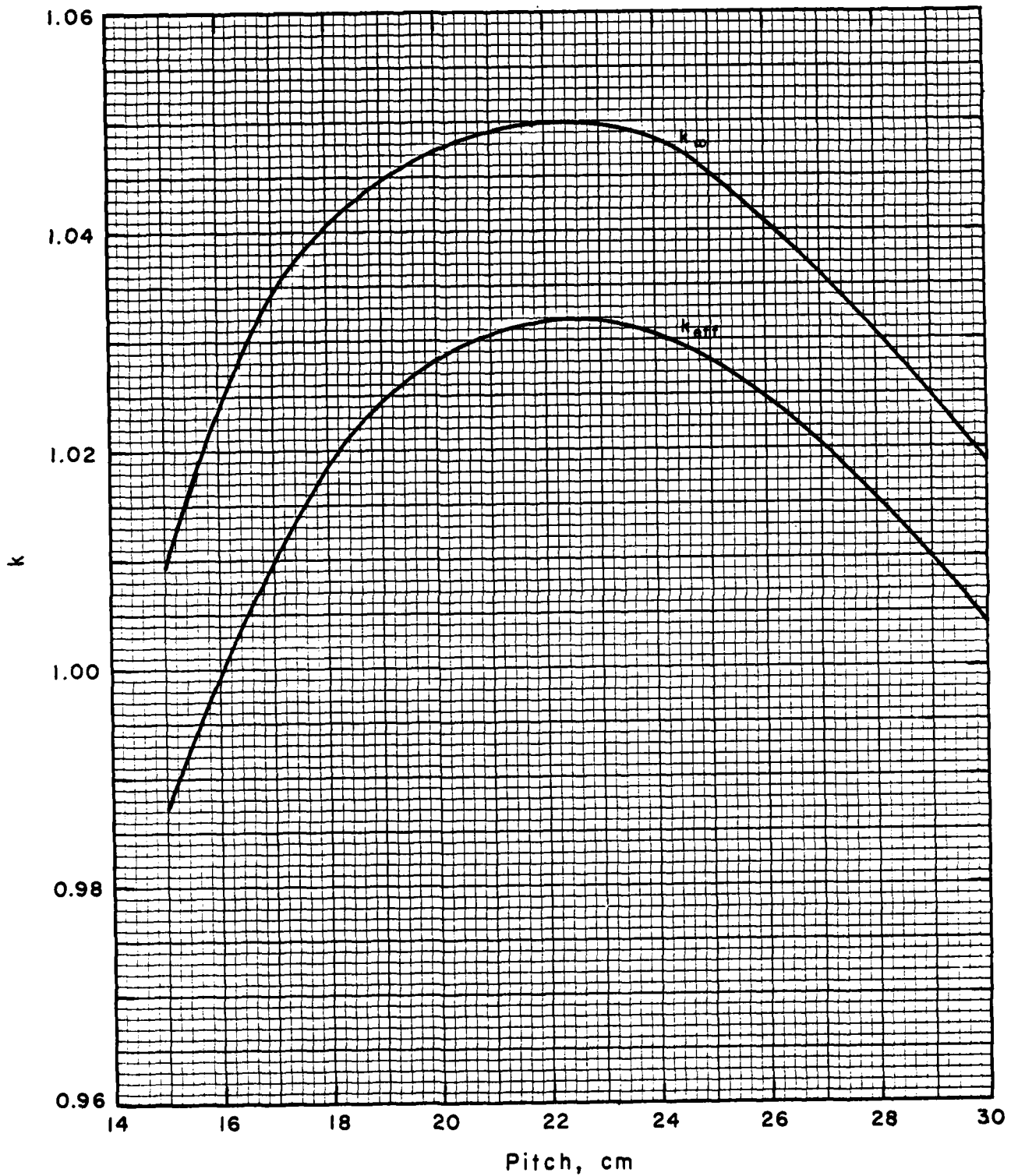


Fig. 6.1 Lattice optimization for natural-uranium-fueled, water-cooled reactor.

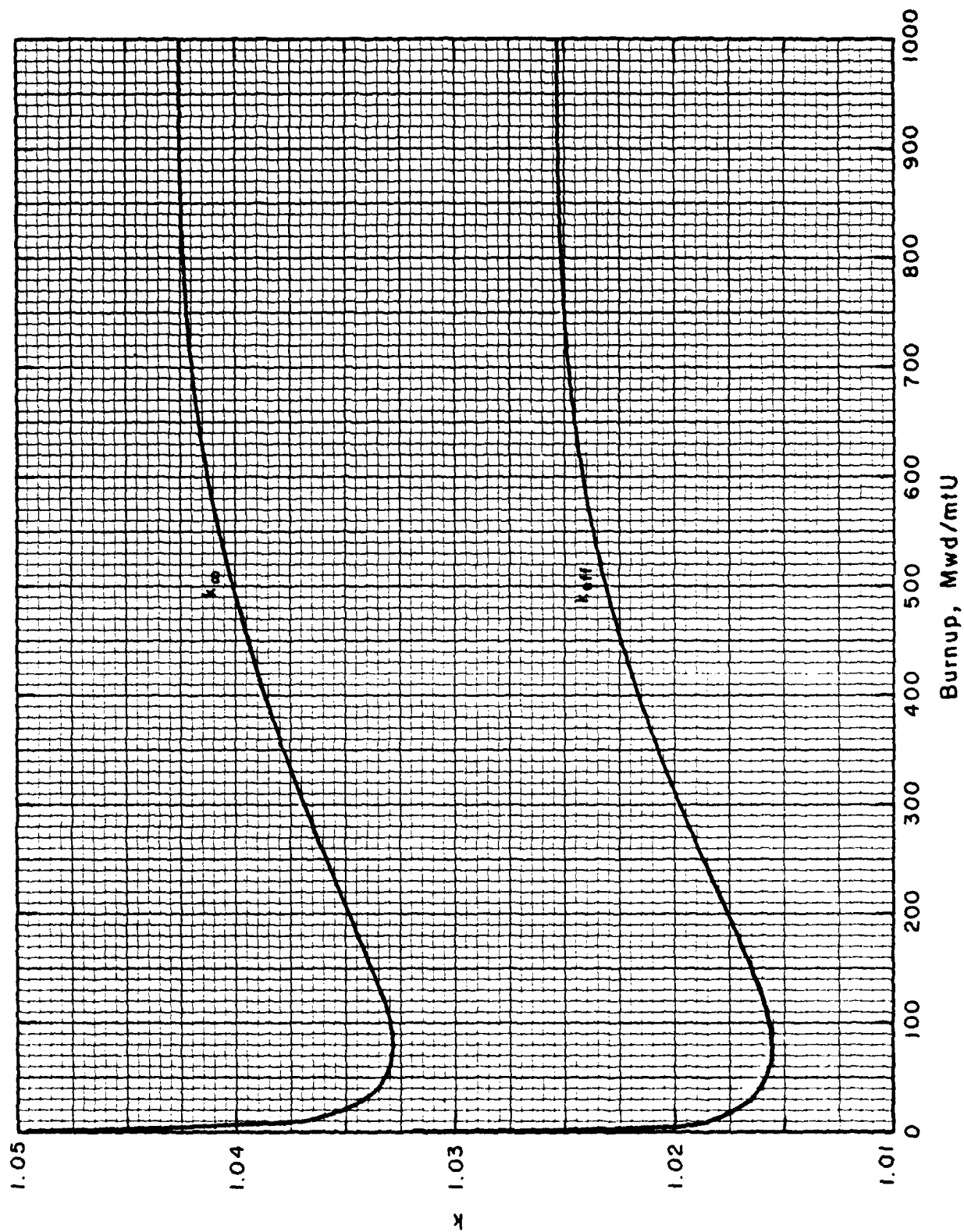


Fig. 6.2 Reactivity variation with fuel burnup for reference natural uranium-fueled, water-cooled reactor (pitch = 22.5 cm, graphite density = 1.65 g/cm³).

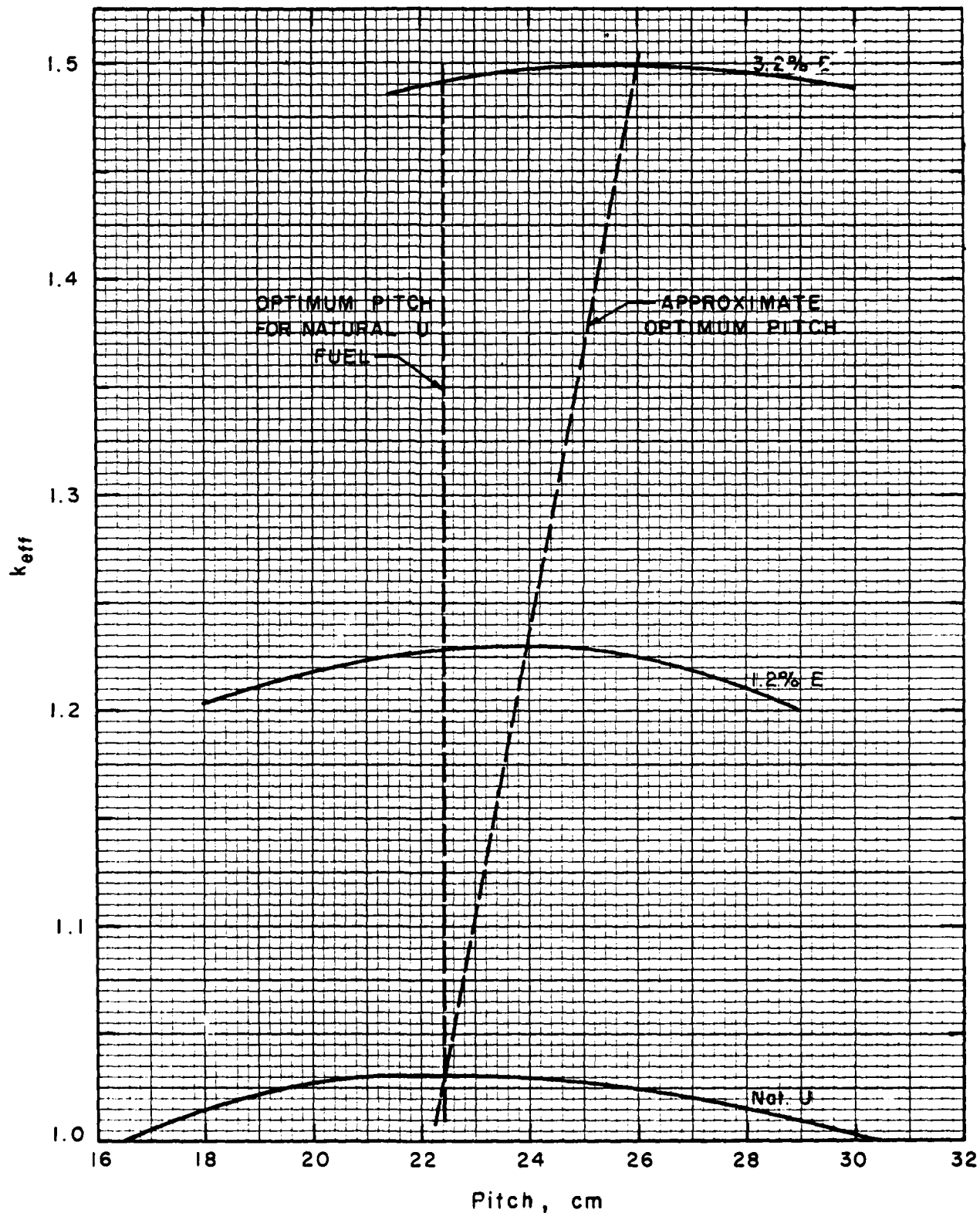


Fig. 6.3 Lattice optimization of k_{eff} for fuel of various enrichments (high-power, water-cooled reactor).

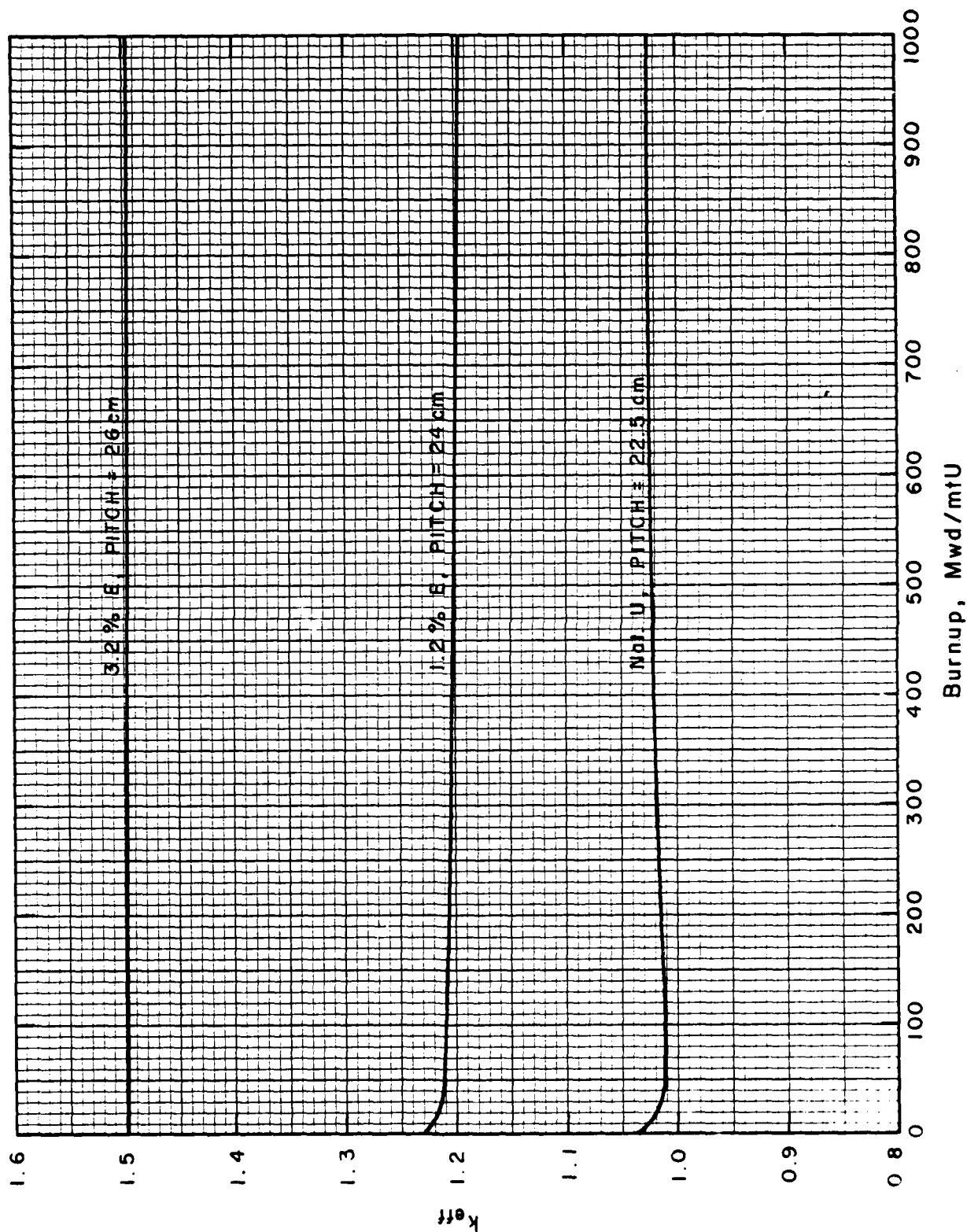


Fig. 6.4 Variation in reactivity with burnup for low-enriched uranium-fueled, water-cooled reactor.

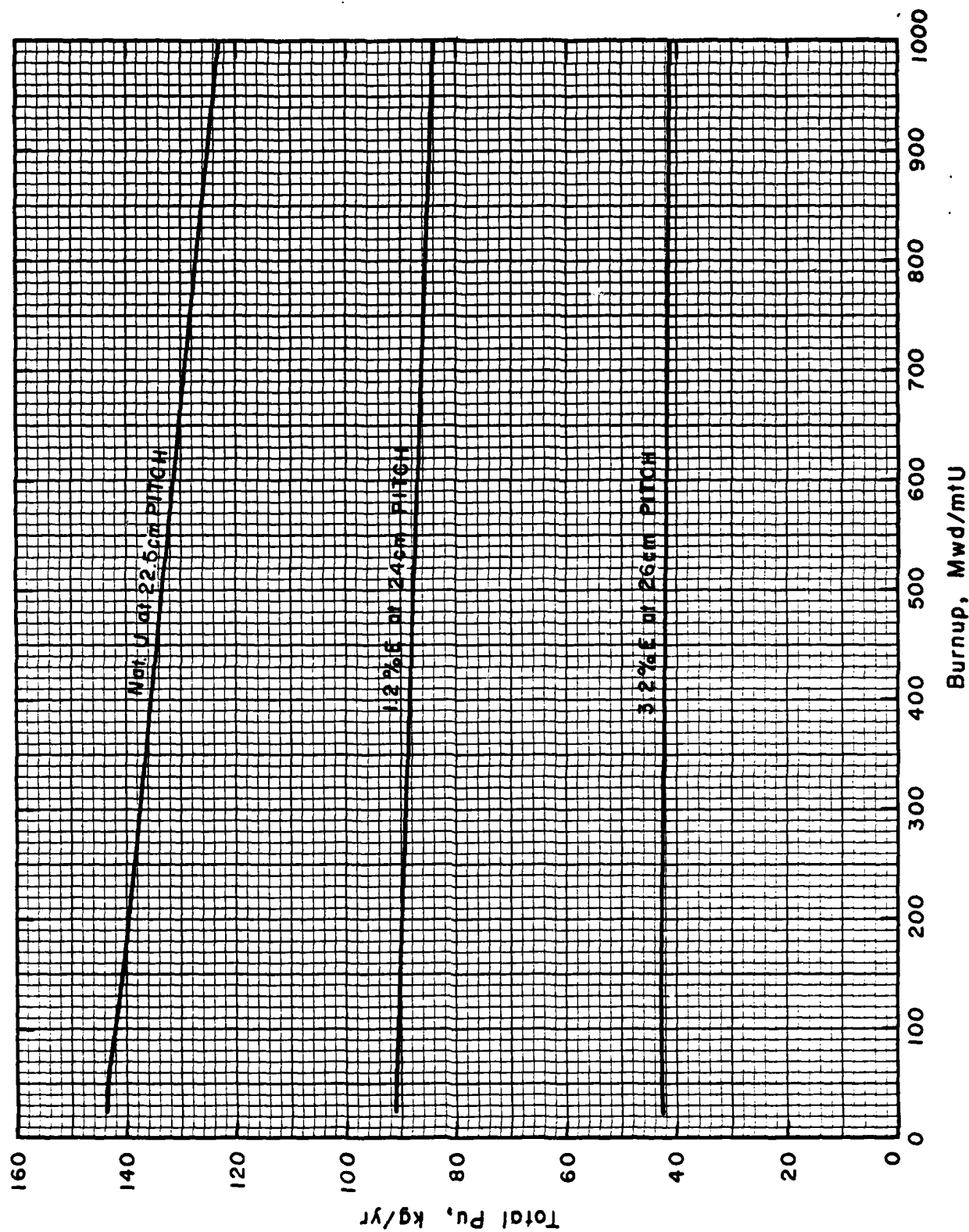


Fig. 6.5 Plutonium production variation with design burnup for low-enriched uranium-fueled, water-cooled reactor.

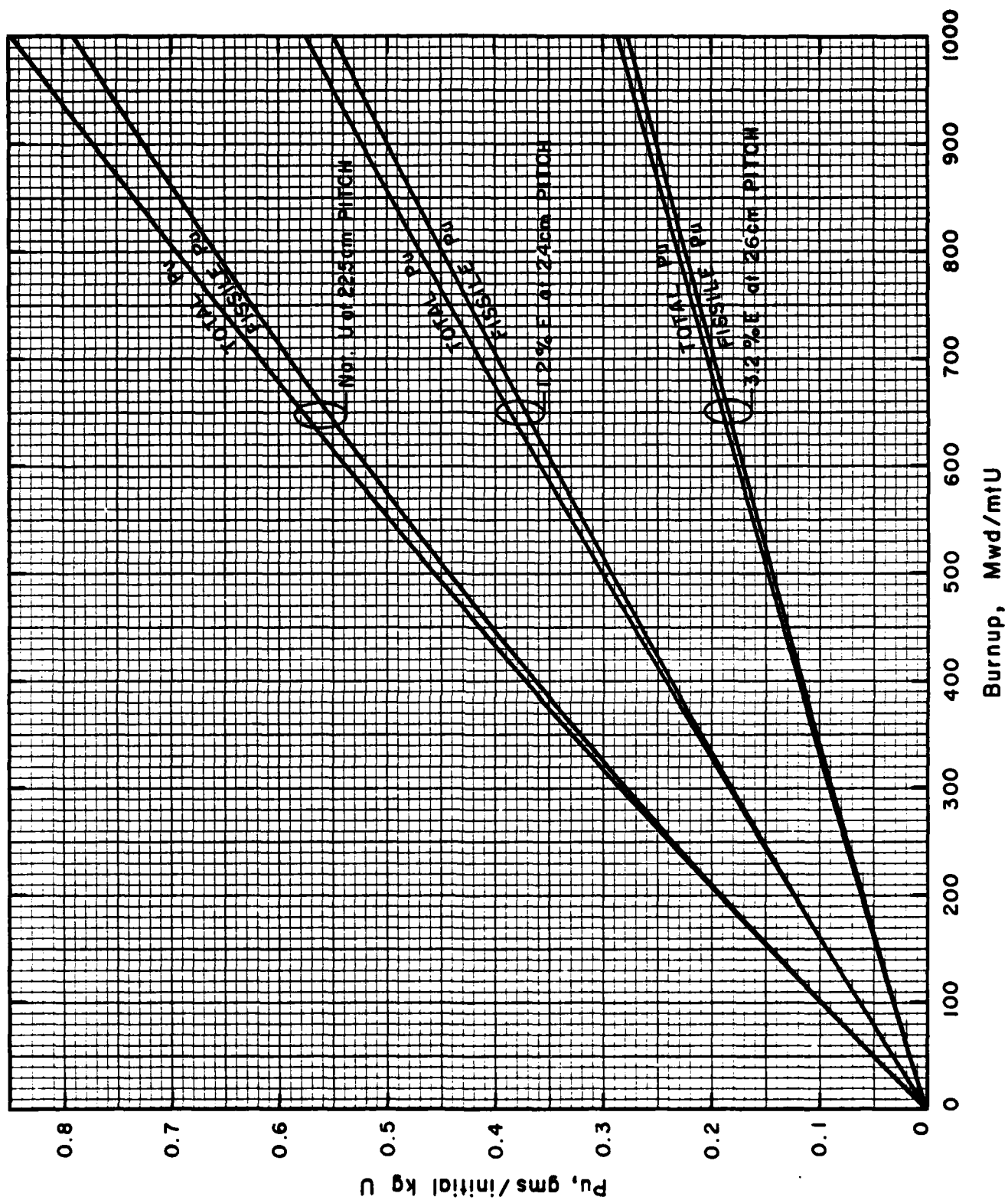


Fig. 6.6 Specific plutonium production for low-enriched uranium-fueled, water-cooled reactor.

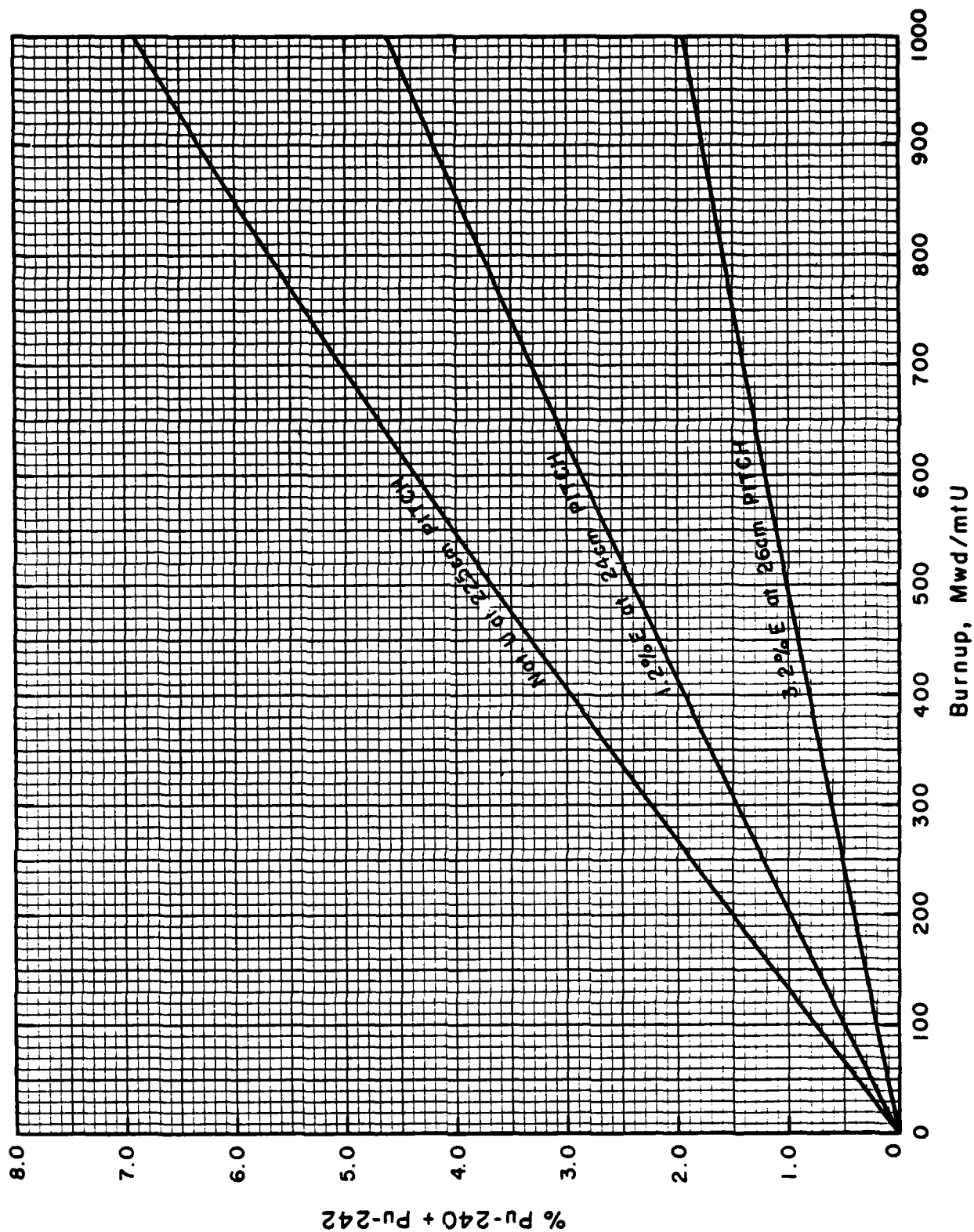


Fig. 6.7 Plutonium isotopic composition in low-enriched uranium-fueled, water-cooled reactor.

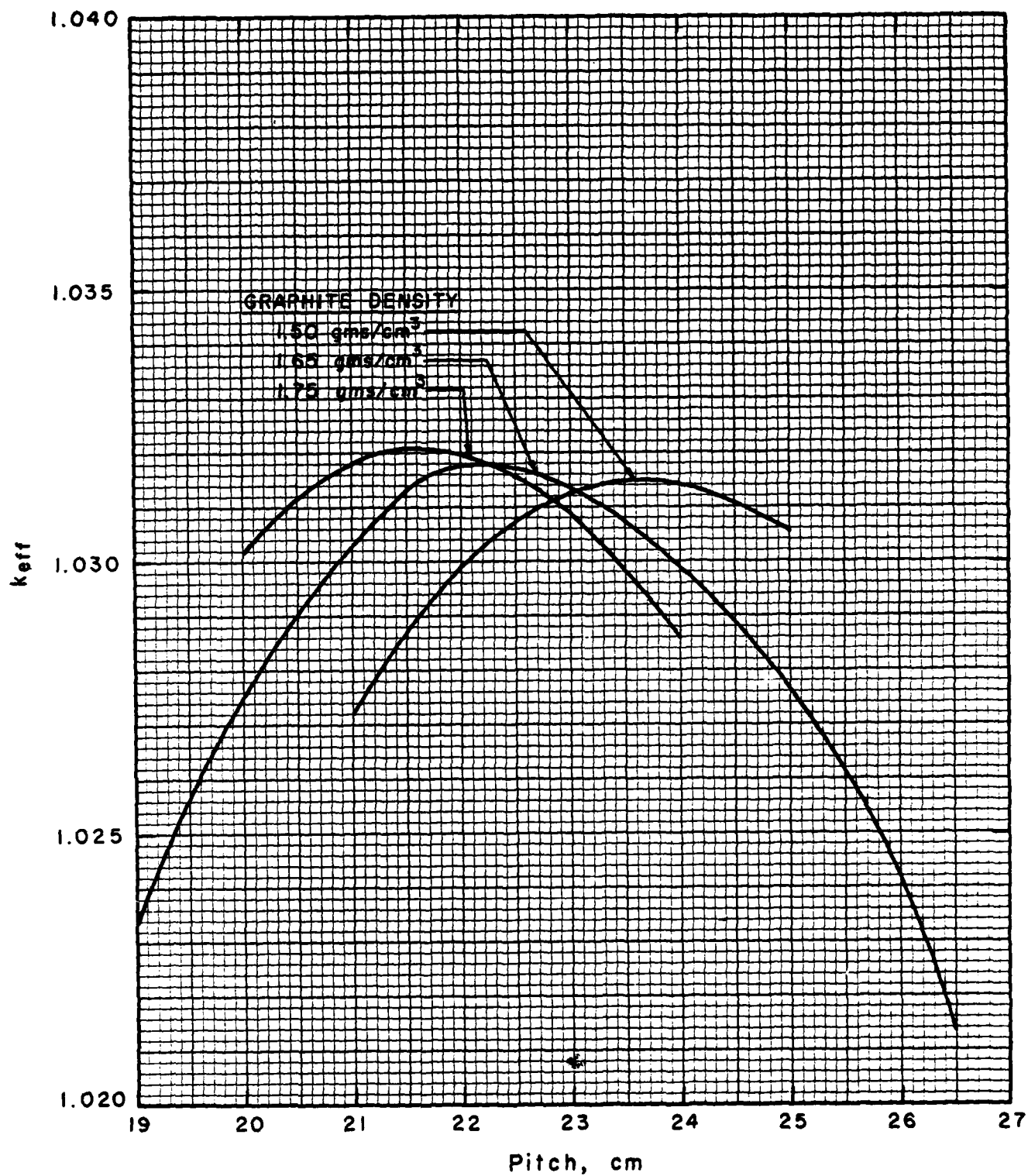


Fig. 6.8 Reactivity variation with pitch for different graphite densities for natural uranium-fueled, water-cooled reactor.

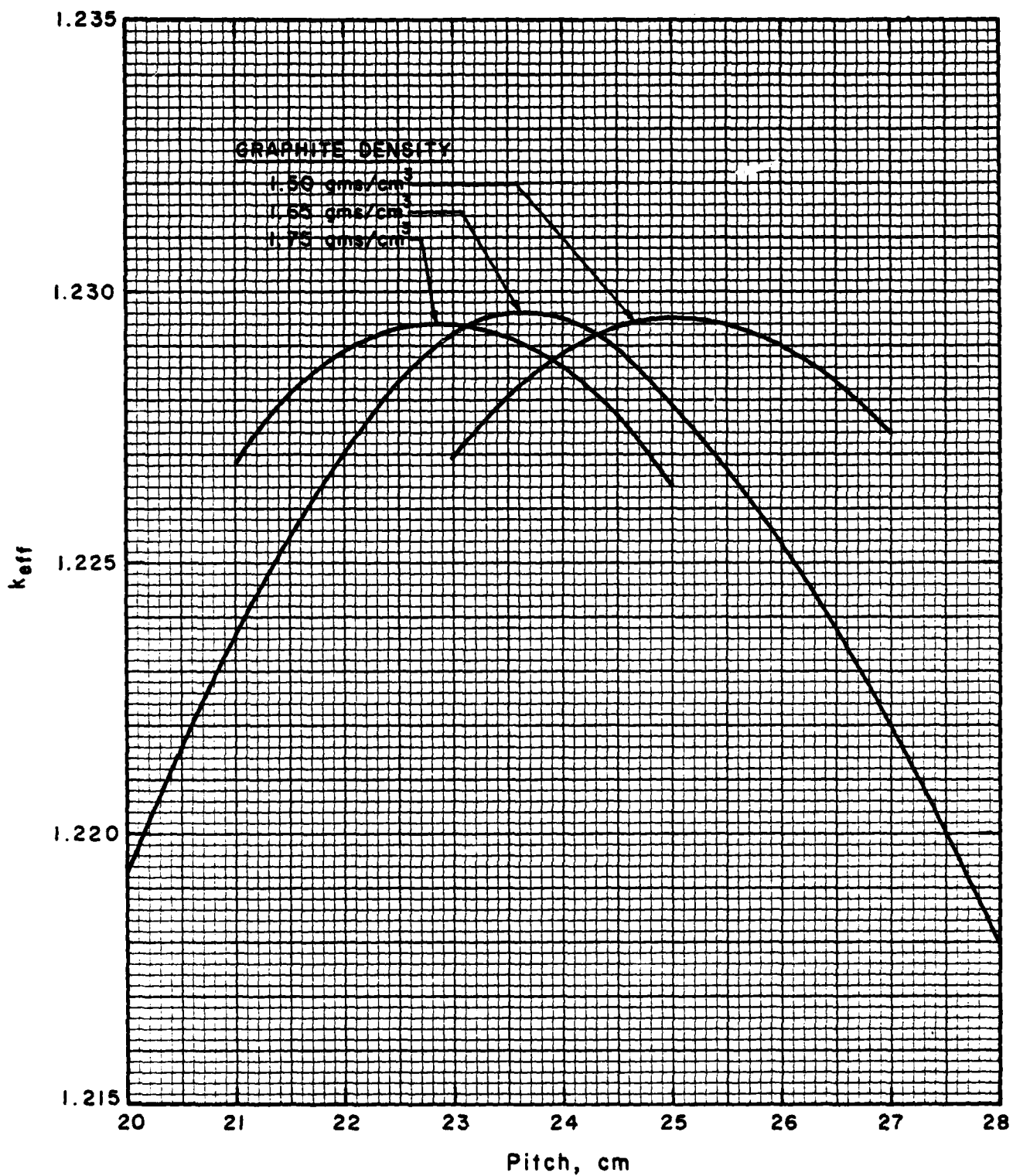


Fig. 6.9 Reactivity variation with pitch for different graphite densities for 1.2%-enriched uranium-fueled, water-cooled reactor.

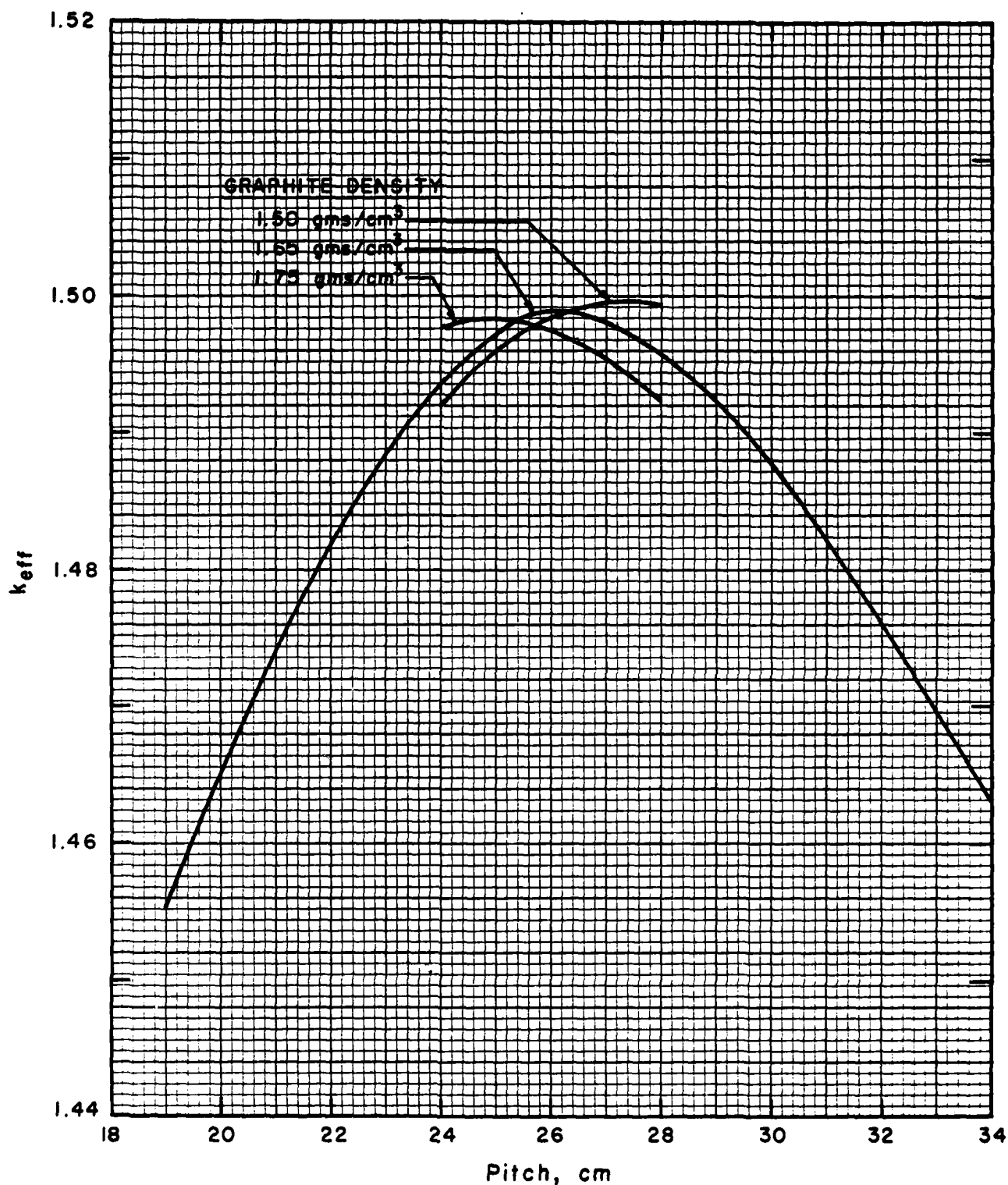


Fig. 6.10 Reactivity variation with pitch for different graphite densities for 3.2%-enriched uranium-fueled, water-cooled reactor.

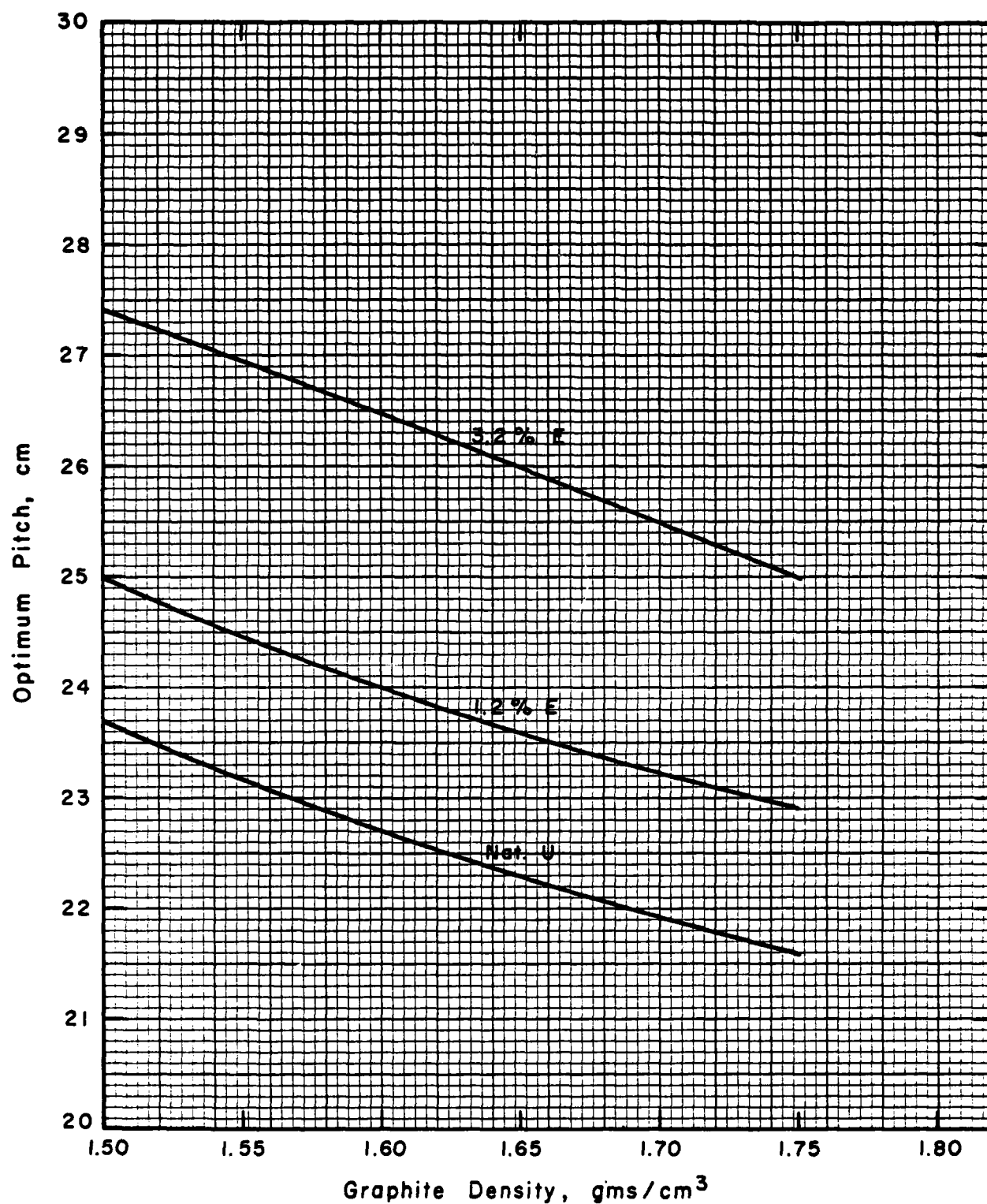


Fig. 6.11 Variation in optimum fuel cell pitch with graphite density for water-cooled reactor.

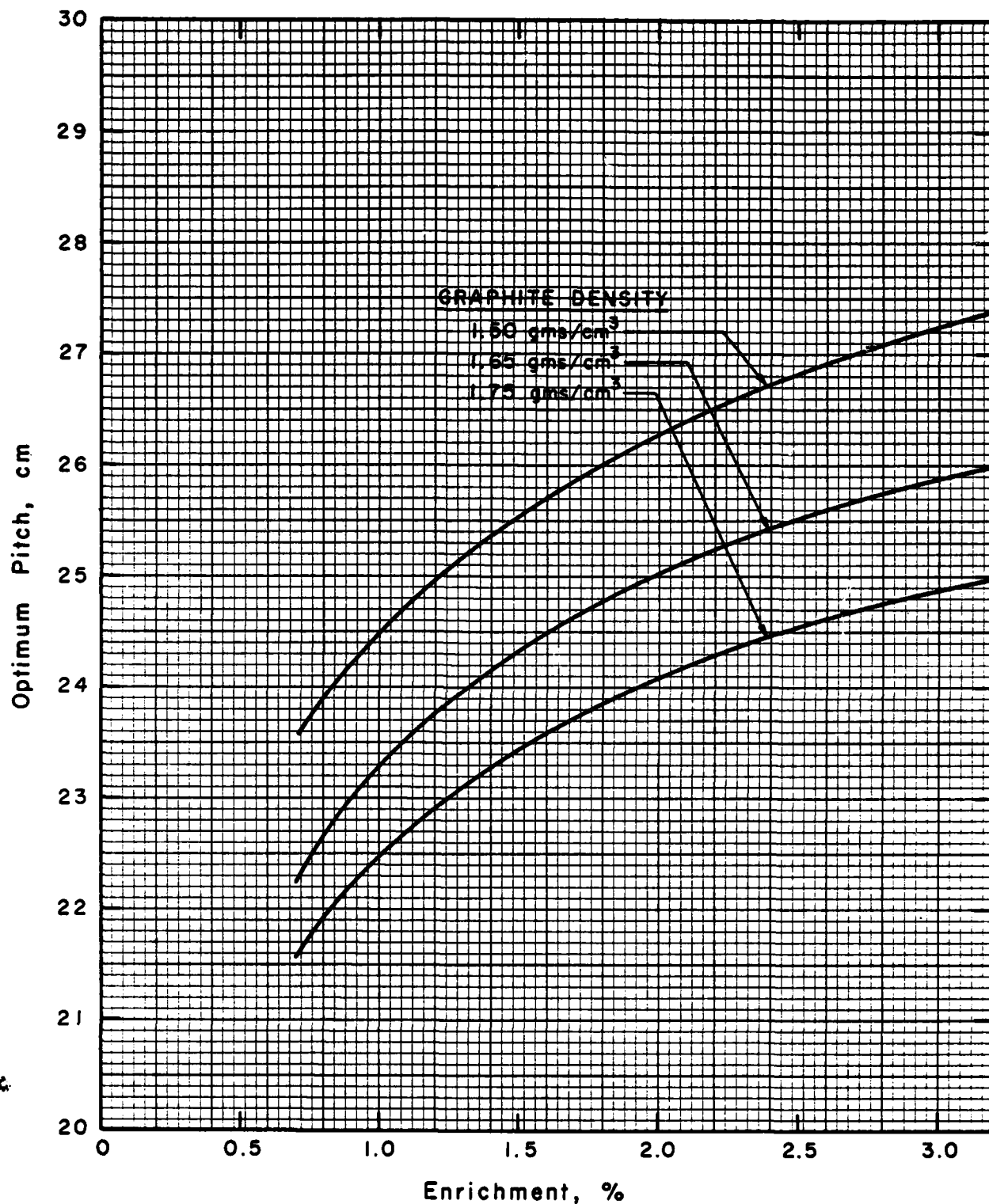


Fig. 6.12 Variation in optimum fuel cell pitch with fuel enrichment for water-cooled reactor.

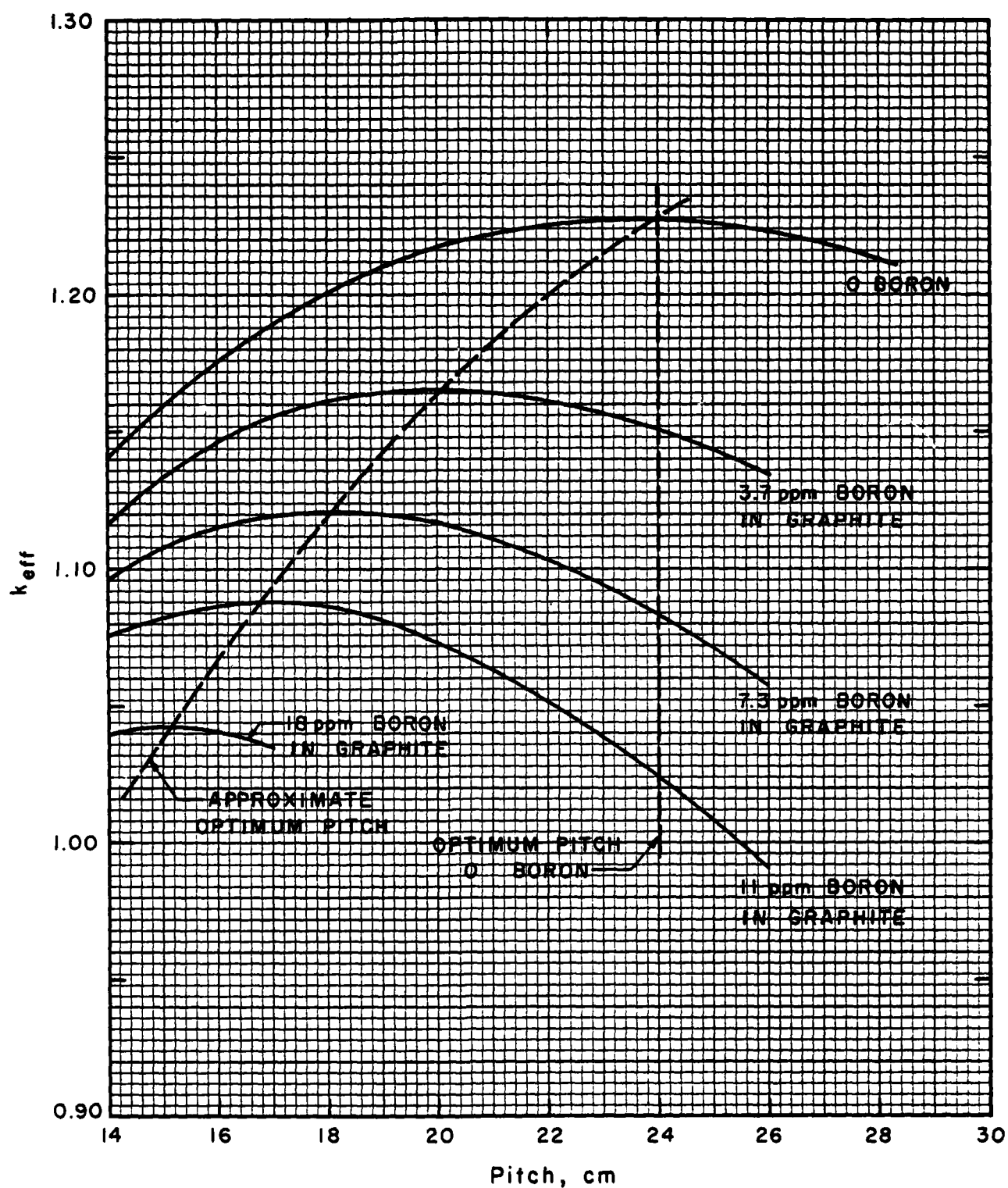


Fig. 6.13 Reactivity variation with pitch for various boron impurity levels; 1.2%-enriched uranium fuel, water-cooled reactor.

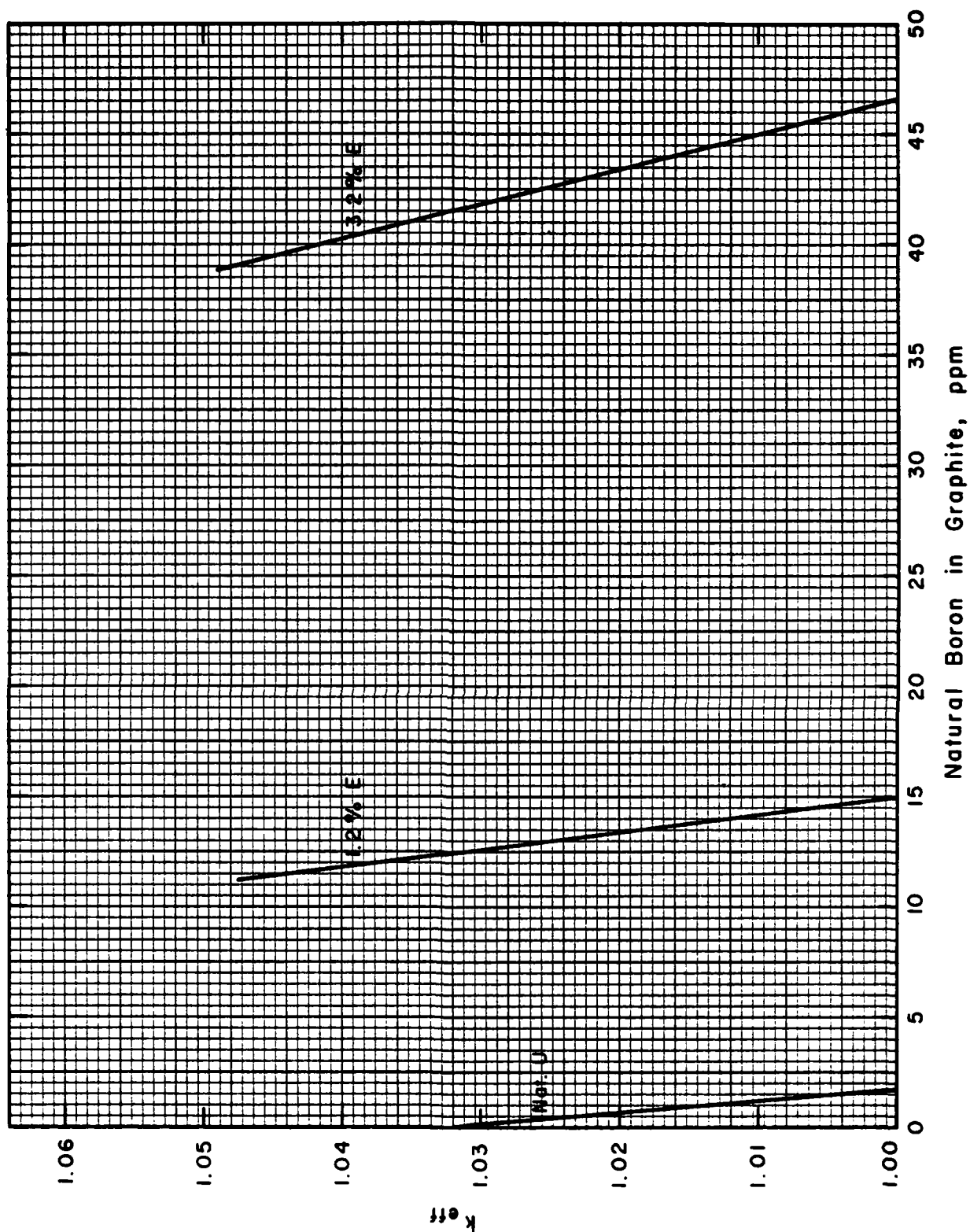


Fig. 6.14 Reactivity variation with graphite impurity level for fuel of natural, 1.2% and 3.2% enrichment (water-cooled reactor).

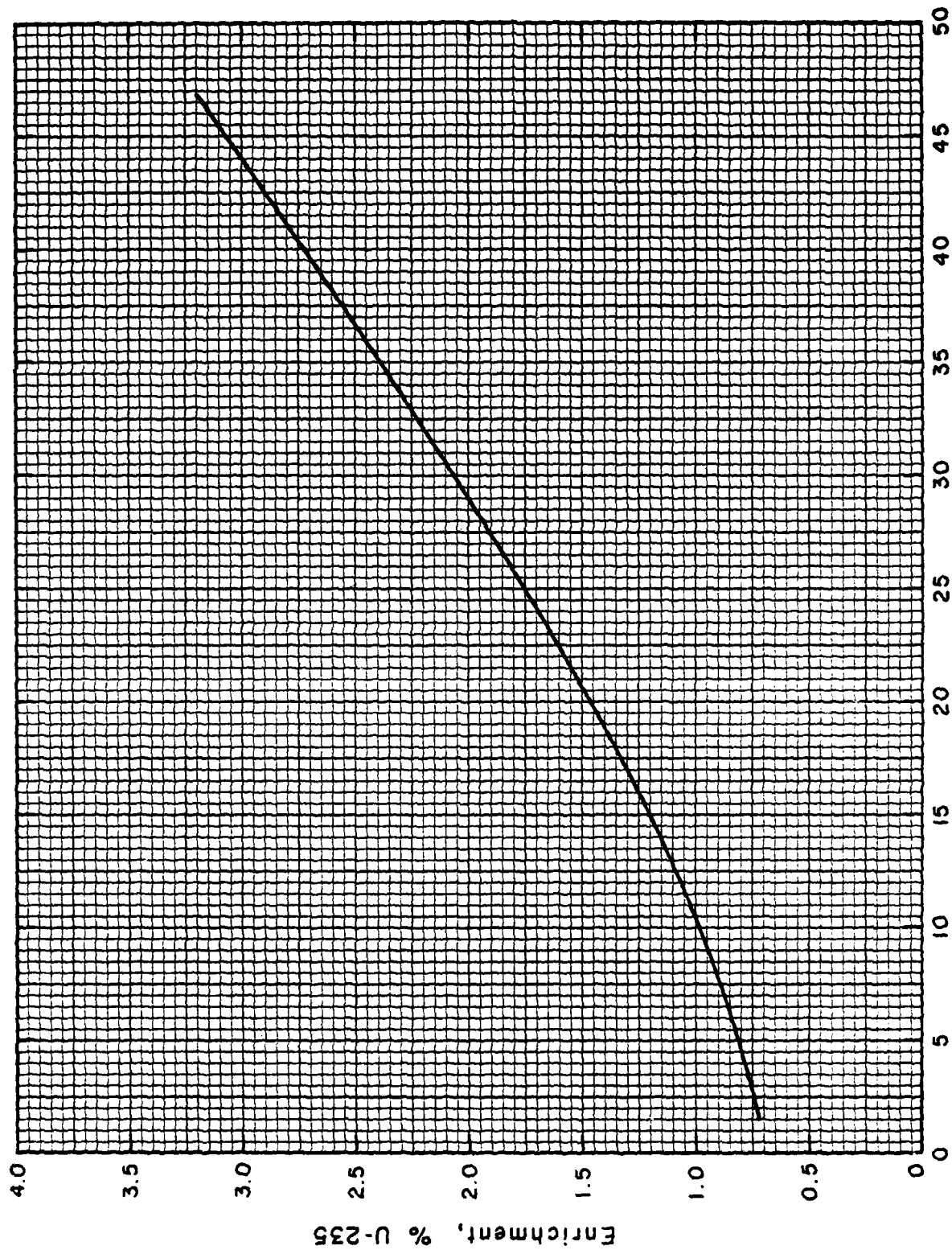


Fig. 6.15 Relationship between enrichment required and impurity level in graphite for the water-cooled reactor (pitch \approx 22.5 cm).

7.0 NEUTRON BURNOUT OF IMPURITIES

Impurities in the graphite will be consumed at a rate dependent upon the neutron flux and the cross-section of the impurity. To a close approximation, the fraction, F , of any impurity remaining after time t is given by

$$F = e^{-(\sigma_a \phi)t},$$

Where σ_a and ϕ are the effective cross-section of the significant isotope and the neutron flux respectively.

Results of calculations of the boron burnout for the three reference design reactors are shown in Figs. 7.1, 7.2, and 7.3 for three different fuel enrichments. As indicated in these figures, a considerably longer time is required for significant boron burnout in the air-cooled reactor than for the other two concepts because of the lower specific power (and hence flux levels). It should be noted that B-10 is the significant isotope of boron for burnout, with a 2200 m/s cross-section of 3860 barns. In each case, with higher enriched fuel, boron burns out at a lower rate because of the reduced neutron flux.

Other impurities have absorption cross-sections different from that of boron-10. A few of the impurities (e.g., iron) produce stable, higher isotopes on capture of a neutron and the poisoning effect is not significantly reduced. Table 7.1 lists the 2200 m/sec cross-section for the various anticipated impurities, together with the time required (years) to reduce the impurity to 10% of its initial value. For example, in the air-cooled concept, vanadium, with a σ_a eff of 4.9 barns and with natural U fuel, would require 9300 years to reduce the vanadium content to 10% of its initial value. Boron, by contrast, would require 11.7 full power years. Thus, except for boron and a few of the high cross-section rare earths, neutron burnout does not appreciably alter the impurity poisoning effects.

AC9NX707

Table 7.1 NEUTRON BURNOUT OF IMPURITIES

Impurity	Significant Isotope	Cross-Section ⁽²⁾	Time in years to consume 90% of impurity						Air-Cooled		CO ₂ -Cooled		H ₂ O-Cooled	
			E=Nat.	E=1.2%	E=3.2%	E=Nat.	E=1.2%	E=3.2%	E=Nat.	E=1.2%	E=3.2%	E=Nat.	E=1.2%	E=3.2%
Boron	B-10	3,860	11.7	16.9	29.9	2.0	3.0	5.4	2.3	3.4	4.8			
Aluminum	Al-27	0.23	197,000	284,000	500,000	33,913	50,500	90,000	38,000	57,000	80,000			
Sodium	Na-23	0.53	85,000	120,000	220,000	14,900	22,000	39,000	16,500	25,000	35,000			
Sulfur	S-32	0.51	89,000	128,000	226,000	15,290	22,800	40,000	17,000	26,000	36,000			
Calcium	Ca-40	0.2	225,000	327,000	577,000	39,000	58,000	100,000	44,000	66,000	92,000			
Vanadium	V-51	4.9	9,230	13,340	23,560	1,600	2,400	4,200	1,780	2,700	3,700			
Chlorine	Cl-35	44	1,028	1,482	2,624	180	260	470	199	300	420			
Lithium	Li-6	950	47.6	68.7	12.1	8.2	12	22	9.2	14	19			
Dysprosium	Dy-164	2,000	22.6	32.7	57.7	3.9	5.8	10.3	4.4	6.6	9.2			
Europium	Eu-151	2,800	16.2	23.3	41.2	2.8	4.2	7.4	3.1	4.7	6.6			
Cadmium	Cd-113	20,000	2.3	3.3	5.8	0.4	.58	1.03	.44	.66	.92			
Samarium	Sm-149	41,500	1.09	1.57	2.78	.19	.28	.50	.21	.32	.44			
Gadolinium	Gd-155 Gd-157	58,000 240,000	.78 .19	1.12 .27	1.99 .48	.13 .03	.20 .05	.36 .09	.15 .04	.23 .06	.32 .08			
Silicon	-	0.16												
Iron	-	2.5												
Titanium	-	6.1												
Molybdenum	-	2.6												

forms higher isotopes and absorption not appreciably reduced

(1) 2200 m/s barns

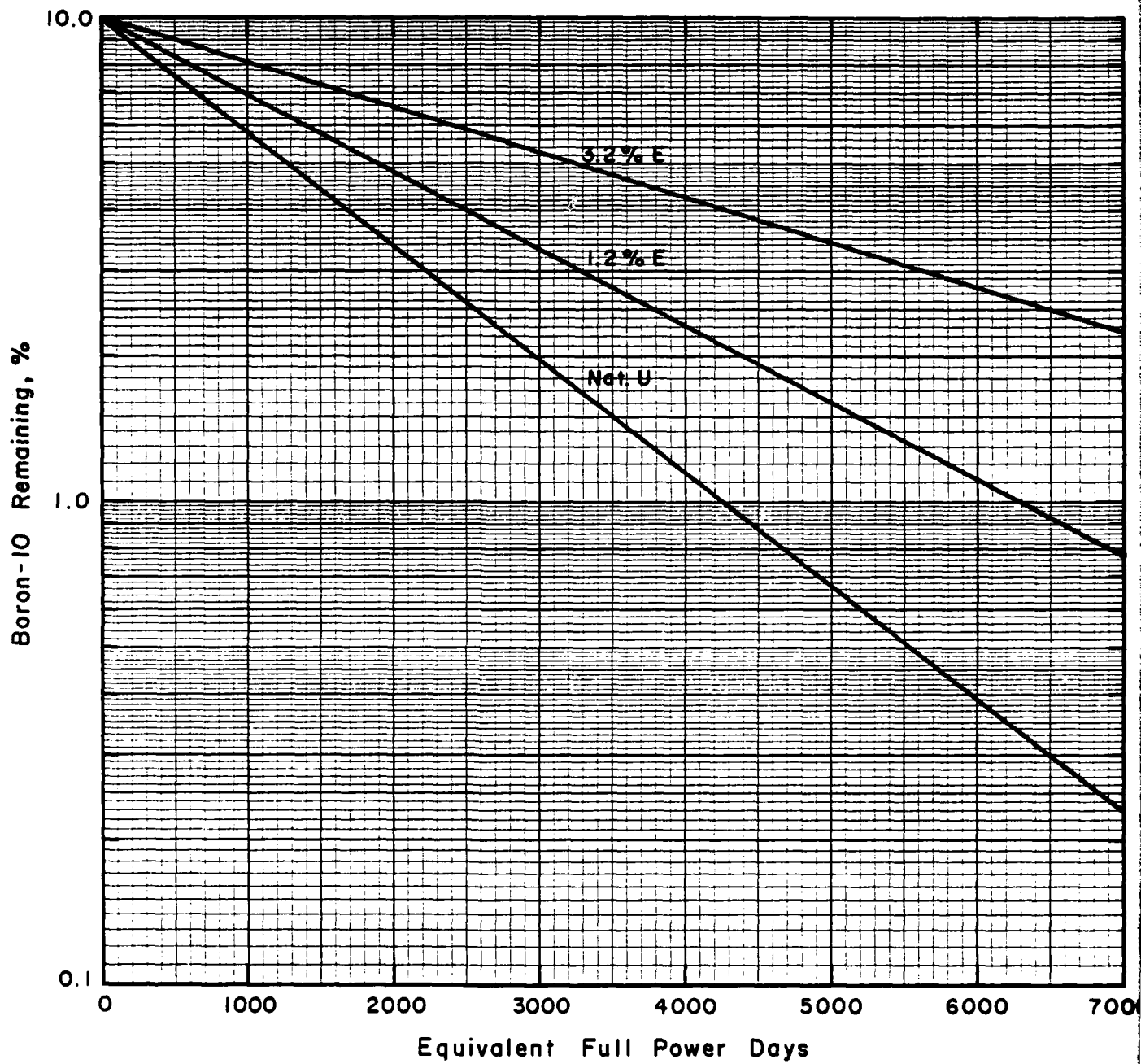


Fig. 7.1 Neutron burnout of boron in the low power air-cooled reactor.

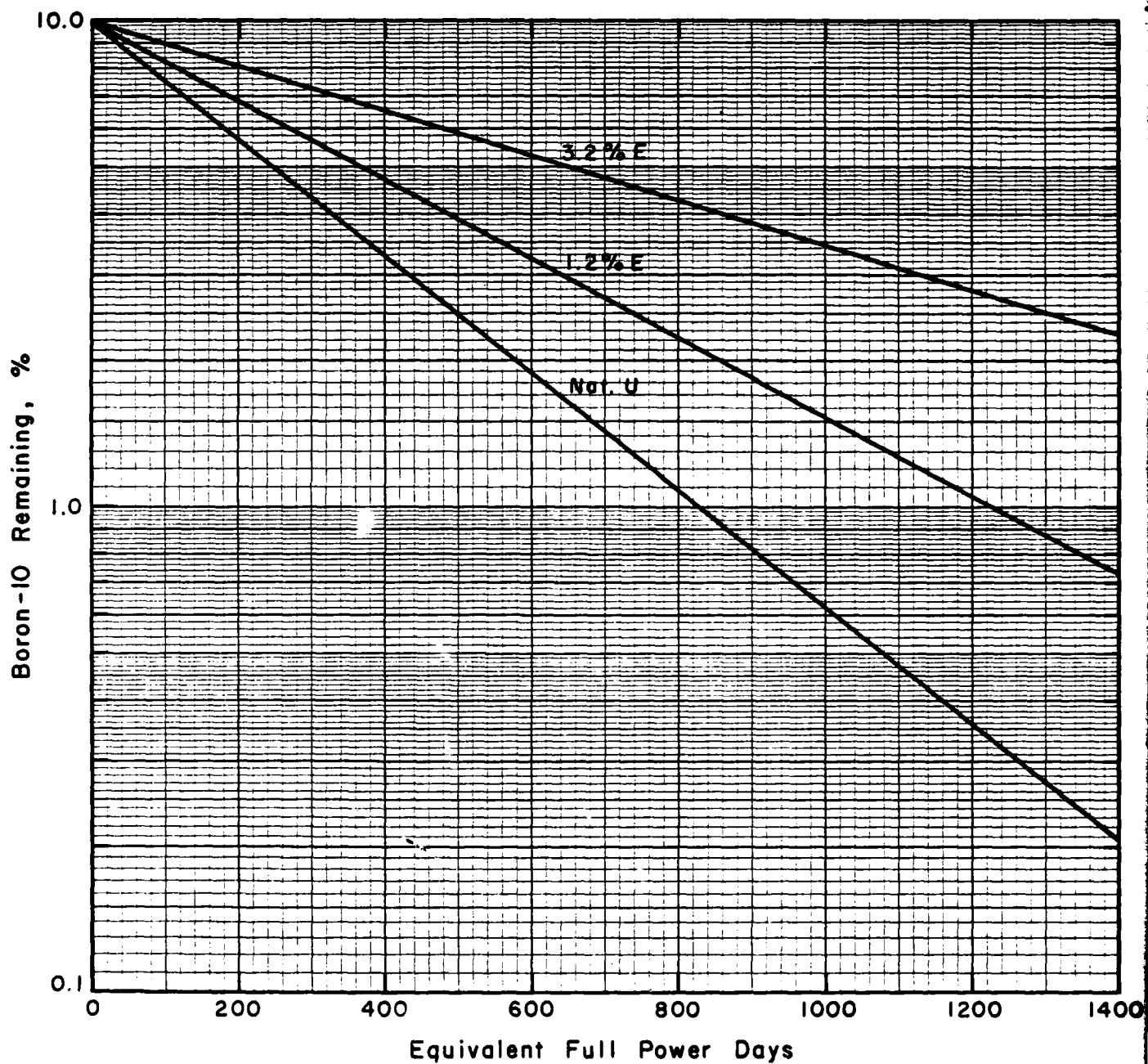


Fig. 7.2 Neutron burnout of boron in the medium power CO₂-cooled reactor.

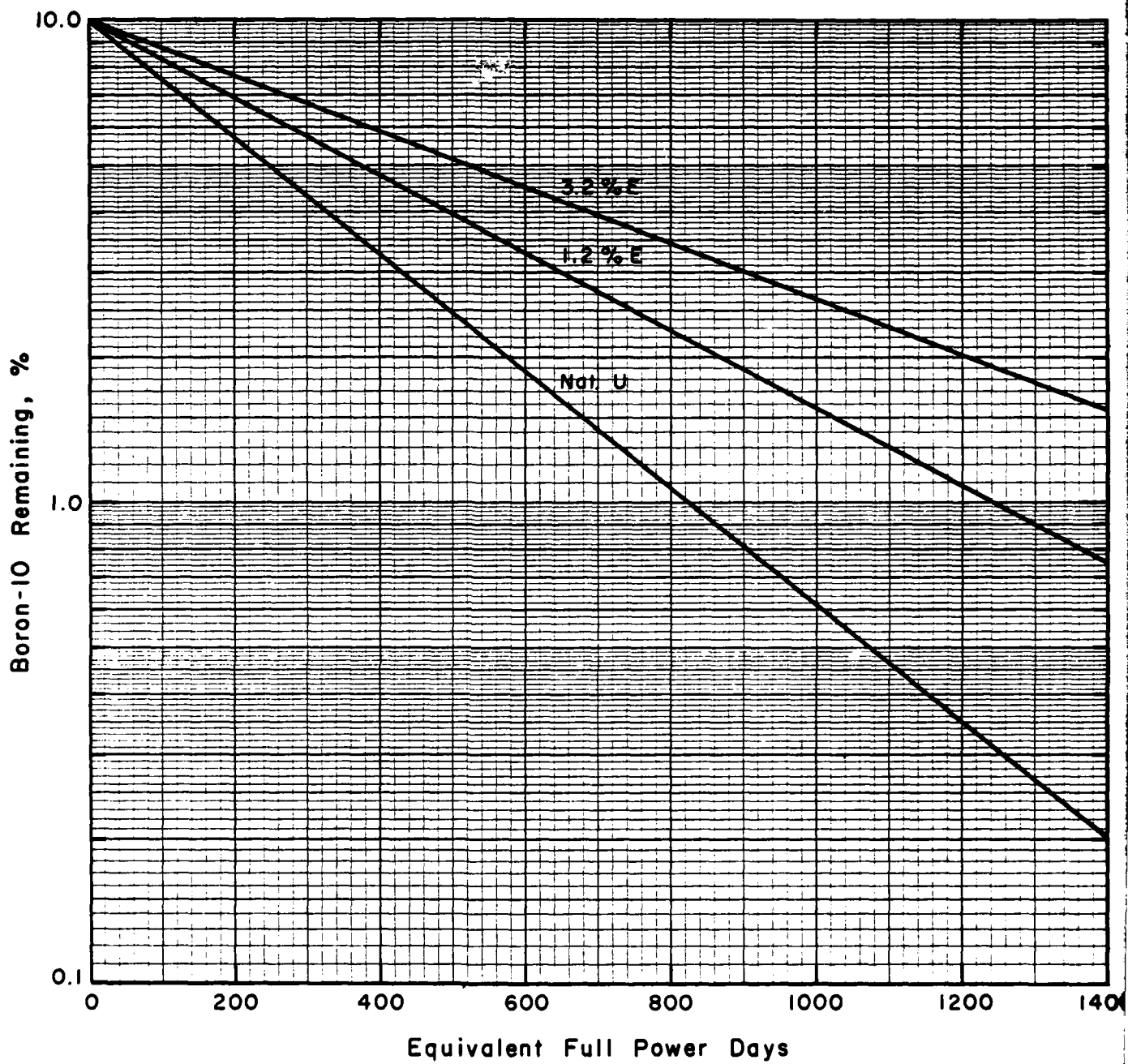


Fig. 7.3 Neutron burnout of boron in the high power water-cooled reactor.

8.0 CONSIDERATION OF COMMERCIALY AVAILABLE GRAPHITE

Graphite is manufactured worldwide in an almost endless variety of shapes, sizes, and combinations of physical, electrical, and thermal characteristics, as well as a wide range of purities. The industry in general has become very adept at tailoring the feed stock and the various manufacturing processes and interim product characteristics to achieve the desired end product characteristics—thus accounting for the extreme variations available.

Nuclear grades for use as reactor moderator tend to be manufactured for low impurity content, especially for those constituents that absorb neutrons, one of the most important being boron, or those constituents that, upon absorption of a neutron, yield unacceptable by-products (e.g., lithium, which yields tritium). Moderator grade graphites also are designed for minimum distortion and gas evolution under irradiation. These physical characteristics are heavily dependent upon the feed source, care in handling during manufacture, and choice of parameters used in the coke calcining, grinding, sizing, blending, baking, soaking, and graphitizing processes employed during manufacturing. These processes will be described in some detail later in this section.

In considering the utilization of commercially available "non-nuclear grade" graphite for a moderator application, at least four properties of the graphite must be evaluated. Two are heavily dependent upon prior manufacturing process parameters and very little improvement could be expected by subjecting the candidate finished graphites to further processing: these are physical size (the pieces can only be used as is or made smaller) and dimensional stability under irradiation. Purity and thermal conductivity, on the other hand, can be improved substantially by high temperature ($\sim 3000^{\circ}\text{C}$) soaking (purification) with or without a surrounding halogen atmosphere. These processes will be discussed further below.

8.1 Manufacture of Graphite

The graphite manufacturing process is relatively simple and the basic facilities required are reasonably inexpensive. The process tends to be labor intensive and is adaptable to a variety of techniques depending upon economic trade-offs and over all plant capacity. Figure 8.1 summarizes the

manufacturing process. Individual processes at each step are widely variable and the choice of operating parameters depends upon feed stock, desired end product characteristics, and consideration of economics and in-place technology. Individual process details available in the literature are adequate to describe the general mechanics and parameters. However, specific production parameters appear to be closely guarded industrial secrets. The extent to which the absence of detailed process data represents a deterrent to a would-be graphite manufacturer is not readily apparent. Certainly some bench scale experiments would be in order to optimize the processes around the intended feed stocks and methods.

The graphite manufacturing process includes generating coke from carbonaceous feed stock (petroleum, coal, etc.). Petroleum is the preferred feed stock for a high purity end product such as required for reactor moderator applications. The feed stock, a normal product of the petroleum refinery process, is converted to coke by heating in the absence of oxygen to drive off the volatile constituents and break down the long chain molecules to yield a high carbon content residual. This petroleum coke is then calcined at temperatures to 2100°F (1150°C) and soaked at this temperature for several days to drive off the volatiles and to thermally decompose any remaining long chain molecules.

The calcined coke is then ground to a fine aggregate ranging in particle size from a few tenths of a millimeter down to a fine dust. This aggregate is then separated for blending into a mixture selected to optimize the finished product density and other physical characteristics. The blend is mixed with a binder, usually of coal tar or petroleum pitch, which has also been finely ground. The resultant mixture is then molded or extruded under pressure and temperature to form "green bricks" of the desired shapes. The green bricks are supported to prevent deformation and baked in an oven in the 900-1600°C (1650-2900°F) range to drive off the volatile constituents of the binder and to harden the brick to protect against deformation at elevated temperatures. The baking can be accomplished in simple, externally-heated kilns, or it can be done in electrically-heated kilns using the product as the electrode. Heating time is typically two or three weeks, with a similar period allowed for cooling, unpacking, repairing, and reloading.

If high product density is required, the baked product is placed under a vacuum and then allowed to soak in hot pitch under pressure for several hours before being subjected to the final purification and graphitization process. Final

purification and graphitization typically take place in an "Acheson furnace" consisting of a long open pit type kiln, into which the bricks are placed, surrounded by graphite powder and/or other materials that serve as both impurity "getter" and insulation. The bricks are then heated electrically to between 2600-3000°C (4700 and 5400°F) using the bricks themselves and their packing material as the resistance heater element. During this graphitization process the individual small crystals (crystallites) are re-aligned and the metallic and refractory impurities are vaporized and deposited in the exterior insulation. This process tends to be catalyzed by some of the impurities being removed and is usually accomplished in very large kilns ten to sixty feet long, four to twelve feet wide, three to six feet deep, and rated at 750 to 7500 kw. Each charge may weigh up to 100,000 pounds. The entire process involves several days to load, two to three days to heat, two weeks to cool and a few days to unpack, repair and re-load.

Generally speaking, low-boiling-point impurities are removed by graphitization; impurities that remain are those which form carbides or are soluble in graphite. Such impurities are extremely stable, often far beyond their vaporization temperatures, since they will frequently be found at imperfections within the graphite crystals. Despite the fact that during thermal purification impurity atoms must diffuse out of the graphite, it has, however, been found quite simple to purify large cross sections.

The ability of halides to penetrate both bulk graphite and graphite crystals, react with impurities, and remove them as volatile halide salts has long been recognized and employed to produce spectroscopic-grade electrodes for chemical analysis. To meet requirements for nuclear material, these techniques have been perfected to produce material of larger cross section in large quantities. The technique utilized most widely in the United States has been purification by Freon-12 or chlorine, although several other gases, including sulfur hexafluoride, carbon tetrafluoride, and carbon tetrachloride have also been tested.

Complete production manufacturing facilities comparable to those in use today could be established for less than \$20 million. Plants capable of the necessary capacity to supply a production reactor program could be built for one-tenth of that or less, especially if the country of deployment opted for more labor-intensive choices.

8.1.1 Graphite Properties

As discussed above, there are many considerations involved in developing a good moderator graphite for use in a natural-uranium reactor. Three of the most important considerations are thermal conductivity, dimensional stability under irradiation, and minimum neutron-absorbing impurities. Table 8.1 lists several graphites that have been used as reactor moderators, as well as some used in non-nuclear applications. The grade designation is based upon manufacturing process and indicates the range of general physical properties and purity. However, based upon discussions with vendors, there appears to be substantial control of the end product by minor changes in the manufacturing processes designated for any particular grade. Therefore, "nuclear" grade materials are usually custom-manufactured on the basis of order specifications.

The thermal neutron absorption cross-section is probably the most important figure of merit when considering graphite for use as a moderator in a natural uranium reactor. For most non-nuclear grades, this figure is not important and therefore has not been measured. Some of these non-nuclear grades have been checked for this figure of merit, or at least the equivalent boron content has been determined, and are included in Table 8.1. ANSI/ASTM standards C626-78 and C624-71, on which these determinations are based, are included here as Exhibit 8.1 for convenience.

8.1.2 After Market Graphite Purification in an Acheson Furnace

It appears that impure graphite might be refined substantially, even subsequent to purchase from a manufacturer, by additional treatment in an Acheson furnace modified for halogen gas treatment of the graphite load. Impure graphite may be returned to an Acheson furnace for further purification at a higher temperature. However, the efficiency of further thermal purification decreases with size of the graphite blocks. The Acheson process, as well as the furnace which was named after him, was first developed by Dr. E. G. Acheson in 1895. The basic structure of the furnace has endured to this day and is shown in Fig. 8.2. It consists of a bed of fire brick tiles laid on concrete piers with a concrete head at each end of the furnace through which

AC9NX707

Table 8.1 SUMMARY OF COMMERCIAL GRAPHITE PROPERTIES

Graphite Grade	Purity Ash & Type	Boron, ppm	Boron Equiv, ppm	Cross- Section mb	Δ ih DIH	Suitability as Moderator (5)		
						Air-Cooled	CO ₂ -Cooled	H ₂ O-Cooled
AGR	1.2		2.8	5.7	- .85(1)	M	M	NU
AGX	1.5		2.8	5.7	- .85(1)	M	M	NU
AGSR	.96	1.3	4.2	6.9(2)		NU	NU	NU
CS Standard (2)	1.2	1.3	1.8 - 4.0	4.9 - 6.7	- .85	U-M	U-M	M-NU
AGSX	1.2	1.5	4.3	7.0	--	NU	NU	NU
ATJ	.16	1.1	1.6	4.7	--	U	U	M
EBP	.005	--	--	--	--	PU	PU	PU
AGOT (now TS 1387)(3)	.07	0.4	1.1	4.3	.25	U	U	U-M
AGOT (now TS 1357) Standard (2)	.09	1	1.9	4.94	0	U	U	M
AGHT				--	--	--	--	--
TS 1240	.008	--	0.7	4		U	U	U
H-452	.008	<2.5 (1.4 nominal)	--	--	--	PM	PM	PMU
TSP (GBF) (3) (Discontinued)	.005	<0.2	.7	3.5-4	+1.0	U	U	U
PGA (Calder Hall)(4)	--	--	.7	4	--	U	U	U
PGB (Calder Hall)	--	--	1.1	4.3	--	U	U	U-M
AVC	.03					--	--	--
French		0.2	.7	4		U	U	U

-- Not available

(1) Private communications with A. Goldman, Carbon Products Division, Union Carbide Company

(2) Purified by high temperature long soak only.

(3) Purified in halogen atmosphere.

(4) Derived from selected very pure feed stock.

(5) U - can be used as moderator

M - marginal, might possibly be used with special operations and sophisticated fuel management scheme (see Text, Section 2.3). Also depends upon purity of individual batch.

AC9NX707

Table 8.1 SUMMARY OF COMMERCIAL GRAPHITE PROPERTIES
(continued)

Graphite Grade	Size, in	Thermal Conduct Cal/cm/Sec°-K	Density g/cc	Thermal Expansion Coeff	Commercial Application
AGR	6" - 12"	---	--	---	Electrodes
AGX	6" - 12"	---	--	---	Electrodes
AGSR	6" - 12"	.321	1.54 1.58	1.88	Crucibles, Boats, Jigs, Furnaces
CS Standard (2)	12"- 18"	.360	1.72	1.35	Pressing Molds, Rocket Inserts, Electrical Resistors, Crucibles & Mold
AGSX	6" - 12"	---	1.67	1.97	Pitch Impregnated AGSR
ATJ	9"x20x24"	.281	1.73	2.19	Pine Grain Molds & Dies, Rocket Motor, Nozzle Inserts
EBP	--	---	--	---	Hi Purity Application
AGOT (now TS 1387) (3)	--	2.27	1.70	2.22	Nuclear Low Boron Appl.
AGOT (now TS 1357) Standard (2)	--	2.27	1.70	2.22	Nuclear Reactor Moderator, Etc.
AGHT	--	---	---	---	Brookhaven Reflector
TS 1240	--	---	1.74	---	Nuclear Application
H-452	--	---	---	---	HTGR Moderator By Great Lake Carbon
TSP (GSP) (3) (Discontinued)	--	2.27	---	2.22	Reactor Appl. Low Gas Evol. & Neut. Cross Sections
PGA (Calder Hall) (4)	--	---	1.7	---	British Pile Grade A
PGB (Calder Hall)	--	---	1.65	---	British Pile Grade B
AVC	--	.404	1.68	1.77	Controlled Purity Const. Molds & Crucible Jigs Resistors for Semi- Conductors
French	--	---	---	---	Lockport graphite (G2 & G3) Reactors)



AMERICAN NATIONAL
STANDARD

ANSI/ASTM C 626 - 78

AMERICAN SOCIETY FOR TESTING AND MATERIALS

1010 River St., Philadelphia, Pa. 19106

Reprinted from the Annual Book of ASTM Standards, Copyright ASTM
It is not listed in the current combined index, and appears in the next edition.

Standard Methods for

ESTIMATING THE THERMAL NEUTRON ABSORPTION CROSS SECTION OF NUCLEAR GRAPHITE¹

This Standard is based under the fixed designation C 626; the number immediately following the designation indicates the year of original adoption or, in the case of revision, the year of last revision. A number in parentheses indicates the year of last revision.

1. Scope

1.1 These methods define the thermal (2200 m/s) neutron absorption cross section, σ_a , of nuclear graphite. Three methods of estimating σ_a are given, one or more of which may be used.

1.2 These methods apply to graphites to be used for moderator or reflector components of nuclear reactors and subcritical test reactors and for thermal columns.

1.3 Excluded from these methods are graphites containing fissionable materials for use as fuel or driver elements and graphites containing materials having high neutron absorption cross sections for use as reactor control or safety devices.

2. Description of Terms

2.1 **Thermal Neutron Absorption Cross Section**—The thermal (2200 m/s) neutron absorption cross section, σ_a (millibarns/atom), of nuclear graphite is expressed in terms of the contributions of impurities by the equation² as follows:

$$\sigma_a = \sigma_c [1 + 0.01 (\sum C_i / A_i)] \quad (1)$$

where:

σ_c = the thermal neutron absorption cross section for carbon (assumed to be 3.4 millibarns/atom).

C_i = the concentration by weight, in parts per million of the i th impurity, and

A_i = the atomic weight of the i th impurity.

Poisson factors are given in Table 1.

C 626

3.4 **DIH Purity**—DIH purity is a measure of the difference in reactivity between the standard graphite and test graphite bars. It is no longer in evidence and Method C 624 has been discontinued.

In the Hanford Test Reactor through arrangement with the United States Atomic Energy Commission.³ This method for determining the DIH purity was given in ASTM Method

¹ Production Reactor Branch, B1100, P.O. Box 356, Richland, Wash. 99352

TABLE 1 Poisson Factors for Common Impurities in Nuclear Graphite

Element	Poisson Factor, f_i , ppm ⁻¹
Aluminum	0.0301
Boron	24.7
Calcium	0.0339
Iron	0.0466
Silicon	0.0326
Titanium	0.043
Vanadium	0.0375

Note—Other impurities that have large Poisson factors are excluded because they are generally present in extremely low concentrations.

The American Society for Testing and Materials takes no position regarding the validity of any patent rights asserted in connection with any item mentioned in this standard. Users of this standard are responsible for identifying their own responsibility of the validity of any such patent rights, and the risk of infringement of such rights, is entirely their own responsibility.

This standard is subject to revision at any time by the responsible technical committee and must be reviewed every five years and if not revised, either approved or withdrawn. Your comments are invited either for revision of this standard or for additional standards and should be addressed to ASTM Headquarters. Your comments will receive careful consideration at a meeting of the responsible technical committee, which you may attend. If you feel that your comments will be considered in a future revision, you should make your views known to the ASTM Committee on Standards, 1910 Ross St., Philadelphia, Pa. 19103, which will schedule a future hearing regarding your comments. Failing submission there, you may appeal to the ASTM Board of Directors.

3. Methods of Estimating σ_a

3.1 Three methods are commonly used for estimating σ_a . These are listed in the following paragraphs in order of increasing reliability. One or more of these methods may be used.

3.2 **Boron and Ash**—The simplest method for estimating σ_a is based on the boron and ash content only. For this method Eq. 1 is applied to boron and ash content only. The Poisson factors used are 24.7 for boron and 0.028 for ash assumed to be entirely titanium dioxide. This method gives a conservative (high) value for the estimated cross section. Concentrations of boron and ash shall be determined in accordance with ASTM Methods C 560, Chemical Analysis of Graphite,⁴ and Method C 561, Test for Ash in Graphite.⁵

3.3 **Common Impurities**—The second method is based upon the concentrations of the common impurities listed in Table 1; these are most likely to be present in significant concentrations in nuclear graphite. The concentrations for the common impurities given in 3.2 shall be determined in accordance with Methods C 560. The σ_a shall be estimated using Eq. 1 with the Poisson factors given in Table 1.

¹ These methods are under the jurisdiction of ASTM Committee C-5 on Manufactured Carbon and Graphite Products.

Current edition approved April 26, 1978. Published June 1978. Originally published as C 626 - 66 T. Last previous edition C 626 - 71 (1977).

² Equation 1 is from R. F. Smith, "Nuclear Graphite," Academic Press, New York, 1962, p. 38.

³ Annual Book of ASTM Standards, Part 17.



Designation: C 624 - 71

American National Standard ISO 6:1973
Approved March 30, 1973
By American National Standards Institute

AMERICAN SOCIETY FOR TESTING AND MATERIALS

1916 Race St., Philadelphia, Pa., 19103

Reprinted from the Annual Book of ASTM Standards, Copyright ASTM

Standard Method of Test for DELTA-IN-HOURS (DIH) PURITY OF NUCLEAR GRAPHITE¹

This Standard is issued under the fixed designation C 624; the number immediately following the designation indicates the year of original adoption or, in the case of revision, the year of last revision. A number in parentheses indicates the year of last revision.

1. Scope

1.1 This method covers the determination of delta-in-hours (DIH) purity of nuclear graphite.
1.2 This method applies to graphites to be used for moderator or reflector components of nuclear reactors and subcritical test reactors and for thermal columns.

1.3 Excluded from this method are graphites containing fissionable materials for use as fuel or driver elements and graphites containing materials having high neutron absorption cross sections for use as reactor control or safety devices.

1.4 The size, number of samples, and authorization required for determining DIH purity are given.

2. DIH Purity

2.1 The DIH purity² of nuclear graphite is determined in the Hanford Test Reactor.³ The difference in thermal neutron absorption between graphite standard and graphite test bars inserted in the reactor is measured in units of in-hours (sometimes called "delta-in-hours" or DIH). The measured DIH is a result of differences in moderating and absorption characteristics between the standard and test bars. A correction for the difference in moderation is applied to measured DIH values and the reported value (DIH purity) reflects only the difference in absorption characteristics between the standard and test bars.

2.2 DIH purity value is positive if the test bars have a lower neutron absorption cross section than the standard bars. Negative DIH

purity values indicate higher absorption cross sections than the standards. The maximum theoretical DIH purity of graphite having a bulk density of 1.70 g/cm³ is +1.16.

3. DIH Sample Bars

3.1 Size—Each test bar, as a whole or composite of smaller pieces, shall have the following dimensions:

3.1.1 Size I—3.750 by 3.750 by 49.150 in. (95.25 by 95.25 by 1248.41 mm), or

3.1.2 Size II—4.187 by 4.187 by 48.000 in. (106.35 by 106.35 by 1219.2 mm).

3.2 Tolerance—Cross section and length tolerances shall be ± 0.005 in. (± 0.13 mm).

3.3 Finish—Surface finish shall be comparable to 125 rms or less.

3.4 Test bars shall be protected from contamination by dust, dirt, moisture, oil, and grease during handling and machining. These precautions shall not, however, exceed those employed in fabrication and delivery of materials for which representative DIH purity values are to be determined.

3.5 Identification shall be stamped or engraved in each test bar.

3.6 Packaging for shipment shall provide protection against exposure to moisture and

¹This method is under the jurisdiction of ASTM Committee C-3 on Manufactured Carbon and Graphite Products.

²Current edition effective Dec. 29, 1971. Originally issued 1968. Replaces C 624-68 I.

³An application for DIH purity testing should be made to the Hanford Test Reactor, Richland, W. Va. 99357.

⁴Revised by F. J. H. and E. M. "Nuclear Properties," American Chemical Society, Chapter 4, Academic Press, New York, 1962, p. 74.

C 624

breakage.

4. Procedure

4.1 Determine DIH purity for one, two, or four test bars in each reactor test. The selection of a representative sampling plan is left at this time to a negotiation between the producer and consumer.

4.2 The standard bars used for reference in these determinations shall be the Hanford Test Reactor Secondary "K" Standards for Size I (see 3.1) and the Secondary "F" Standards for Size II (see 3.1).

4.3 Reactivity of the standards bars shall be the average of four reactivity tests or "drifts."

Make two of these standard bar determinations prior to insertion of test bars and two after the removal of the test bars. Do not make more than six test bar reactivity determinations between standard bar reactivity determinations.

By publication of this standard no guarantee is given with respect to the validity of any purity value in comparison with work, and the American Society for Testing and Materials disclaims any liability for any damage or injury resulting from the use of this standard.

4.4 Reactivity of the test bars shall be the average of two tests which may include one, two, or four bars per test.

4.5 Derive the DIH purity from the differences in standard and test bar reactivities and report it in the manner recommended.⁴

4.6 Conversion of DIH purity values to an estimate of thermal neutron absorption cross section may be made using Eq. 2 of ASTM Method C 626, for Estimating the Thermal Neutron Absorption Cross Section of Nuclear Graphite.⁴

5. Precision

5.1 The precision of DIH purity values reported shall be within ± 0.03 .

⁴Each, C. E. "Reporting IIR Graphite Test in Light of Recent Changes," USARC Report HWR-4198, May, 1970, Nuclear Reactor Assets Products Operations, Richland, W. Va. 99357.

⁵Annual Book of ASTM Standards, Part 11.

graphite electrodes are connected to energize the pile. The carbon bars to be graphitized are placed crosswise, one on top of the other to form stacks of carbon. Granular coke is placed between successive stacks and enough stacks are loaded to fill the length of the furnace. The whole pack is surrounded-top, sides and bottom-with layers of finely-divided carbon, coke, silicon carbide, and sand for thermal insulation. The side insulation is held in place by removable concrete blocks. The stacked carbon blocks and the granular coke between them form the resistor element of this high-temperature, resistance type furnace. Power is usually supplied at 600 to 7500 kw, depending on the size of the furnace and type of graphitizing charge. Total energy input ranges from 1.6 to 5.0 Kwh per pound of finished graphite, depending on the type of furnace and the type of graphite desired. The heating cycle lasts from three to four days, following which the graphite must be cooled for about two weeks before it can be exposed to air. The peak temperature reached in the graphitization process ranges from 2600 to 3000°C. During the graphitization process, the physical properties of the carbon change markedly, and many of the ash constituents are vaporized, thus improving the purity.

Graphite purity can be further improved in an Acheson furnace by a high temperature halogen gas extraction process, a technique developed sometime ago and now generally known in principle worldwide. The process essentially incorporates the Acheson furnace principles but is modified to expose the graphite to a halogen gas environment at high temperatures. The halogen gas serves to reduce the boiling points of the impurities, thus improving their ability to diffuse from the graphite to be redeposited in the cooler insulation layer surrounding the graphite blocks. Figure 8.3 illustrates typical modifications to the original Acheson process. Halogen gas purification can and has been used to further purify commercial graphite that had been previously manufactured.

It should be pointed out that the illustrations show rather elaborate provisions for accomplishing the graphitization process quickly and economically under production conditions. These furnaces could be made much more simply and cheaply for a "one shot" endeavor where competitive economy was not an important factor. For example, the French employ halide-bearing salts instead of gas for the halogen source.

8.2 Suitability of Commercially Available Grades for Use in Production Reactors.

As can be seen from the data presented in Table 8.1 above, many of the purer grades of graphite commercially available today have boron or equivalent poison contents sufficiently low to make them suitable for use as moderator material in a natural uranium fueled reactor. The primary constraints would be adequate material availability, cost, and graphite piece size. Furthermore, if one wished to consider a low-enriched fuel (say, 1%), the naturally-occurring neutron absorbers in a very wide variety of graphite would present little or no problem relative to the use of these graphites as moderator materials. Other properties of the purer, well-graphitized, non-nuclear grades would also probably make them suitable for application as moderator material. Thermal conductivity, dimensional stability under irradiation and temperature gradients, and strength characteristics should all prove to be acceptable, especially for relatively short-term or low-power-density applications.

Most of the graphites commercially available, if subjected to an additional purification step as described in Section 8.1.2, could be adapted for use as a moderator material with equivalent boron content well below the 1 ppm limit. The additional purification step might be accomplished at a relatively small cost compared to the original acquisition cost of the graphite. This is especially true in areas where electric power of the order of 5 Kwh per pound of required product is readily available. Assuming the purification pit (furnace) is sized for a load of 50,000 pounds, the total energy input would be approximately 250,000 Kwh over a period of approximately four or five days. Maximum power input capacity would approximate five megawatts, assuming a 100% reserve for control purposes. The furnace could be made smaller to accommodate restrictions in power availability at the expense of proportionately increasing the number of batches required and slightly increasing the overall schedule requirements.

8.3 Neutron Absorber Spikants to Deter the Use of Commercially Available Graphite in Reactors

Commercially available graphites could be spiked at the manufacturing plant with neutron-absorbing materials such as boron or some of the rare earths. This would easily render

the graphite unusable in a natural uranium reactor without further treatment. Spiking to a level of 20 to 100 ppm boron could probably be accomplished without seriously interfering with the manufacturing process or final machinability of the end product. There does not appear to be any spikant material that could not be removed by the steps outlined in Section 8.1.2, nor does the literature indicate that any unusual difficulty can be expected in such an endeavor. Thus, it would seem that spiking would make the use of commercially available graphites slightly more expensive, as indicated in Section 8.2-but not impossible. The intended commercial end use of many grades of graphite require graphite of high purity. Any intentional addition of impurities (spikants) may serve to make the product less competitive in the world market and unusable in those commercial applications requiring pure graphite.

8.4 Bibliography for Section 8.0

The Industrial Graphite Engineering Handbook, Union Carbide Corporation, Carbon Products Division, New York, 1969.

Legendre, A., et al., General Study on Nuclear Graphites Produced in France, Proceedings of the Second United Nations Internatinal Conference on the Peaceful Uses of Atomic Energy, 4, 243-56 (1958).

Mantell, C. L., Carbon and Graphite Handbook, Interscience Publishers, New York, 1968.

Nightingale, R. E., Nuclear Graphite, Academic Press, New York, 1962.

Currie, L. M., et al., The Production and Properties of Graphite for Reactors, First United Nations International Conference on The Peaceful Uses of Atomic Energy, Geneva, Switzerland, August 8-20, 1955.

Private communication, A. Goldman, Union Carbide Corporation, Carbon Products Division.

Private communication, W. P. Eatherly, Union Carbide Nuclear Corporation.

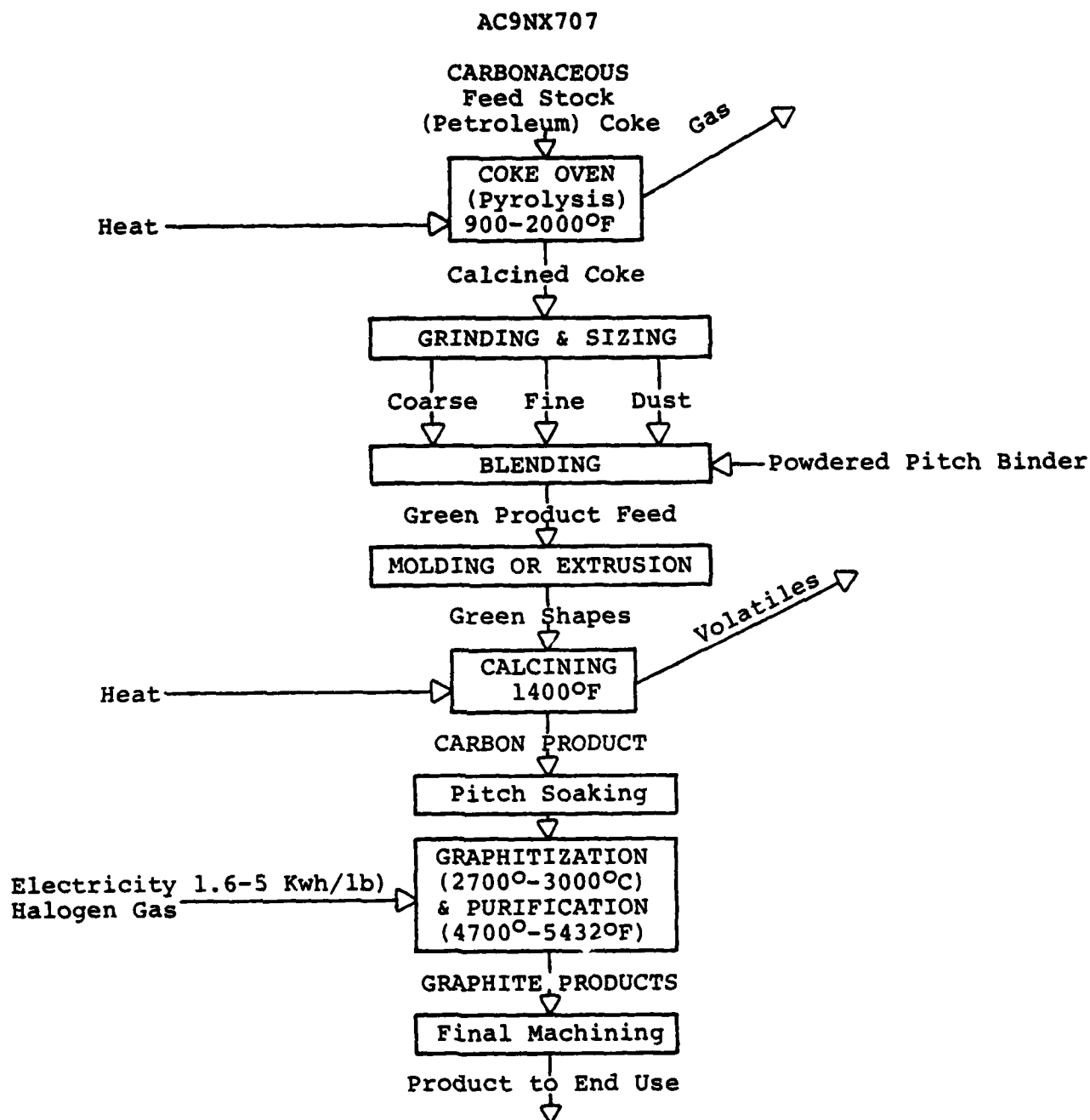


Fig. 8.1 Graphite manufacturing process.

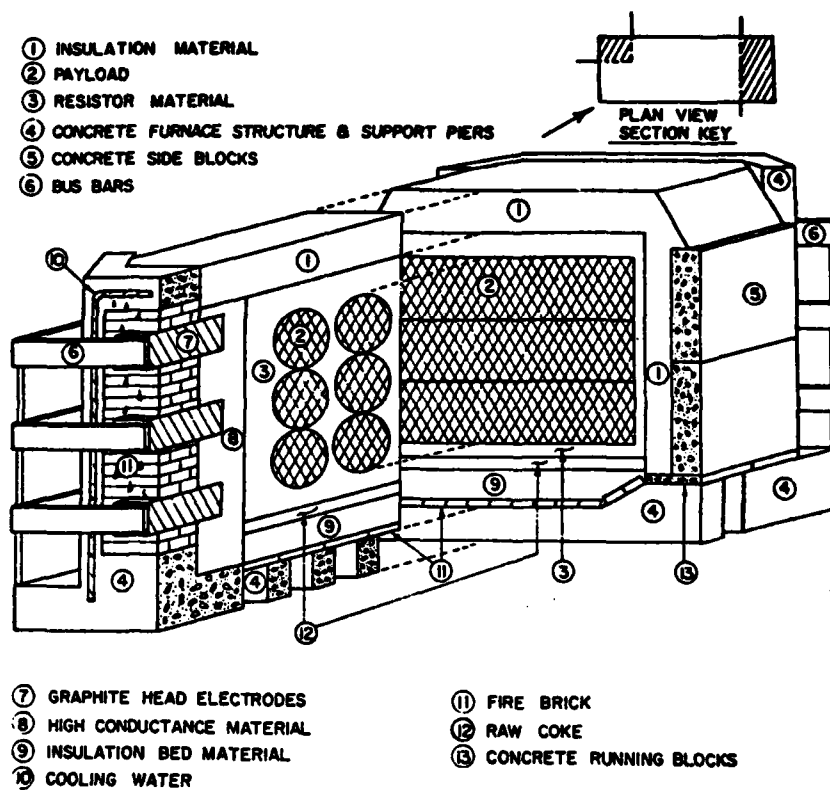
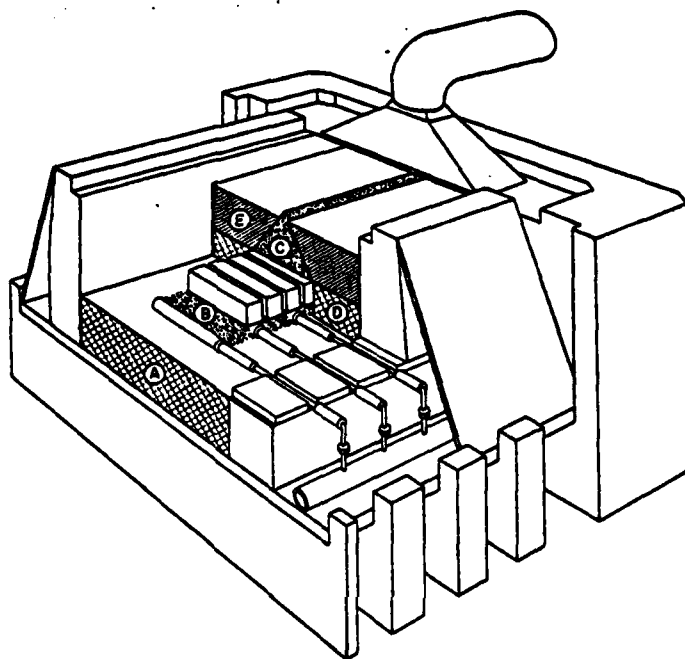


Fig. 8.2 Packing of a normal Acheson furnace.



A, D & E Low permeability mixture
 coke and flour

B & C Coke only (gas region)

Fig. 8.3 Packing of an Acheson furnace for gas purification.

9.0 EFFECT OF REACTOR SIZE

To a first approximation, the rate of plutonium production is directly proportional to the thermal power of the reactor. Because of thermal limitations, an increase in reactor power would necessitate increasing the number of fuel channels and, hence, the reactor size. This in turn, will decrease neutron leakage, affording a higher reactivity. Conversely, a decrease in reactor size increases neutron leakage and reduces the available reactivity. Figure 9.1 shows the change in k_{eff} for different size reactors of the three types considered.

Using the medium power reactor as an example, an increase in reactor size from the reference 250 Mw to 280 Mw ($\frac{280}{250}$ = ratio of 1.12) would increase the production rate of plutonium (annual fuel cycle) from 89 kg/year to 100 kg/full power year. The increase in reactor size necessary to accomplish this will increase the available reactivity from 1.052 to 1.0536, a Δk of .0016. Conversely, decreasing the size of the reactor to 140 Mw (~ 50 kg plutonium/full power year) would increase leakage and reduce the initial k_{eff} to 1.042, a loss of 1% in reactivity.

Of equal (or greater) significance is the increase in reactor power level (and hence, plutonium production) that could be achieved in later fuel cycles by judicious selection of fuel management schemes. By utilizing a carefully-designed fuel management scheme after the initial cycle, a considerable degree of flattening in power distribution can be accomplished, allowing the average power of the reactor to be increased (by perhaps 15 to 20%) without exceeding thermal performance limitations in the maximum power channel (limiting channel).

It should also be recognized that the thermal performance parameters represent nominal values only. By careful (and flow distribution and orificing) and relaxation of margins to some of the limiting criteria, it would be possible to achieve somewhat higher power levels, particularly for the water-cooled reactor design, without an increase in size (i.e., number of fuel channels).

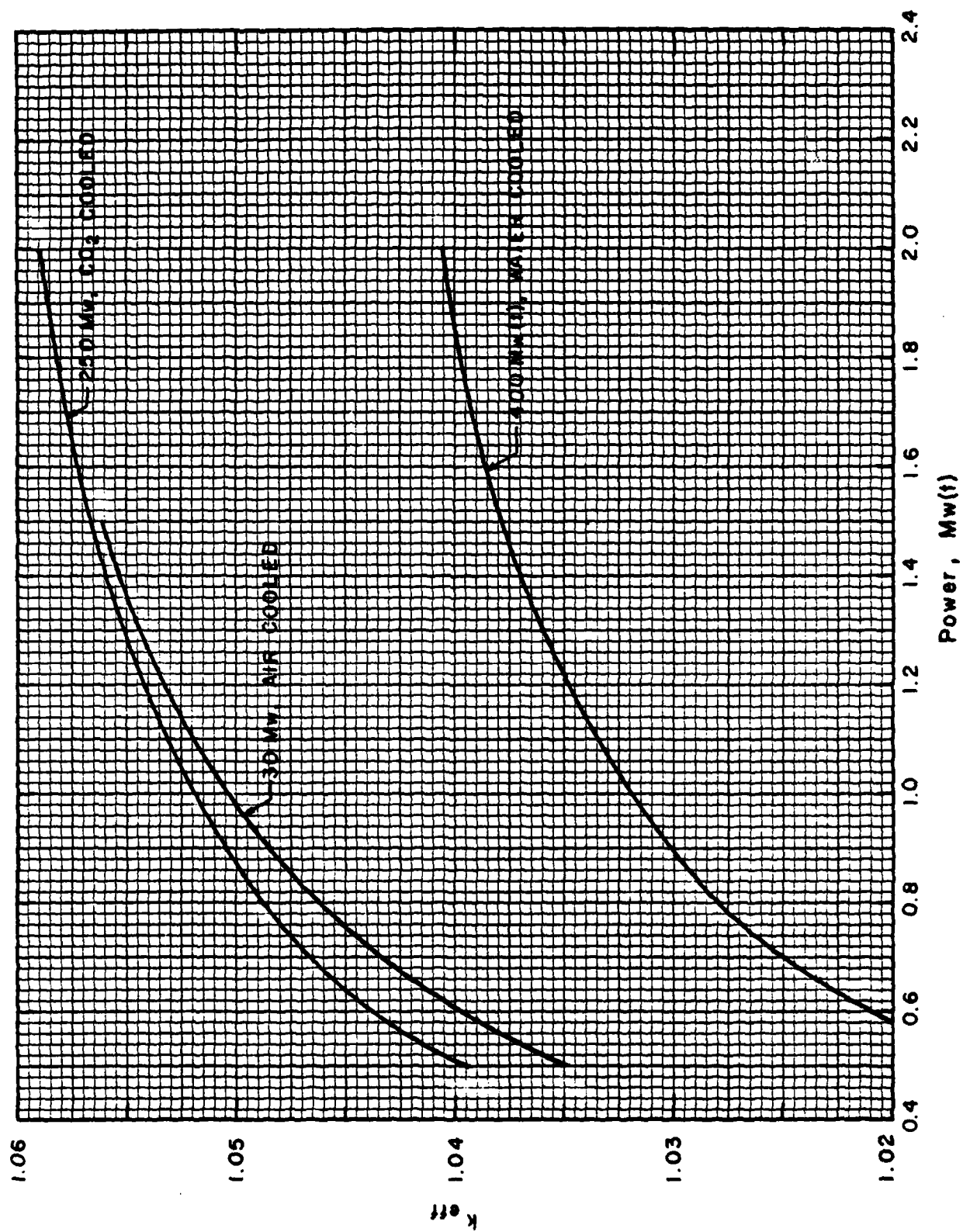


Fig. 9.1 Change in initial reactivity with reactor design power level.